Steady-state and Stopped-flow Fluorescence Measurements of The Interaction of Translational Initiation Factors with mRNA and The Interaction of Transcription Stimulatory Factor USF with DNA

By

Ma Sha

A dissertation submitted to the Graduate Faculty in Biochemistry in partial fulfilment of the requirements for the degree of Doctor of Philosophy, The City University of New York

1995

This manuscript has been read and accepted for the Graduate Faculty in Biochemistry in satisfaction of the dissertation requirement for the degree of Doctor of Philosophy.

7/11/95
Date

Chair of Examining Committee

7/11/95
Date

Executive Officer

Supervisory Committee

The City University of New York

Abstract

Steady-state and Stopped-flow Fluorescence Measurements of The Interaction of Translational Initiation Factors with mRNA and The Interaction of Transcription Stimulatory Factor USF with DNA

by

Ma Sha

Adviser: Professor Dixie J. Goss

The binding of oligoribonucleotides or m^7GTP to wheat germ protein synthesis initiation factor eIF-4B, eIF-(iso)4F and the purified subunits (p28, 28 kDa and p86, 86 kDa) of eIF-(iso)4F were measured by direct fluorescence techniques. Analysis of the equilibrium association constants (Keq) indicates that eIF-4B RNA binding is not affected by the m^7GTP cap structure or the AUG initiation codon of translation. eIF-4B is insensitive to hairpin structures within the oligoribonucleotide. The binding site size of mRNA on eIF-4B is approximately 18 bases. A specific anion effect of Cl^- on eIF-4B binding to oligoribonucleotides was found when comparing the ionic strength effect of $KC_2H_3O_2$ and KCl. The binding of m^7GTP to p28 as a function of pH, temperature and ionic strength is described. Iodide quenching shows

that all 9 tryptophan residues in p28 are exposed while only 6 out of 16 tryptophan residues are exposed on the intact eIF-(iso)4F. As in the eIF-(iso)4F protein, a specific anion effect of Cl^- on p28 binding to m^7GTP was found. The binding of p28, p86, and eIF-(iso)4F with m^7GTP and mRNA analogues was measured and compared. The second part of this thesis was devoted to the study of transcription upstream stimulatory factor USF. USF is a human transcriptional activation factor, which uses a basic/helix-loop-helix/leucine zipper (b/HLH/Z) motif to form a homotetramer and recognize specific sequences in the promoter region of both nuclear and viral genes transcribed by RNA polymerase II. Steady-state fluorescence spectroscopy demonstrated that the b/HLH/Z domain of USF binds to its DNA targets with high affinity and specificity, whereas removal of the leucine zipper yielding the b/HLH minimal DNA-binding region reduces both affinity and specificity. Stopped-flow measurements provided kinetic evidence for a two-step binding process, involving rapid formation of a protein-DNA intermediate followed by a slow isomerization step. Titration studies revealed that the first binding event has a equilibrium constant $K_{eq}= (2.2\pm2.0)\times10^9 M^{-1}$ for MLP (Adenovirus Major Late Promoter) DNA, whereas the second binding occurs with a remarkably reduced affinity $K_{eq}= (1.2\pm0.8)\times10^8 M^{-1}$. This anti-cooperative feature of DNA binding by the homotetramer suggests that USF stimulates transcription by mediating DNA looping between nearby recognition sites located in nuclear and viral gene promoters.

Abbreviations

Ac	acetate
BME	2-mercaptoethanol
DTT:	dithiothreitol
EDTA:	ethylenediaminetetraacetate
eIF:	eukaryotic initiation factor
HEPES:	N-(2-hydroxyethyl)piperazine-N'-2-ethanesulfonic acid
kDa:	kilodalton
m^7G:	7-methylguanosine
PEG	polyethylineglycol
PMSF	phenylmethylsulfonyl fluoride
SDS	sodium dodecyl sulfate
STI	soybean trypsin inhibitor
Tris	tris(hydroxymethyl)aminomethane

Acknowledgments

I would like to thank some of the many people who have made this work possible. To Dr. Dixie J. Goss, my mentor who have taught me everything I needed to learn. To all of my committee members who have kindly supported me through out my study: From Hunter College: Dr. William Sweeney, Dr. Maria Tomasz, Dr. Gary Quigley and from City College Dr. Horst Schulz and Dr. David Calhoun. To my wife, my parent and my little sister who have loved me and supported me for all these years. To Dr. Steven K. Burley from Rockfeller University and Dr. Karen Browning from University of Texas Austin with whom I had the pleasure to collaborate. I would like to thank some of the members of my lab whom I have worked with, laughed with and learned from, especially, Dr. Luisa M. Balasta, Yahong Wang, Chen Tang, Ting Xiang and Jianhua Ren.

Table of Contents

List of Tables

List of Figures

Chapter 1

Introduction

Overview of Protein Synthesis

Proteins are the end products of many biological systems. A typical cell requires thousands of different proteins at any moment. These proteins must be synthesized according to the cell's current needs. In eukaryotic cells, protein synthesis requires the participation of over 70 different ribosomal proteins; 20 or more enzymes to activate the amino acid precursors; a dozen or more initiation factors and many elongation and termination factors and additional enzymes for post translational modification. Thus several hundred different macromolecules must cooperate to synthesize polypeptides. Many of these macromolecules are organized into the three-dimensional complex of the ribosome to carry out stepwise translation of the mRNA. In some systems, protein synthesis can account for up to 90% of the chemical energy used by a cell for all biosynthetic reactions. In *E. coli*, the types of proteins and RNA molecules involved in protein synthesis are similar to those in eukaryotic cells. Both eukaryotic and prokaryotic cells contain thousands of copies of each protein. When totaled, there are about 20,000 ribosomes, 100,000 related protein factors and enzymes, and 200,000 tRNAs present in a single bacterial cell.

Despite this complexity, proteins are made at very high rates. A complete peptide chain of 100 residues is synthesized in an *E. coli* cell at 37 ^{o}C in about 5 s. The

synthesis of the thousands of different proteins is so well regulated that only the required number of molecules are made. To maintain the appropriate mix and concentration of proteins in a cell, the targeting and degradative process is also regulated to coordinate with protein synthesis.

In order to understand this very complicated protein synthesis mechanism, we began by trying to understand the initiation process of translation.

Three steps in the initiation of eukaryotic protein synthesis

The initiation of eukaryotic protein synthesis can be simplified as the following three major steps:

Step 1. Ribosome dissociation:

The 80s eukaryotic ribosome dissociates into 60S and 40S small subunits with the help of eukaryotic initiation factor eIF-2, eIF-3, eIF-4C and eIF-6.

Step 2: mRNA binding:

The small subunit of the ribosome (40S) binds to the 5' end of mRNA with the help of eIF-4A, eIF-4B and eIF-4F (plus eIF-(iso)4F in wheat germ) to form the initial 40S-mRNA complex.

Stem 3: 80S translation complex formation:

The initiation factors from the 40S-mRNA complex were removed with the help of eIF-5. The 60S ribosome subunit join the 40S-mRNA complex to form the active 80S ribosome-mRNA translation complex and start protein synthesis.

After protein synthesis, the mRNA dissociates from the 80S ribosome and the ribosome can initiate another round of translation starting from dissociation. Although this thesis focused on the study of those initiation factors involved in the second step of translational initiation, the mRNA binding step, a background review of all the initiation factors described above is helpful in understanding the whole initiation process.

Initiation factors of eukaryotic protein synthesis

As mentioned earlier, the eukaryotic protein synthesis initiation process contains three steps. These three steps involved many initiation factors including eIF-1, eIF-2, eIF-3, eIF-4A, eIF-4B, eIF-4C, eIF-4D, eIF-4F (plus eIF-(iso)4F in wheat germ), eIF-5 and eIF-6, plus the hydrolysis of ATP, unwinding of double stranded RNA in a mechanism that is not well understood. A general description is given below for the above initiation factors with emphasis on some of the wheat germ initiation factors studied in this thesis.

eIF-1

Eukaryotic initiation factor type 1 (eIF-1) is one of the smallest and least studied protein synthesis initiation factors. It was purified more than 15 years ago (Benne et al., 1978; Voorma et al., 1979) by gel filtration and SDS electrophoresis. eIF-1 appears to be a single polypeptide with a molecular mass of 15 kDa. Radioactivity labeled eIF-1 did not appear to form a stable complex with 40S, 60S, or 80S ribosomes and thus, like all the other translation factors, it cycles on and off the ribosome. The reason that this protein has not been well studied is that it has only a slight stimulation on protein synthesis, about 20% or less (Benne et al., 1978), and

even this slight stimulation is scattered among several steps rather than focused on one. The absence of eIF-1 does not affect in vitro protein synthesis significantly.

eIF-2

eIF-2 contains three subunits named α, β and γ with molecular mass of 35 kDa, 38 kDa and 52 kDa respectively. The human DNA sequences for α (Ernst, H. et al., 1987) and β (Pathak et al., 1988) subunits have been obtained from cDNA cloning. The complete γ DNA sequence has not been cloned. The primary function of eIF-2 is to bind the initiation Met-tRNA, and then bind with the small subunit of the ribosome during the first step (after ribosome dissociation) of protein synthesis initiation. Earlier cross-linking studies have shown that the Met-tRNA binds predominantly on the β subunit of eIF-2 (Nygard et al., 1980). Later studies found out that the initiator tRNA also cross-links to a peptide from the γ subunit (Kinzy, 1991). There is no evidence that the α subunit is involved in the binding of Met-tRNA. Some interesting results showed that an eIF-2 lacking the β subunit still functioned with only slightly reduced activity (Anthony et al., 1990). Obviously, many questions are left to be answered regarding to eIF-2.

eIF-3

eIF-3 is the largest of the initiation factors, with an overall molecular mass of about 650 kDa (Heufler et al., 1988). The mammalian protein contains 8 different subunits (35, 36, 40, 44, 47, 66, 115 and 170 kDa respectively) where the wheat germ eIF-3 contains 10 different subunits (28, 34, 36, 41, 45, 56, 83, 87, 107, 116 kDa respectively) (Heufler et al., 1988). The major role of eIF-3 is to bind to the small subunit of ribosome to facilitate the 80s eukaryotic ribosome dissociation during the first step of translation initiation. Hydrodynamic analysis of rat liver eIF-3 combined with electron-microscopic results suggest eIF-3 has a flat triangular shape with sides of 17, 17 and 14 nm long and a thickness of 7 nm.

eIF-4A

eIF-4A is a single subunit protein of 45 kDa. It has two separate functional genes which share 98% homology (Nielsen et al., 1988). The two eIF-4A gene products, however, are identical. eIF-4A has been characterized as RNA-dependent ATPase (Abramson et al., 1987), an activity characteristic of RNA helicases (the unwinding proteins). Many other proteins were found to share a particular sequence motif with eIF-4A, and they were all found to have RNA helicases activity. The sequence of eIF-

4A is highly conserved among species. The rabbit eIF-4A and the mouse eIF-4A share 100% sequence homology (Conroy et al., 1990). In fact, for most of the translational initiation factors, the sequences among different species share a tremendous amount of sequence homology and many researchers believe there is a general mechanism for protein synthesis which applies to all eukaryotes.

eIF-4B

eIF-4B has been generally characterized by gel electrophoresis from mammalian sources as an 80-kDa polypeptide. eIF-4B is required for 40S subunit binding to mRNA (Edery et al., 1983) in the second step of protein synthesis initiation (the mRNA binding step). It was also found that eIF-4B stimulates the helicase activity (Lawson et al., 1989) and RNA-dependent ATPase activity (Rozen et al., 1990) of other initiation factors. Mammalian eIF-4B was sequenced from a human cDNA library (Milburn et al., 1990). The DNA encodes a protein comprising 611 residues with a mass of 69,843 daltons. The amino-terminal domain of eIF-4B contains a consensus RNA binding domain present in a number of other RNA binding proteins. However, most assays of eIF-4B have required other initiation factors to bind mRNA or stimulate the synthesis of polypeptide chains, and thus a specific function of eIF-4B independent of other translational factors has not been found. Similar results have been obtained with wheat germ eIF-4B as described later in the this thesis.

Wheat germ eIF-4B is a 59-kDa protein that was originally designated eukaryotic initiation factor eIF-4G when it was first purified (Browning et al. 1987). It was soon found to be a functional equivalent of the 80-kDa mammalian eIF-4B, and the designation for the 59-kDa factor was changed from eIF-4G to eIF-4B (Browning et al. 1989). Recent sequence information for eIF-4B provided by the Browning group (K. Browning, personal communication) indicates that the wheat germ protein lacks the consensus sequence for the RNA binding, it also lacks an ATP binding site. However, this wheat germ eIF-4B sequence has a short piece of the N-terminus missing, where the RNA consensus binding sequence occurs in mammalian eIF-4B. Since the function of wheat germ eIF-4B was poorly understood and its binding specificity was not well determined, much effort was given to characterizing the binding properties of the protein in this thesis study. In order to investigate the binding of eIF-4B to the 5' terminus of mRNA, a series of oligonucleotides with or without cap, AUG, and hairpin structures were constructed. The fluorescence quenching of eIF-4B upon binding to these oligonucleotides was measured and the binding equilibrium constant was calculated (detail in **Chapter 4, Interaction of eIF-4B with oligonucleotides**).

eIF-4C

Like eIF-1, eIF-4C also has a very small molecular mass of only 17 kDa. It is also found in both mammalian and wheat germ systems (Dever et al., 1989). In the wheat

germ system, eIF-4C appears to be a heat-stable initiation factor, maintaining more than 85% of its activity after being heated to 90 ^{o}C for 5 min. (Seal et al., 1982). eIF-4C is about 153 amino acids long and the wheat germ and mammalian proteins share a 75% sequence homology. No particular sequence motifs were found in eIF-4C except the polar nature (positive charges on one end and negative charges on the other end) between the C and-N terminal. 10 of the first 22 N-terminal residues are basic, and 13 out of the 20 C-terminal amino acids are acidic. The major role of eIF-4C is to bind to the small subunit of the ribosome to facilitate the eukaryotic 80S ribosome dissociation during the first step of translational initiation.

eIF-4D

Like eIF-4C and eIF-1, eIF-4D is a low molecular mass (16 kDa) protein except that eIF-4D has not had a specific function assigned during protein synthesis initiation. It was found that eIF-4D could undergo a post-translational modification with spermidine to yield a modified lysine called hypusine (N-4amino-2-hydroxybutyl-lysine) (Cooper et al., 1983). This unique labeling with spermidine allowed for the analysis of different eukaryotic organisms, with the result that this protein with its unique modification is conserved among eukaryotes (Gordon et al., 1987). Studies on the Enzymology of hypusine biosynthesis indicated that it occurs by a two-step process which involves first the transfer of the 4-aminobutyl group from spermidine to the e-

amino group of lysine and then the hydroxylation of the deoxyhypusine to yield hypusine (Murphey et al., 1987). It was found that the formation of hypusine is not regulated but is subject to the availability of spermidine within the cell (Park et al., 1987). However, once the modification is finished, it is not easily reversed (Gordon et al., 1987). Thus, regulation of eIF-4D activity by removal of the spermidine modification is not likely to happen.

eIF-4F

eIF-4F contain two subunits: a 220 kDa large subunit and a 26 kDa small subunit. The small subunit also referred to as eIF-4E, has been cloned in mouse (Altman et al., 1988), human (Rychlik et al., 1987) and also yeast cells. This subunit is responsible for recognition of the m^7GTP cap structure at the 5' end of eukaryotic mRNAs. The eIF-4F was also discovered in wheat germ and contains similar subunits as the mammalian eIF-4F, with 26 kDa small subunits and the 220 kDa large subunit in a 1:1 molar ratio (Lax et al., 1986). It was proposed that the recognition of the m^7GTP cap structure might occur through π-π stacking between a tryptophan residue of eIF-4E and the cap (Ishida et al., 1983; Brun et al., 1975; Lawaczek & Wagner, 1974). An Isozyme of eIF-4F called eIF-(iso)4F was also found in wheat germ and is described below.

eIF-(iso)4F

eIF-(iso)4F has only been described in the wheat germ system and is the equivalent initiation factor of eIF-4F. eIF-(iso)4F, which contains two subunits of 82 and 28 kDa, was designated "eIF-4B" at the beginning by Lax et al (Lax et al., 1986a) and was subsequently designated eIF-(iso)4F after the discovery of "true" eIF-4B (Browning et al., 1989). eIF-(iso)4F is one of the two wheat germ initiation factors that has cap binding ability (the other is wheat germ eIF-4F). Although eIF-(iso)4F and eIF-4F was antigenically distinct (Lax et al., 1985, 1986b), some structural and functional similarity exists between the two initiation factors. Both wheat germ eIF-4F and eIF-(iso)4F have RNA-dependent ATPase activity. Only one wheat germ factor was required for ATP hydrolysis and stimulation of protein synthesis in an eIF-4F or eIF-(iso)4F deficient translation system (Lax et al., 1985, 1986b). Wheat germ eIF-(iso)4F can substitute for mammalian eIF-4F in an RNA-dependent ATPase activity and in cross-linking of mammalian eIF-4A to the cap of oxidized mRNA (Abramson et al., 1988). Separate subunits of eIF-(iso)4F are not functionally active as measured by the ability to stimulate polypeptide synthesis. However, when both subunits are added, activity was equal to native eIF-(iso)4F (Heerden et al., 1994). These results indicate that the two subunits are able to associate to form an active complex. In order to understand the RNA binding ability of the intact protein and the function of the individual subunits, the binding and physical properties of the separated subunits, reconstituted protein and native eIF-(iso)4F with m^7GTP cap structure and some 5' end rabbit globin mRNA analogs were studied in this thesis and described in detail **(Chapter 5, Interaction of eIF-(iso)4F and its Subunits P28 and P86 With m^7GTP and mRNA Analogues).**

eIF-5

eIF-5 is a single polypeptide chain of molecular mass of 125 kDa with a ribosome-dependent GTPase activity (Benne et al., 1978). Little is known about this initiation factor except that it is believed to be involved in protein synthesis initiation in a later stage (the third step: 80S ribosome formation) than other initiation factors. It is one of the most active GTPase proteins. Merely 100 ng of protein is enough for it's activity assay. However, it exists in very low abundance, making it a difficult protein to purify.

eIF-6

To make people like me who feed on wheat germ feel better, the eIF-6 was originally purified from wheat germ (Russel et al., 1979), then obtained from calf liver (Valencia et al., 1982) and rat reticulocytes (Raychaudhuri et al., 1984). eIF-6 is a small single polypeptide of 25 kDa. The major role of eIF-6 is in the ribosomal dissociation for preparing 40S subunit-mRNA binding.

Transcription Stimulation Factor USF

The detailed mechanism and research progress about DNA transcription is not described in this thesis. Since only one transcription factor has been investigated, all the introduction is limited to this particular transcription factor, USF, upstream stimulatory factor.

The human transcription factor USF is involved in the regulation of both cellular and viral genes. USF belongs to the basic (B)-helix-loop-helix (HLH)-leucine zipper (Z) family of transcription factors and stimulates transcription by binding to a specific E-box motif (CACGTG) upstream of many cellular and viral promoters. Earlier studies identified USF as a cellular factor which activates the intrinsically strong adenovirus major late promoter by binding to an E-box located at position -60 with respect to the cap site (Carthew et al., 1985; Miyamoto et al., 1985; Sawadogo et al., 1985), and stimulate transcription, possibly by direct interaction with the transcription factor TFIID (Sawadogo, 1988; Meisterernst et al., 1990; Bungert et al., 1992). USF contains three major domains: b, basic domain; HLH, helix loop helix domain and Z, leucine zipper domain. The leucine zipper domain was believed to be necessary for high-affinity DNA binding by b/HLH/Z (Ferr D'Amar et al., 1994). The present

studies used the b/HLH and b/HLH/Z domains of USF. The recent cocrystal structure of b/HLH•DNA has shown that b/HLH binds to one duplex DNA as a dimer and other studies suggested that the b/HLH/Z binds 2 duplex DNAs at the same time as a homotetramer (Ferr D'Amar et al., 1994), but little is known about the binding affinity, specificity or the rate of this reaction. The duplex DNA oligomer containing a palindromic E-box (underlined) was used in this study:

MLP: 5'-TAGGCCACGTGACCGG
3'-ATCCGGTGCACTGGCC

A non-specific (NS) sequence, which contains three mutations (labeled with *) on one half of the sequence, was designed to alter the E-box:

NS: 5'-TAGGCCACCTGCCTGG
3'-ATCCGGTGGACGGACC
(* * * mark the mutated positions)

Recent studies showed that USF is a component of human beta-globin locus control region (LCR) transcription complex with a binding site very much like our NS sequence (Bresnick et al., 1993).

LCR 5'-TAGACCACCTGACTGG
3'-ATCTGGTGGACTGACC

The comparison of the association constants of USF with LCR, NS and the intrinsically strong MLP sequence will shed light on the sequence specific interaction of USF with DNA.

Figure 1.1: Schematic drawing of the stoichiometry of interaction between b/HLH and b/HLH/Z with DNA.

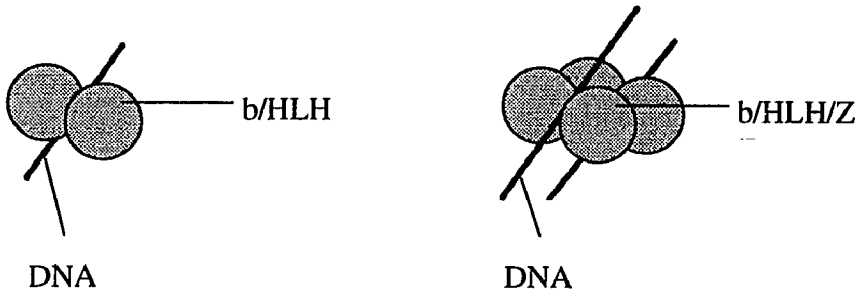

Chapter 2

Protein Purification

All the protein initiation factors studied in this thesis including eIF-4A, eIF-4B, eIF-4F and eIF-(iso)4F were purified in our lab from wheat germ. Among them, three translational initiation factors, wheat germ eIF-4B, eIF-4F and eIF-(iso)4F have been purified by myself based on the protocol of Lax et al. (1986a,b) and Browning et al. (1987) with many modifications. The detailed purification procedures for each of the three factors are described below.

Materials

Buffer E, used in obtaining the wheat germ 120 supernatant extract, consisted of 20 mM HEPES-KOH, pH 7.6, 1mM $Mg(Ac)_2$, 2mM $CaCl_2$, 6mM BME, 120 mM KCl, 0.1 mg/ml of STI, and 0.5 mM PMSF (from a 50 mM solution of PMSF in isopropanol prepared just prior to use). Buffer B, used in isolation of the wheat germ factors, consisted of 20 mM HEPES-KOH, pH 7.6, 0.1 mM EDTA, 1 mM DTT, 10% glycerol, and KCl as indicated. All chemicals were reagent grade or better. m^7GTP was purchased from Sigma Chemical Co. (St. Louis, MO), and m^7GTP-Sepharose was obtained from Pharmacia P-L Biochemicals Inc. (Piscataway, NJ). DE-52 and phosphocellulose P11 were purchased from Whatman BioSystems Inc. (Clifton, New Jersey). Sephadex G-200, Sephadex G-100, Sephadex G-75 and Sephadex G-25 were also obtained from Pharmacia P-L Biochemicals Inc. (Piscataway, NJ).

Wheat germ extract

The purification of eIF-4B, eIF-4F and eIF-(iso)4F shared a common start from the 120 mM KCl supernatant wheat Germ extract as described bellow. All procedures were carried out at 0-4 °C unless indicated otherwise. 200 grams of wheat germ were reduced to a fine powder by grinding in a Waring blender at medium speed at 15-sec intervals. The powdered wheat germ was mixed thoroughly with 340 ml of Buffer E and centrifuged for 20 minutes at 15,000 g. The fatty layer on top was removed; the supernatant was poured out and passed through a Sephadex G-25 column. The effluent from the column, about 450 ml, was centrifuged for 20 minutes at 30,000 g. The supernatant was ultra-centrifuged for 3.5 hr at 170,000 g. The final supernatant, designated 120 mM KCl wheat germ extract supernatant, was separated and stored in a -150 °C freezer before being used for the next step of wheat germ initiation factor purification.

Ammonium sulfate precipitation

The entire 120 mM KCl wheat germ extract supernatant as described above (400 ml containing about 15 g of protein) was removed from the -150 °C freezer and thawed slowly in a 4 °C cold box to prevent cracking of the plastic storage tubes. The

supernatant was brought to 40% saturation by gradually adding the ammonium sulfate (24.3g/100ml). The ammonium sulfate must be reduced to a fine powder prior to use to facilitate the fast dissolving in solution and prevent the formation of local over saturation of ammonium sulfate (which will cause more unwanted protein to precipitate). After stirring for 30 minutes in the 4 ^{o}C cold box, cloudy precipitation was observed and the solution was centrifuged at 15,000 g (about 12,500 rpm in our Sorvall centrifuge) for 20 min. The pellets were resuspended in small amount of buffer B(40), about 2 ml per 30 ml centrifuge tube, and dialyzed in B(40) overnight at 4 ^{o}C.

DE-52 column chromatography

The protein synthesis initiation factors eIF-4B, eIF-4F and eIF-(iso) are present in the 40% ammonium sulfate fraction until the completion of the DE-52 column chromatography step. This made it possible to get three factors from one set of purification procedures, it also made the DE-52 column chromatography a crucial step in the purification of all the eIF factors studied in this thesis.

Column packing

The fresh DE-52 cellulose had to be washed in acid and base before use in the ion exchange column. The DE-52 cellulose powder was stirred in 25 volumes of 0.5N NaOH and left for 5 minutes. The supernatant was removed and the medium washed in a funnel until the pH was 11.0 or below. The DE-52 cellulose powder was stirred in 25 volumes of 0.5N HCl and left for 5 minutes. The supernatant was removed and the medium washed in a funnel until the pH was above 3.0. In order to avoid excessive hydrolysis and swelling changes, it was important not to exceed the 5 minute incubation time in acid or base. Before loading the DE-52 resin into a column, it was very important to remove all fine particles from the resin, as those fine particles would clog the column mesh filter, reduce the column flow rate and resolution significantly. To remove the fine particles, large amounts of distilled water were added to the large beaker that contained the DE-52 cellulose resin. The resin was stirred and allowed to settle for several minutes. The cloudy supernatant was removed and discarded. Distilled water was again added and this step repeated until all the resin precipitated quickly to give a very clear supernatant. A little patience in this step paid off later. The DE-52 resin with enough distilled water was then poured into a column.

Column Equilibration

The 200-ml DE-52 column (2.5x41cm) was washed with Buffer-B(40) at pH 7.6 overnight with about 5 to 10 column volumes. The pH of the incoming and outgoing buffer was measured and the column equilibrated until these two pHs were exactly the same. If reusing a previously used DE-52 column, the column packing step was skipped, but the column was washed with the high salt B(500) to remove any residue of protein. The column was washed until the absorbance at 280 nm was below 0.2 O.D. before re-equilibrating the column.

Sample loading

A smooth baseline must be obtained before loading the sample. The B(40) dialyzed sample from the ammonium sulfate precipitation was loaded into the DE-52 column. If the sample appeared cloudy, an extra step of centrifuging (15,000g and 15 minutes) was applied to remove the undisolved precipitate before loading the sample. The column was washed with B(40) to remove all the non-bound proteins until the absorbance returned to the baseline.

B(80) peak collection

The column was then washed with B(80), the peak that eluted was collected. There was only one major peak at this point as we were not using a salt gradient. This B(80) peak contained eIF-(iso)4F and eIF-4B. The column was then washed continuously with B(80) without collecting until the absorbance returned to the baseline.

B(120) peak collection

The above column was then washed with B(120) and the peak that eluted was collected. There was also only one major peak in the B(120) wash as we were again not using a gradient. This B(120) peak contained the wheat germ protein synthesis initiation factor eIF-4F. The column was washed with B(500) to remove any remaining proteins until the absorbance returned to the baseline. The B(500) fraction was discarded.

Protein purification of eIF-(iso)4F

The B(80) peak from the DE-52 column which contained the eIF-(iso)4F and eIF-4B was concentrated by 80% ammonium sulfate precipitation (ammonium sulfate was added 51.6 g/100 ml, at 4 ^{o}C) and centrifuged at 15,000 g in a Sorvall centrifuge (12,500 rpm) for 25 minutes. The precipitate was resuspended in 10 ml of B(120) and dialyzed overnight against 500 ml B(120). The sample was then applied to an m^7GTP-Sepharose column as described below:

m^7GTP column cleaning

A 1 ml m^7GTP column was used as an affinity column for the purification of eIF-(iso)4F. The eIF-(iso)4F was bound to the column and eIF-4B was washed out as the flow-through. If the column was clean and well stored, only 20 ml B(120) was needed to wash the column before sample loading. However, if the column looked dirty or was not well stored, a regeneration step was necessary. First, the column was washed with 2 ml 100 mM Tris base pH 8.5 containing 500 mM KCl; second, the column was washed with 3 ml 100 mM pH 4.5 acetate buffer containing 500 mM KCl. Then the column was washed with 20 ml B(120) before sample loading.

m^7GTP column chromatography

The clean m^7GTP column was loaded with 10 ml dialyzed sample, the flow-through was collected for the purification of eIF-4B. This column was then washed with about 20 ml of B(120). No detector was connected to the small column as the operation was very simple, and the sample amount was too small to go through the tubing before collection. Ten ml freshly prepared 70 μM m^7GTP solution in Buffer (120) was added to the column. About 5 ml of the m^7GTP solution was allowed to pass through the column and collected; then the flow of the column was stopped for about 5 minutes before the rest of the m^7GTP solution was allowed to pass through and collected.

Dialyzing the eIF-(iso)4F after the m^7GTP column

It was very important for the 10 ml eIF-(iso)4F sample to be completely dialyzed to remove the m^7GTP (cap) from the solution. The 10 ml eIF-(iso)4F sample was dialyzed in 1000 ml of B(120) for 4 hours with stirring at 4 $^{\circ}C$. The sample was then dialyzed overnight in B(120) containing 10% PEG to further remove the m^7GTP and to concentrate the sample to about 0.5 ml. If the dialyzed tube was completely shrunken the next day, it was opened up and 0.5 ml B(120) added to rinse the tube and the sample collected. The purity of eIF-(iso)4F was then checked on a 7% SDS

denaturing mini-gel electrophoresis with a 4% stacking gel. Two bands, 82 kDa and 28 kDa respectively, were observed as corresponding to the large and small subunits of eIF-(iso)4F.

G-100 column chromatography

The eIF-(iso)4F obtained from the m^7GTP affinity column should contain only two visible bands on the mini-gel, the large and small subunits of eIF-(iso)4F. However, if undesired bands were present due to various reasons (like dirty m^7GTP column, incorrect solution concentrations or wrong pH), the impure eIF-(iso)4F was further purified by a G-100 gel filtration column.

Column preparation

The preparation of Sephadex G-100 column was much simpler than the ion-exchange DE-52 column. The way that the Sephadex G series columns worked was that they allowed smaller proteins to be trapped inside the pore of the special resin particle and travel a longer distance before being eluted so that the larger proteins were eluted earlier. The charge and buffer concentration was not very important. The column material was prepared from the dry resin powder by boiling in distilled water for about

two hours or by letting it sit at room temperature for about 72 hours, which ever was preferred. The fine particles were removed exactly as described earlier for DE-52 column preparation. The column materials were then loaded into a 25 ml column (1 cm x 35 cm) with B(120).

Column running

The column was equilibrated by passing through 100 ml of B(120) and the concentrated sample of eIF-(iso)4F (no more than 0.5 ml sample) was loaded into the G-100 column (25 ml). The column was washed with B(120) and the peaks collected separately. The mini-gel was again used to check the purity of the eIF-(iso)4F.

Protein purification of eIF-4F

Wheat germ eIF-4F is also an m^7GTP binding protein that was purified almost exactly like the eIF-(iso)4F. The B(120) peak from the DE-52 column described earlier which contained the eIF-4F was concentrated with 80% ammonium sulfate (51.6 g/100 ml) and centrifuged at 15,000 g in a Sorvall centrifuge (12,500 rpm) for 25 minutes. The precipitate was resuspended in 10 ml of B-120 and dialyzed overnight

against 500 ml B(120). The sample was then applied to the m^7GTP-Sepharose column. The 10 ml eIF-4F sample after the m^7GTP-Sepharose column was also completely dialyzed to remove the m^7GTP to prevent any interference in the protein-cap binding study. The 10 ml eIF-4F sample was dialyzed in 1000 ml of B(120) for 4 hours with stirring at 4 ^{o}C. The sample was then dialyzed overnight in B(120) containing 10% PEG to further remove the m^7GTP and to concentrate the sample to less than 0.5 ml. The purity of eIF-4F was also checked on a 7% SDS denaturing mini-gel with 4% stacking gel. Two bands of 220 kDa and 26 kDa were observed as the large and small subunits of eIF-4F.

G-200 column chromatography

A Sephadex G-200 column was used for the final purification of eIF-4F after the m^7GTP step if the sample was still not pure. The Sephadex G series of column materials from Pharmacia contained G-10, G-15, G-25, G-50, G-75, G-100, G-150, G-200 et al.. An easy way of selecting the appropriate resin to use was to use the resin with the number close to the protein molecular mass in kilodaltons. For eIF-4F, with a large subunit of 220 kDa, G-200 resin was used. Similar preparation procedures apply for all the G series gel-filtration materials as described earlier for the G-100 column. A sample chart for the separation of two marker proteins of apoferritin (443 kDa) and egg albumin (45 kDa) was shown in Figure 2.1. It should be pointed out that the two

protein were still not completely separated even with the large molecular mass difference. The surest purification was to make sure that the m^7GTP affinity column step was performed perfectly, so that the G series column need not be used.

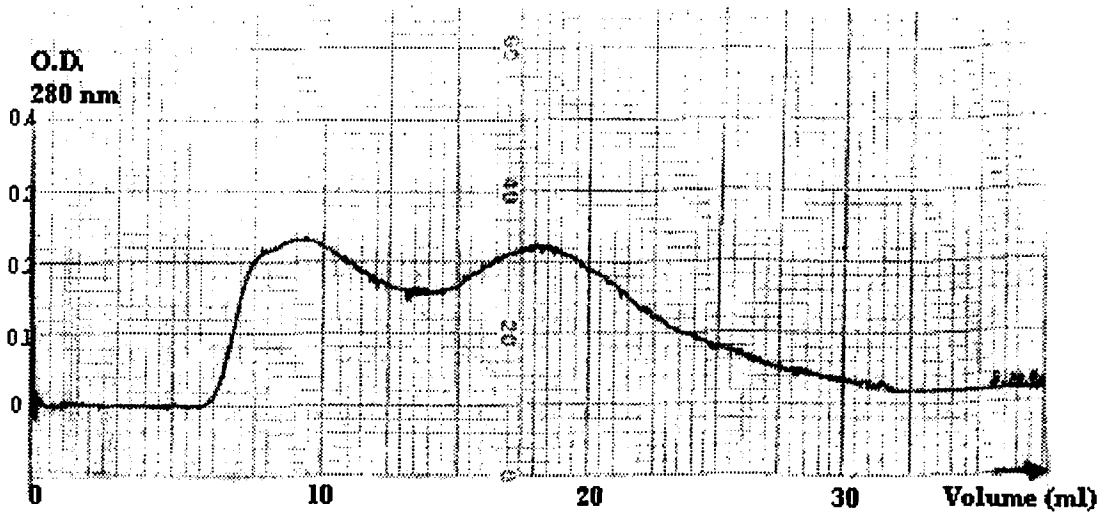

Figure 2.1. Sephadex G-200 Gel-filtration column of marker proteins. A 25 ml column (1x35 ml) was used. A mixture of the two protein samples, 2.5 mg each, was loaded with a total volume of 0.2 ml. The left peak was the larger apoferritin (443 KDa) which was eluted earlier, and the right peak was the smaller egg albumin (45 KDa) which was eluted later. The 280 nm UV absorbance detection was set with a sensitivity of 0.5.

Protein Purification of eIF-4B

Wheat germ eIF-4B exists in very low abundance, which made it more difficult to purify.

Sample preparation

5 to 10 batches of the m^7GTP-Sepharose flow-through from eIF-(iso)4F purification were pooled together with a total volume of 50 to 100 ml. The pooled eIF-4B was then concentrated with 80% ammonium sulfate precipitation (51.6 g/100 ml) and centrifuged at 15,000 g in a Sorvall centrifuge (12,500 rpm) for 25 minutes. The precipitate was resuspended in 3-5 ml (the minimal amount was used) of B(100) and dialyzed overnight against B(100).

P11 column preparation

The column used for wheat germ eIF-4B purification was the phosphocellulose P11 from Whatman Inc. This phosphocellulose P11 is a double featured column material that allows regular ion-exchange chromatography on general proteins plus special affinity chromatography effects on ATP binding proteins. The preparation of the P11 resin was exactly as described for DE-52 column earlier, including the 0.5N acid and

base wash, except that the column had to be made fresh for each use. The fine particle were also be removed exactly as described earlier for DE-52 column preparation.

Running of P11 Column

A 20 ml phosphocellulose P11 column (1.5x15) was packed and equilibrated with 200 to 500 ml buffer B(100). The pH of the incoming and outgoing buffer was measured until these two pHs were exactly the same and the baseline absorbance at 280 nm was stabilized bellow 0.05 O.D. The 3-5 ml sample from previous step was then loaded into the column. If the sample appeared cloudy, an extra step of centrifuge (15,000g and 15 minutes) was performed to remove the undisolved precipitate. The column was washed with B(100) buffer to remove all the non-bound proteins until the absorbance returned to the baseline, this sometimes took a long time (2~4 hr) but was important for obtaining pure eIF-4B. The huge peak observed with the flow-through represented the majority of unbound, unwanted proteins. The 280 nm absorption was usually over the maximum scale of the instrument; this was normal as the O.D. decreased with more B(100) washing.

Eluting with 100-400 mM KCl gradient

The column P11 was then developed with 120 ml (60 ml of B(100); 60 ml of B(400)) a linear KCl gradient from 100 mM to 400 mM in Buffer B. At the end of the gradient, the column was continuously washed with B(400) until the baseline was near zero. Two or three small peaks should be observed after the large peak of flow-through. Usually the second peak contained the eIF-4B, but the conditions changed from different preparations, so the conclusions were only be drawn from the mini-gel containing the eIF-4B band of 59 kDa. Small 2 ml fractions were collected continuously instead of collecting only the peaks, as there were sometimes overlap between the peaks. After checking on the mini-gel, the desired fractions were pooled and dialyzed against 500 ml of 33% ammonium sulfate in B(100) for 5 hours. The precipitated protein was collected by centrifugation at 15,000 g for 25 minutes, suspended in 0.4 ml buffer B(100) and dialyzed overnight against B(100). The eIF-4B activity was then assayed for stimulation of poly U dependent eIF-4A ATPase activity as described in **Chapter 4, Interaction of eIF-4B with oligonucleotides.**

G-75 column chromatography

A 25 ml Sephadex G-75 gel-filtration column (1 cm x 35 cm) could be used for further purification if the eIF-4B obtained from P11 column did not meet the desired purity. The column preparation and sample loading and elution procedures were the same as the G-100 column described earlier for eIF-(iso)4F purification.

Chapter 3

Instrumentation

Fluorescence of Amino Acids

The absorption of light by a molecule can excite an electron into a higher energy level, after relaxation, the exited molecule may drop back to the ground level with the emission of certain amount of energy, in the forms of fluorescence or phosphorescence. The excited states can be divided into two major types: singlet and triplet. In a singlet excited state, the excited electron has the opposite spin orientation as the second electron in the lower orbital (paired). In a triplet excited state, the excited electron has the same spin orientation as the second electron in the lower orbital (unpaired). The emission from a singlet state to the ground state is called fluorescence and the emission from a triplet state to the ground state is called phosphorescence. The 2 unpaired electrons in the triplet state (same spin orientation) are extremely unstable, thus phosphorescence is rare and usually not observed for amino acids. Among 20 native amino acids that make up a protein, three are known to be fluorescent. They are: tyrosine, phenylalanine and tryptophan. Figure 3.1 is an example of the energy diagram for tryptophan fluorescence excited at 280 nm. If the emission is after a period of relaxation which loses some energy, the fluorescence will have less energy compared to the excitation light, which means that the emission is at a longer wavelength than the excitation.

Because the tryptophan absorption is around 280 nm, the protein fluorescence study of eIF-4B, eIF-(iso)4F and USF in this thesis generally use the excitation wavelength around 280 nm. Among the three fluorescent amino acids, the excitation maxima of phenylalanine is about 250 nm, sufficiently far away from the absorbance of 280 nm that phenylalanine fluorescence can be separated from tryptophan fluorescence. Although both tyrosine and tryptophan residues are excited at 280 nm,

they have different fluorescence emission spectra. According to Table 3.1, tyrosine has an emission maximum around 300 nm, while tryptophan has an emission maximum about 340 nm depending on the environment. The source of the protein fluorescence can be determined from the protein emission maxima.

Table 3.1. Absorption and emission maxima of fluorescent amino acid residues in protein: phenylalanine, tyrosine and tryptophan (Data from Lakowicz, 1983).

Amino acids	Excitation maxima	Emission maxima
phenylalanine	255 nm	280 nm
tyrosine	280 nm	300 nm
tryptophan	280 nm	340 nm

Figure 3.1. A simple Jablonski diagram of tryptophan fluorescence. Tryptophan absorbs near 280 nm, its fluorescence emission maxima ranges from 320 nm to 350 nm.

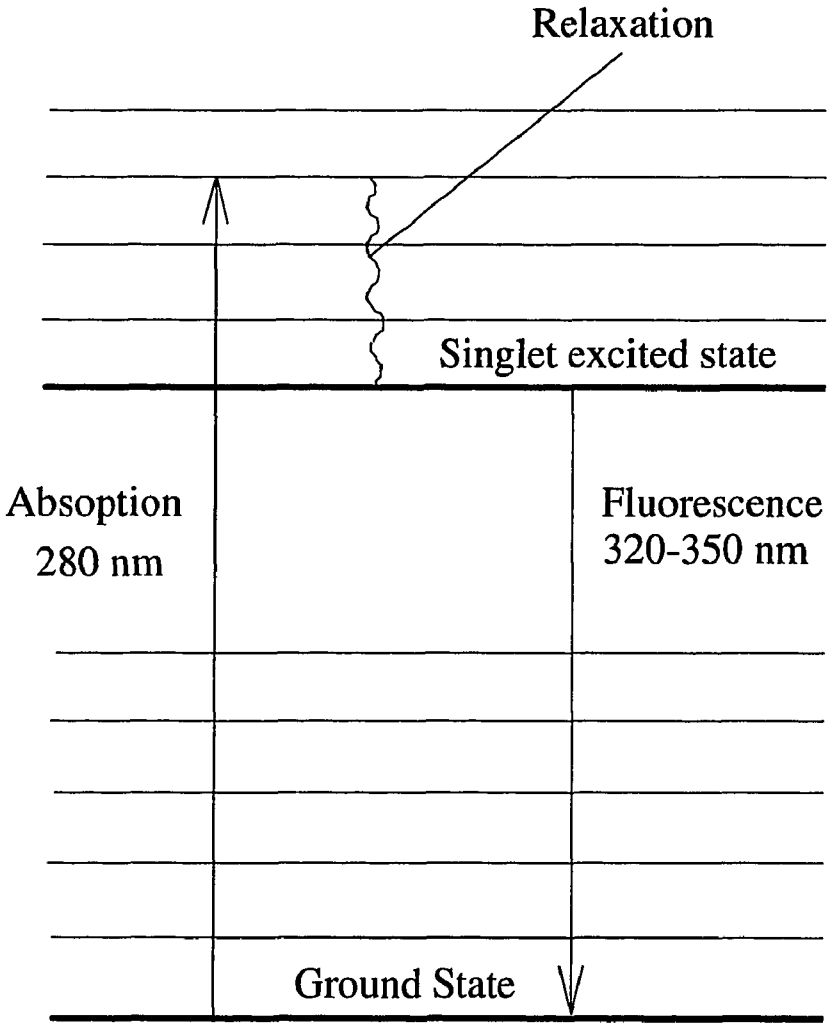

Instrumentation

The fluorescence instrument used in this thesis study was a SPEX Fluorolog-τ 2 system consisting of six major components: lamp, excitation monochromator, modulator compartment, sample compartment and the detector-emission monochromator. The broad range of light generated by the lamp was passed through the monochromator, a single wavelength of light was selected and sent to the sample chamber. The wavelength was close to 280 nm to excite the protein molecule in the cuvette. The fluorescence signal was collected at 90 degrees to the incoming light. The fluorescence intensity as a function of wavelength was collected and processed by a Gateway 2000 computer.

Lamp—A 450W ozone-free xenon arc lamp has been used to provide continuous light output from 250 nm to 700 nm, except for a number of sharp lines near 467 nm. The lamp emitted light as a result of the recombination of electrons with ionized Xe atoms. These ions were generated by collisions of the Xe atoms with the electrons which flow across the arc. The broad continuos light output was from the ground state atoms, while the sharp lines around 467 nm were from excited atoms.

Figure 3.2. Spectral output of the Xenon arc lamp used in this thesis study.

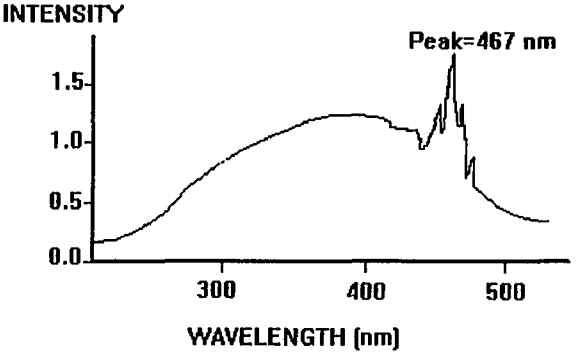

Excitation Monochromator— An excitation monochromator was used to select a single excitation wavelength. A modified Czerny-Turner single-grating monochromator was used to disperse the light from 200 nm to 900 nm. The monochromator was motorized to allow automatic scanning of wavelength. Two slits were used to control the amount of light passing through the sample chamber.

Modulator Compartment—The modulator compartment in the SPEX Fluorolog-τ 2 system contains a beam spliter to provide two beams of light, one for sample (s) and one for reference (r) to allow the measurement of s/r mode. Variation in the intensity of the arc lamp by voltage fluctuations is corrected by the division of the signal of the sample by that of the reference.

Sample Compartment—The sample compartment was a motorized cuvette holder where the protein sample was located. Mode switches allowed manual or automatic control of the sample by the computer. A programmable shutter was also in the sample chamber. The shutter had three modes of operation: Manual, Automatic and Minimum. Manual allowed the operator to control the shutter; automatic allowed opening the shutter during detection and closing the shutter after the scan. Minimum controlled the shutter opening time to be a minimum while engaging the automatic mode, ideal for some protein samples that photobleach.

Emission monochromator—The emission monochromator is connected to a emission signal detector which was a Hamamatsu R928-P photomultiplier mounted in a room temperature housing. Only a narrow range of fluorescence wavelength passed through the emission monochromator at a time to allow the signal detector to record the fluorescence intensity at a certain wavelength. The photomultiplier amplified and transferred the photon signal into an electronic signal which was recorded and stored in the computer. Figure 3.3 shows a schematic diagram of the Fluorolog-τ2 spectrofluorimeter with the six components.

Figure 3.3. Schematic diagram of the Fluorolog-τ2 spectrofluorimeter.

From SPEX Fluorolog-τ2 Operation Manual 4-7.

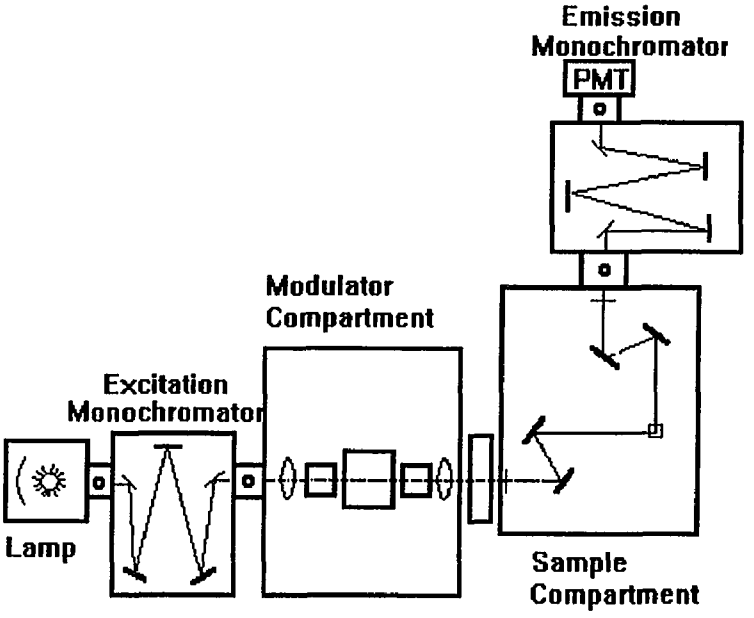

Mechanisms

Michaelis-Menten theory—The general enzymatic reaction can be described

$$E+S \underset{k_{-1}}{\overset{k_1}{\rightleftharpoons}} ES \xrightarrow{k_2} E+P \qquad (1.1)$$

The enzyme reaction is divided into two steps. The enzyme reversibly binds the substrate first to form a complex, ES. Then the ES complex decomposes to form the product by a irreversible process and the free enzyme is released unchanged. The steady-state assumption assumes that as the reaction reaches equilibrium, the rate of ES formation will be the same as the rate of ES decomposition. From Equation 1.1:

$$\frac{d[ES]}{dt} = 0 = k_1[E][S]-k_{-1}[ES]-k_2[ES] \qquad (1.2)$$

$$k_1[E][S] = k_{-1}[ES] + k_2[ES] \qquad (1.3)$$

The free enzyme concentration, [E], and the total enzyme concentration, [E_o] are related by

$$[E]=[E_o]-[ES] \tag{1.4}$$

Substituting equation 1.4 into equation 1.3 gives

$$k_1([Eo]-[ES])[S] = k_{-1}[ES] + k_2[ES] \tag{1.5}$$

$$k_1[Eo][S]-k_1[ES][S] = k_{-1}[ES] + k_2[ES] \tag{1.6}$$

$$k_1[Eo][S] = [ES](k_1[S] + k_{-1} + k_2) \tag{1.7}$$

$$[ES]=\frac{[Eo][S]}{\frac{k_{-1}+k_2}{k_1}+[S]} \tag{1.8}$$

Let $\frac{k_{-1}+k_2}{k_1} = K_m$ (Michaelis constant)

$$[ES]=\frac{[E_o][S]}{K_m+[S]} \tag{1.9}$$

The rate of product formation, v, can be calculated by

$$v = k_2[ES] \tag{1.10}$$

Substituting equation 1.9 gives

$$v = k_2 \frac{[E_o][S]}{K_m + [S]} \tag{1.11}$$

where $k_2[Eo] = V_{max}$

$$v = \frac{V_{max}[S]}{K_m + [S]} \tag{1.12}$$

Equation 1.12 is the Michaelis-Menten Equation that describes most single substrate enzyme reactions. A plot of v against [S] gives a saturation curve where the v levels off when approaching it's maximum reaction rate V_{max} (Figure 3.4).

Figure 3.4. The plot of v against [S] for an enzymatic reaction obeying Michaelis-Menten (or saturation) kinetics.

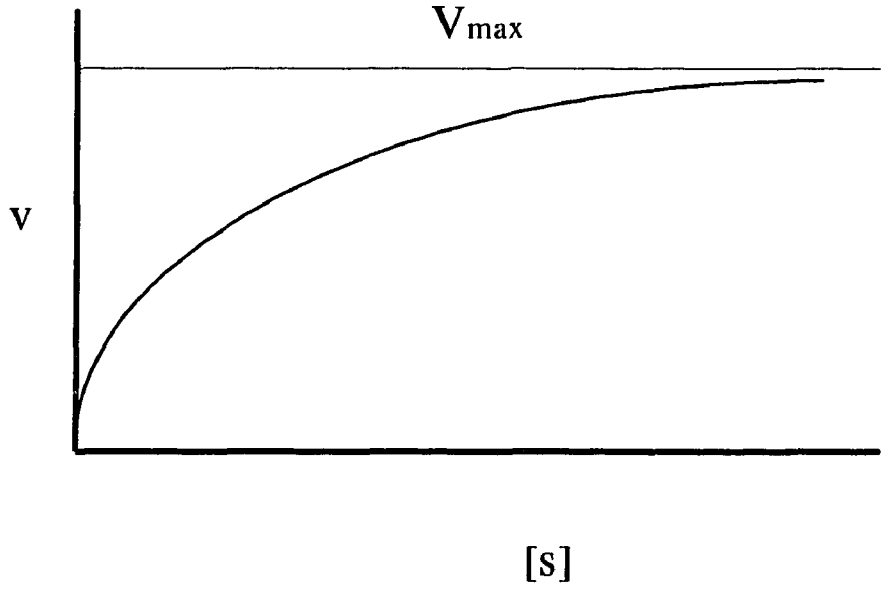

The Michaelis constant, $K_m=\frac{k_{-1}+k_2}{k_1}$, when $k_{-1} >> k_2$, represents the dissociation constant. The K_{eq} described later in this thesis is the association equilibrium constant, which is equivalent to $\frac{1}{K_m}$.

From equation 1.12, $v=\frac{V_{max}[S]}{K_m+[S]}$, when $v=\frac{1}{2}V_{max}$

$$\frac{1}{2}V_{max}=\frac{V_{max}[S]}{K_m+[S]} \qquad (1.13)$$

$$K_m+[S]=2[S] \qquad (1.14)$$

$$K_m=[S] \qquad (1.15)$$

Thus, K_m is also described as the substrate concentration when the reaction reaches half the maximum rate. It can be used to approximate the K_m or K_{eq} from a saturation curve.

A very useful way of plotting the Michaelis-Menten Equation was developed by Eadie-Hofstee (Eadie, 1942).

From equation 1.12

$$v=\frac{V_{max}[S]}{K_m+[S]} \qquad (1.16)$$

$$v(K_m+[S])=V_{max}[S] \qquad (1.17)$$

$$K_m \frac{v}{[S]} + v = V_{max} \qquad (1.18)$$

$$v= - Km \frac{v}{[S]} + V_{max} \quad \text{(Eadie-Hofstee equation)} \qquad (1.19)$$

This plot of v vs v/[S] gives a linear plot, and K_m can be calculated from the slope (Figure 3.5).

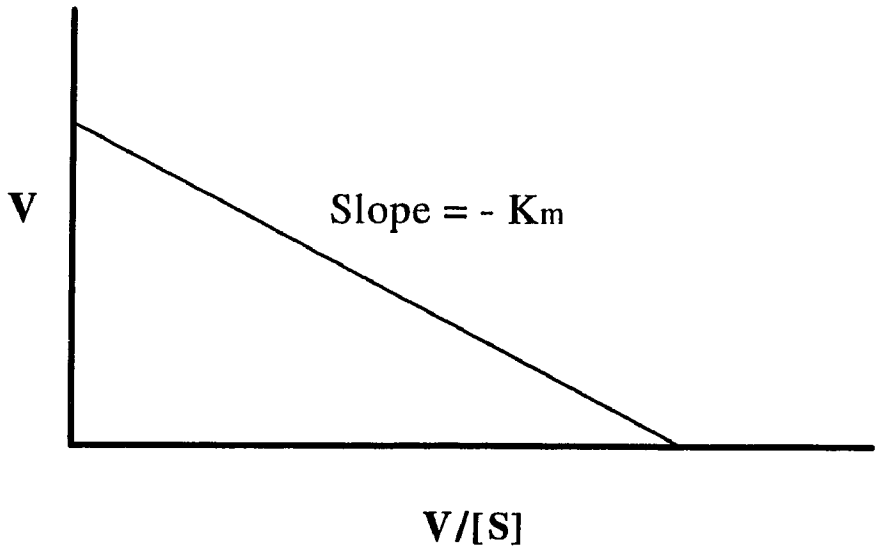

Figure 3.5: Eadie-Hofstee plot for an enzymatic reaction obeying Michaelis-Menten mechanism.

The equation for fluorescence measurements of protein-RNA binding— The Michaelis-Menten equation and the Eadie-Hofstee equation can not be applied to the protein RNA binding interactions. Equation 1.1 does not represent the binding mechanism between protein and RNA. The major difference is that the protein-RNA binding does not produce P, product, instead the complex dissociates into free enzyme and substrate as shown in equation 1.20:

$$E+S \underset{k_{-1}}{\overset{k_1}{\rightleftharpoons}} ES \qquad (1.20)$$

Under the steady-state assumption, the rate of ES formation will be the same as the rate of ES decomposition.

$$\frac{d[ES]}{dt} = 0 = k_1[E][S]-k_{-1}[ES] \qquad (1.21)$$

Substitution of the free enzyme concentration, [E], by [E_o]-ES] as in equation 1.4.

$$k_1([Eo]-ES])[S]=k_{-1}[ES] \qquad (1.22)$$

$$[Eo][S]=(\frac{k_{-1}}{k_1}+[S])[ES] \qquad (1.23)$$

$$[ES]=\frac{[Eo][S]}{\frac{k_{-1}}{k_1}+[S]} \qquad (1.24)$$

Equation 1.24 is the equivalent of the Michaelis-Menten equation for enzymatic reactions described earlier, where $\frac{k_{-1}}{k_1}$ is the equivalent of K_m, the Michaelis constant.

From equation 1.23

$$[Eo][S]-[ES][S]=\frac{k_{-1}}{k_1}[ES] \qquad (1.23)$$

We can also derive the equivalent of an Eadie-Hofstee plot (1.29)

$$[ES][S]=[Eo][S]-\frac{k_{-1}}{k_1}[ES] \qquad (1.25)$$

$$[ES]=[Eo]-\frac{k_{-1}}{k_1}\bullet\frac{[ES]}{[S]} \qquad (1.26)$$

The association constant is defined as $K_{eq}=\frac{k_1}{k_{-1}}$

$$[ES]=[E_o]-\frac{1}{K_{eq}}\bullet\frac{[ES]}{[S]} \qquad (1.27)$$

Keq can be calculated from the slope of a plot of [ES] versus [ES]/[S]. But this equation cannot be used directly in fluorescence measurements since [ES] is not known. However, because [ES] is directly proportional to the change in the fluorescence signal being observed, we have

$$\Delta F=\Delta F_{max}-\frac{1}{K_{eq}}\bullet\frac{\Delta F}{[S]} \qquad (1.28)$$

A plot of ΔF against ΔF/[S] gives a slope of $-\frac{1}{K_{eq}}$, which is the equivalent Eadie-Hofstee plot for treatment of fluorescence quenching data, and is used throughout the thesis.

Chapter 4

Interaction of eIF-4B with nucleotides and mRNA analogs

ATPase Activity Assay

The enzymatic hydrolysis rate of adenosine triphosphate (ATPase activity) by eIF-4B and eIF-4A can be assayed by measuring the inorganic phosphate (Pi) produced as a function of time. Very early studies of colorimetrically measured Pi as a complex of molybdovanadophosphoric acid (Mission et al., 1908) or moylbdophosphoric acid (Fiske et al., 1925) have provided a simple, sensitive, and reliable method for Pi determination. When the ATPase activity was measured, the reactions were stopped after 30-37 °C water bath incubation and the mixture was deproteinized by precipitation before Pi determination. These methods employed perchloric acid (or trichloroacetic acid) to stop the reaction and precipitate the protein. However, perchloric acid caused some non-protein reagents to precipitate; furthermore, the subsequent removal of the precipitate by centrifugation complicated the colorimetric determination, e.g., by reducing the color intensity, and causes errors in the readings. Later, Dulley et al. (1975) modified the method of Fiske et al. and SDS was used to stop the catalysis and cause the protein precipitation. In the eIF-4B ATPase activity study, a further modified method developed by Lin et al. (1977) was used. This colorimetric assay used a one-step procedure that combines the above two methods in which perchloric acid was replaced by nitric acid and 2% SDS solution was incorporated into the mixed reagent without causing protein precipitation. The reagents for phosphorus determination were prepared as follows: (a) ammonium molybdate: 10 g of ammonium molybdate ($(NH_4)_6Mo_7O_{24}\cdot 4H_2O$), and 1 ml of ammonia were dissolved in water to make 100 ml. (b) ammonium metavanadate: 0.235 g of ammonium metavanadate were added to 40 ml of hot water and cooled under tap water as soon as they dissolved; 0.61 ml of concentrated nitric acid diluted

with 1.4 ml of water were added to the above solution and made up to 100 ml with water. (c) 20% SDS solution: 20 g of SDS was dissolved in water to make 100 ml of solution. (d) mixed reagent: The above solutions were mixed together with 37 ml of concentrated nitric acid and made up to 1 liter with water.

The eIF-4B was assayed for stimulation of poly U dependent eIF-4A ATPase activity as reported by Browning et al. (1989). The ATPase activity of eIF-4B, eIF-4A and eIF-4A•eIF-4B complex was tested in a reaction mixture containing 15 mM HEPES-KOH, 80mM KCl, 5 mM $M_g(C_2H_3O_2)_2$, 1mM DTT, pH 7.5, 0.2 O.D. poly U, 0.1 μM eIF-4A, and 0.033 μM eIF-4B for complex activity. Following addition of 2 mM ATP, the reaction mixture was incubated in a 35 °C water bath for 30 min. The reaction was then stopped by placement in ice bath and the addition of the mixed reagent (d). The solution quickly turned yellow and the absorption was measured at 350 nm. The O.D. was recorded and used to find the corresponding P_i concentration (hydrolyzed by the ATPase) from the calibration curve (Figure 4.1). The activity of this ATPase was defined as molar Pi generated per milligram of enzyme per minute. The calibration curve was made by adding mixed reagent (d) into potassium phosphate (P_i) solution at various concentrations. The absorption (O.D.) at 350 nm was then measured and plotted against P_i concentration (Figure 4.1).

The results showed that wheat germ eIF-4B alone did not have poly U dependent ATPase activity, but it stimulated the poly U dependent ATPase activity of eIF-4A by 2 fold (eIF-4A: $(2.4\pm0.2)\times10^{-7}$ mol Pi/mg·min; eIF-4A•eIF-4B: $(4.1\pm0.3)\times10^{-7}$ mol Pi/mg·min). Similar results were reported for mammalian eIF-4B (Browning et al. 1989).

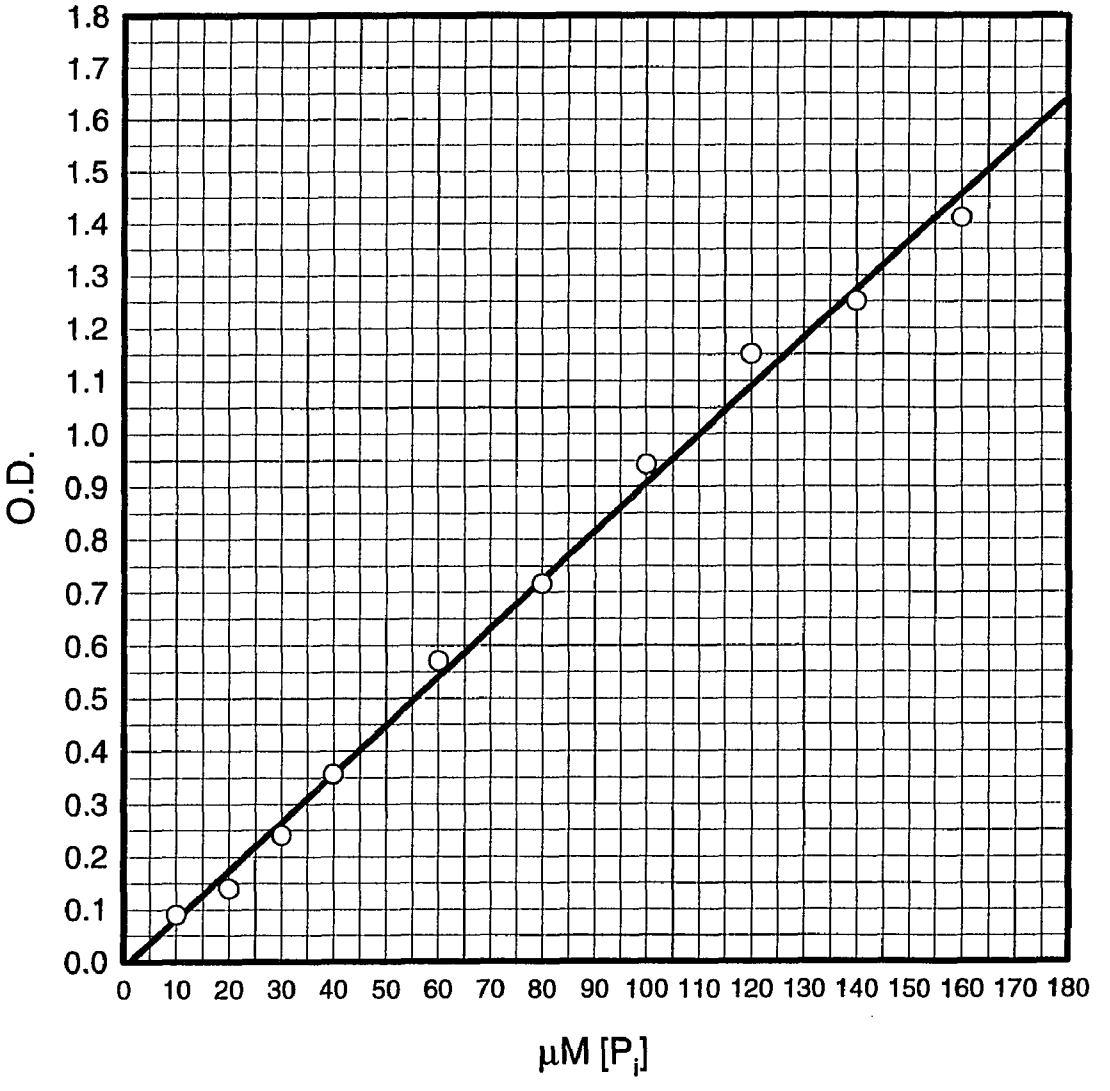

Figure 4.1. Calibration Curve for ATPase Assay. The absorbance of the mixture of potassium phosphate with the mixed reagent (d) plotted vs. the concentration of p_i.

Oligonucleotide Preparation and Fluorescence Measurements

The oligoribonucleotides studied in this chapter were chosen to contain structural features of the 5'-terminus of mRNA, the RNA concentration used in these calculation was mole of RNA single strand. They were prepared by cell-free transcription in a T7 RNA polymerase system according to the method of Milligan et al. (1987) and purified by the method of Draper et al. (1988). The details of this protocol have been described elsewhere (Carberry et al., 1992). All chemicals used were reagent grade or better.

Buffer A, the solution for the fluorescence studies was prepared in 20 mM HEPES-KOH, 1 mM DTT, 1 mM $MgCl_2$, 100 mM KCl, adjusted to pH 7.6. For the pH dependence studies of binding, the buffer was adjusted to the desired values. Fluorescence measurements were carried out at 23 ± 0.2 °C, and data were collected and analyzed according to the protocol of Carberry et al., (1989, 1990). The wheat germ protein synthesis initiation factor eIF-4B was purified according to the procedure described in detail in **Chapter 2, protein purification**.

Results

Fluorescence of eIF-4B•oligoribonucleotide Complexes — The fluorescence maximum of eIF-4B was approximately 336 nm. Figure 4.2 showed the fluorescence emission spectra of eIF-4B•oligoribonucleotide complexes as a function of oligoribonucleotide concentration. There was a decrease in the protein fluorescence intensity at all wavelengths upon eIF-4B•oligoribonucleotide complex formation. Since the position of the emission maximum of eIF-4B (336 nm) was similar to that of a free tryptophan residue (348 nm), tryptophan residues were most likely involved in this interaction. The relative fluorescence intensity changes at 336 nm in free and complexed eIF-4B emission spectra were used to calculate the Keq between eIF-4B the oligoribonucleotides by construction of an Eadie-Hofstee plot (Eadie, 1942, inset of Figure 4.2). Bujalowski and Lohman had suggested earlier about some more complex methods for fitting of similar data (Bujalowski and Lohman, 1986; Bujalowski et al. 1988). However, their data analyses were unnecessary to obtain binding equilibria since the fluorescence decrease was linear in an Eadie-Hofstee plot. A simple equilibrium model was adequate for data fitting. The oligonucleotide models of the 5'terminus of mRNA and their equilibrium binding constants (Keq) with eIF-4B were shown in Figure 4.3. Oligonucleotides V and VII, VI and VIII were designed with the following differences: Oligonucleotide VII and VIII had the m^7GTP cap structure at their 5' end; oligonucleotide V and VI shared the same sequence with VII and VIII respectively with the exception of cap. eIF-4B was shown not to preferentially bind to the cap structure, because the capped (VII, VIII) and uncapped (V, VI) oligonucleotides bound to eIF-4B with similar affinity.

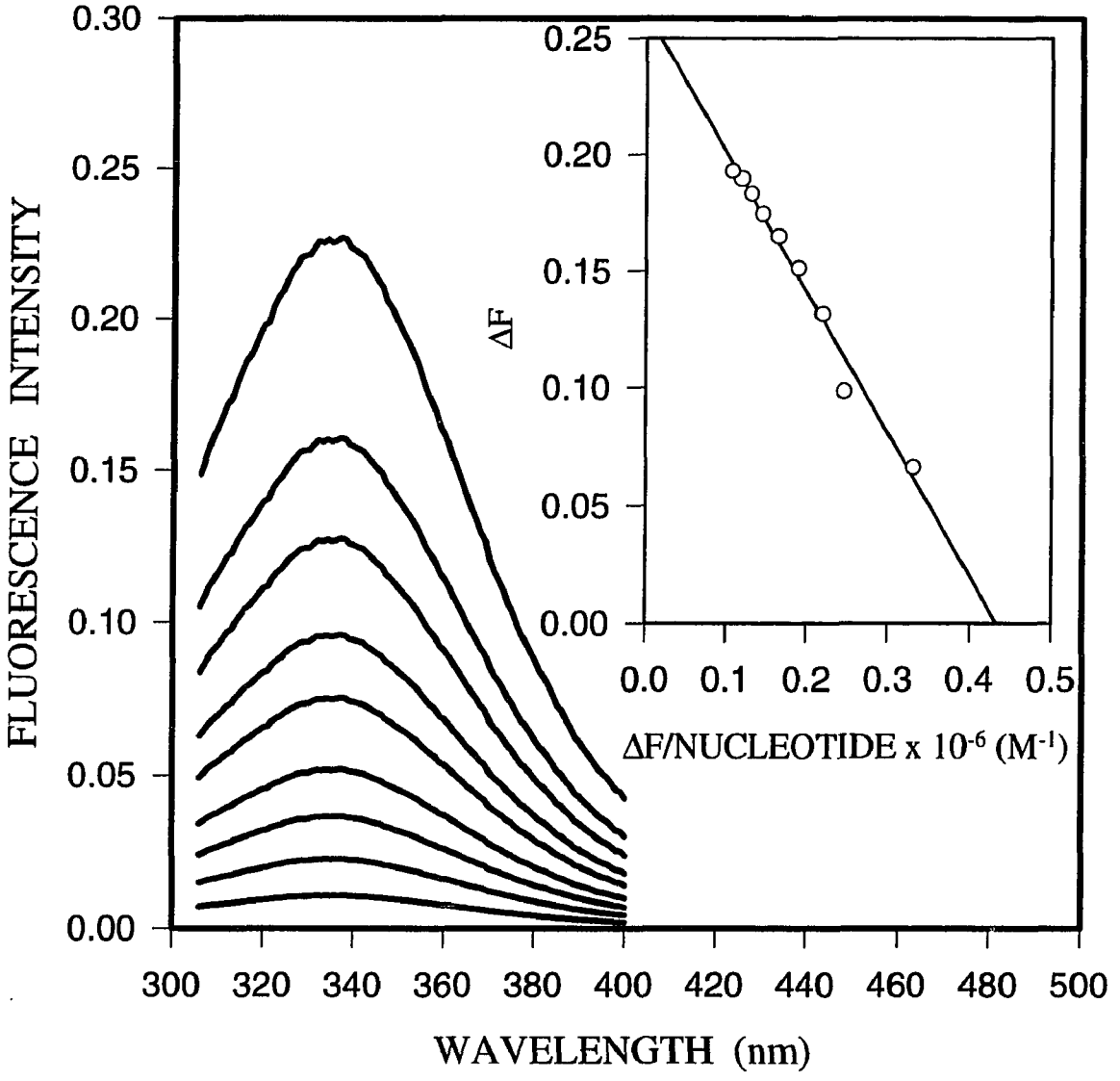

Figure 4.2. Fluorescence emission spectra of eIF-4B (2μM) titrated with oligonucleotide V in buffer A, pH 7.6, at 23 °C. The oligonucleotide concentration (*top to bottom*) was 0, 0.2, 0.4, 0.6, 0.8, 1.2, 1.6, 3.2 and 5.6 μM. The excitation wavelength 275 nm, and a 1.4 mm slit was employed. Emission maxima were observed at 336 nm. *inset*: Eadie-Hofstee plot of fluorescence data. ΔF was calculated at 336 nm where $\Delta F=F_{eIF\text{-}4B}-F_{eIF\text{-}4B+oligonucleotide}$

Model	Structure	Keq x 10^{-6} (M^{-1})
I	5'-GGCGCUCUACC	1.84±0.07
II	5'-GGCGCUCUACCAUG	1.62±0.05
III	5'-GGCGCUCUACCAUGGUAU	2.87±0.03
IV	5'-GGCGCUCUACCAUGGUAUUAUA	2.68±0.05
V	U-G G A A A C-G C-G U-A G-C G-C 5'-GGCGCUCGAUACCU ACCAUAGCGGUAUA	2.41±0.01
VI	U-G G A A A C-G C-G U-A G-C G-C 5'-GGCGCUCGAUACCU ACCAUAAUGGUAUA	2.32±0.05
VII	U-G G A A A C-G C-G U-A G-C G-C 5-m^7G_{ppp} GGCGCUCGAUACCU ACCAUAGCGGUAUA	2.32±0.01
VIII	U-G G A A A C-G C-G U-A G-C G-C 5-m^7G_{ppp} GGCGCUCGAUACCU ACCAUAAUGGUAUA	2.46±0.09

Figure 4.3. Structures of the oligonucleotides used for studies reported in this chapter and their association equilibrium constants (K_{eq}) with eIF-4B.

The binding of eIF-4B to oligonucleotides was not enhanced by the initiation codon AUG. The oligonucleotides with AUG (VI, VIII) and the oligonucleotides without AUG (V, VII) bound to eIF-4B with similar affinity. The binding of eIF-4B to oligonucleotides was also not enhanced by the hairpin structures or linear mRNA (linear mRNA III, IV and oligonucleotides with a hairpin structure V, VI, VII, VIII, had similar Keqs). The binding of eIF-4B to oligonucleotides was found to require a minimum number of 18 bases for optimum binding (Keq with oligonucleotide II, 14 bases, 1.62×10^6 M; Keq with oligonucleotide III, 18 bases, 2.87×10^6 M). A longer oligonucleotide did not increase the binding affinity (Keq with oligonucleotide IV, 22 bases, $2.68 \pm 0.05\, 10^6$ M).

pH Dependence — The binding of protein to mRNA was sensitive to pH, because various interactions existed between the protein factors and mRNA. Figure 4.4 showed a pH dependence curve of oligoribonucleotide V binding to wheat germ eIF-4B. A sigmoidal-shaped curve with a dramatic change around pH 7 showed increased binding at higher pH. This change in binding with pH probably reflected titration of an amino acid residue with a pKa near pH 7.

Temperature Effects — A Van't Hoff plot of $-\ln(K_{eq})$ vs the reciprocal of temperature (T^{-1}) was used to calculate the thermodynamic parameters of entropy (ΔS) and enthalpy (ΔH). Figure 4.5 showed the Van't Hoff plot based on oligoribonucleotide V binding to eIF-4B, the values of ΔH and ΔS were obtained from the intercept and slope, respectively.

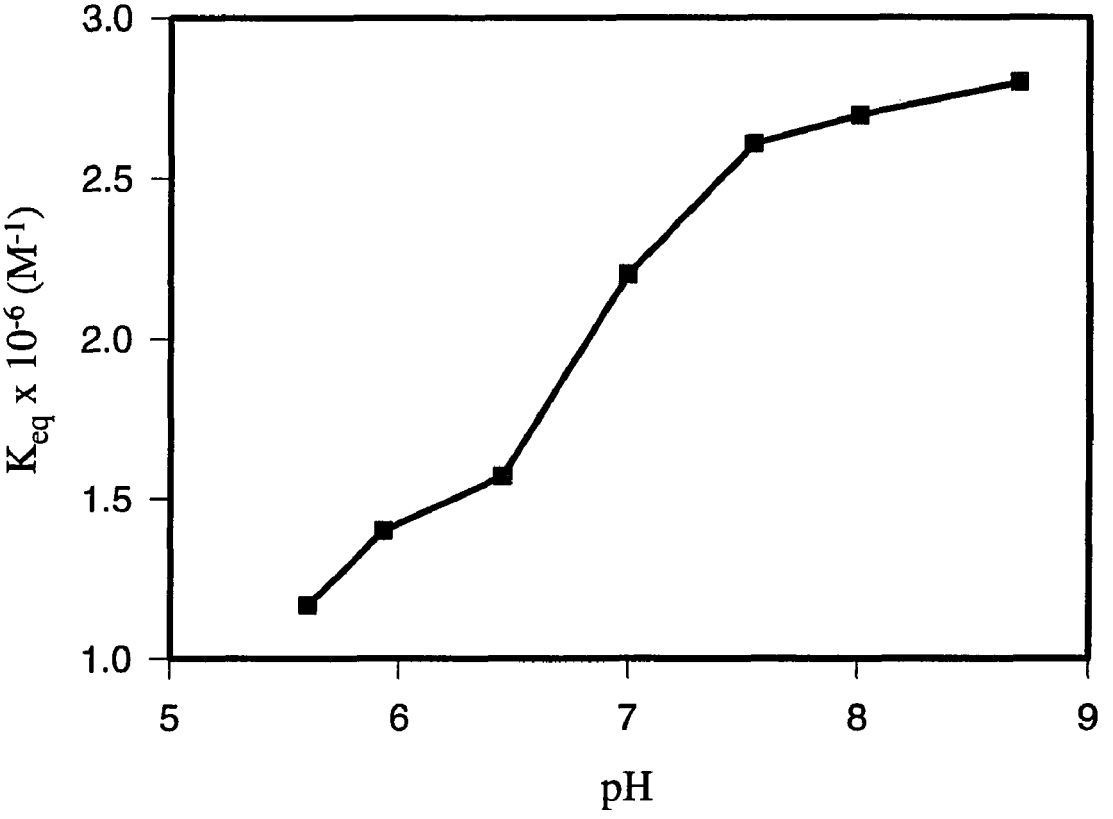

Figure 4.4. Binding of oligonucleotide V and eIF-4B as a function of pH. All solutions were prepared in buffer A, adjusted to the appropriate pH at 23 °C. Other conditions were the same as in Figure 4.2.

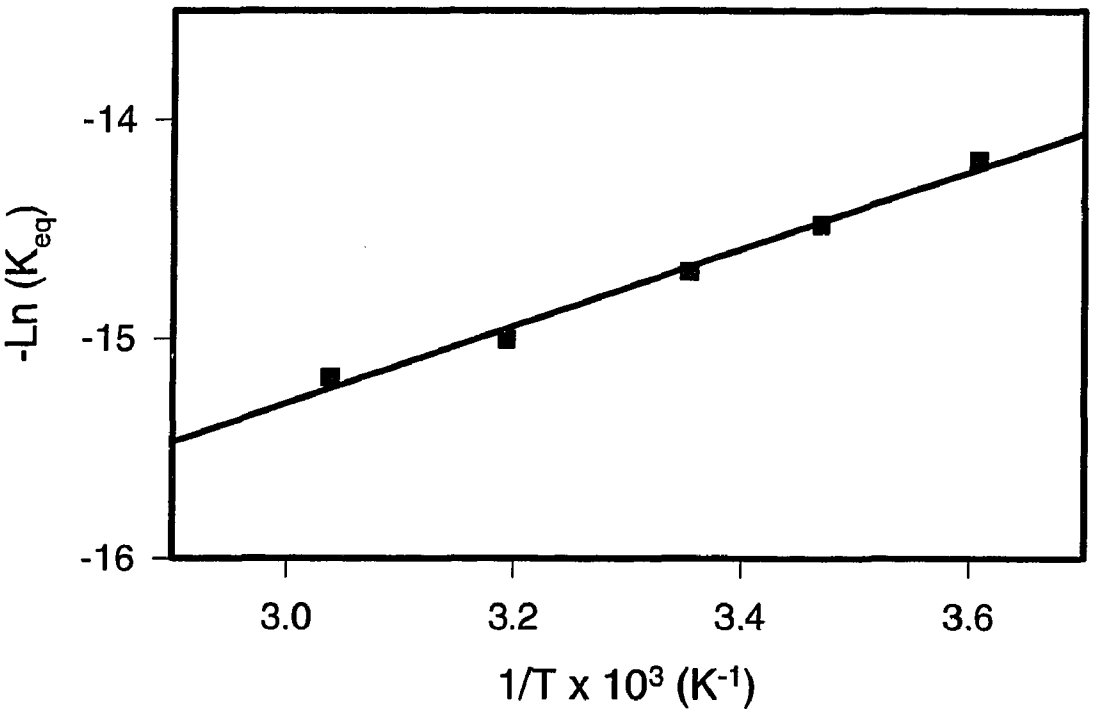

Figure 4.5. van't Hoff plot for oligonucleotide V - eIF-4B interactions.
All experimental conditions were as in Figure 4.2.

The thermodynamic values of ΔH and ΔS were obtained as 3.5 ± 0.2 kcal/mol and 40.9 ± 0.1 cal/(mol °C), respectively. These parameters were similar to the m^7GTP• eIF-4E interaction (ΔH, 6.25 ± 0.25 kcal/mol; ΔS, 46.1 ± 1.8 cal/(mol °C), Carberry et al., 1989). Similar values were also obtained for the m^7GTP•eIF-4F interaction, where ΔH was found to be 6.84 ± 0.7 kcal/mol and ΔS was 47.4 ± 5.0 cal/(mol °C) (Carberry et al., 1991). An interpretation has been given (Ross et al., 1981) that positive ΔH and ΔS values suggest either hydrophobic (Gill et al., 1967, 1976) or ionic (Pimentel & McClellan, 1971) interactions. The ionic strength dependence of oligoribonucleotide binding with eIF-4B was investigated in order to determine if the interaction was hydrophobic or ionic.

Ionic Strength Dependence — Figure 4.6 (A) showed the binding of oligoribonucleotide IV to wheat germ eIF-4B as a function of KCl and $KC_2H_3O_2$ concentration. Figure 4.6 (B) showed the treatment of the same data according to the Debye-Huckel theory. A straight line passing through the origin with a slope of $1.02Z_AZ_B$ was obtained from the Debye-Huckel plot of log (K/K_o) versus the square root of the ionic strength. In the Debye-Huckel plot, K and K_o were the equilibrium constants in the presence of KCl and $KC_2H_3O_2$ respectively, and Z_A and Z_B were the respective charges of the reactants. A Z_AZ_B of -1 was obtained for the interaction of a single positive and negative charge. A Z_AZ_B value of -0.165 was obtained for the interaction of oligonucleotide IV with eIF-4B in KCl.

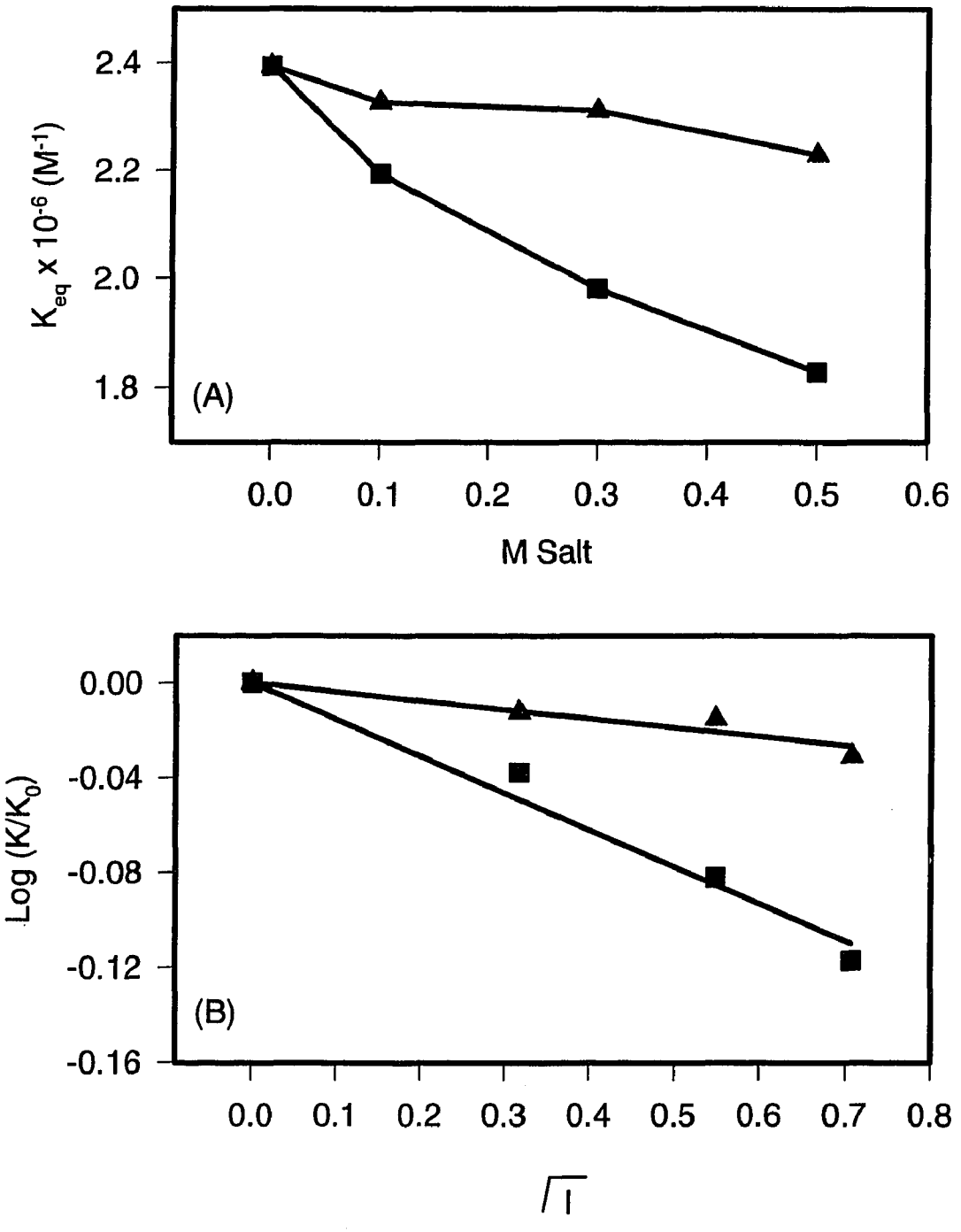

Figure 4.6. (A), Keq values of oligonucleotide IV and eIF-4B as a function of KCl (■)and KAc (▲) concentrations. All solutions were prepared in buffer A, pH 7.6. Experimental conditions were as in Figure 4.2. **(B), Debye-Huckel analysis of the data in (A).**

A Z_AZ_B value of -0.039 was obtained for the interaction of oligonucleotide IV with eIF-4B in $KC_2H_3O_2$. This result demonstrated that the binding of oligonucleotide IV to eIF-4B had little dependence on ionic strength, there were no significant ionic interactions involved in the binding of oligonucleotide IV to eIF-4B. The value of Z_AZ_B was -0.165 when KCl was used to vary ionic strength. This difference between KCl and $KC_2H_3O_2$ suggested a possible uptake of Cl^- by the protein. Bujalowski et al., (1988) had reported similar special effects of anions on protein-DNA binding.

Surface Accessibility of Tryptophan Residues in eIF-4B — Iodide (Lehrer, 1971) and oxygen (Lakowiczet et al., 1973) were shown as quenchers for tryptophan residues in proteins. But the quenching of tryptophan fluorescence by iodide was sometimes less than the amount of quenching by an equivalent concentration of oxygen. It was reported that this difference was caused by the inability of iodide to penetrate into the interior of the proteins (Lakowicz, 1983). This suggested that iodide quenching could be used to determine the fraction of the total fluorescence emitted by the surface tryptophan residues. Figure 4.7(A) showed the iodide quenching of eIF-4B plotted by the Stern-Volmer method (Lakowicz, 1983). The iodide quenching of tryptophan fluorescence was generally characterized by downward curving Stern-Volmer plots. At higher iodide concentrations essentially all surface residues were quenched. The remaining fluorescence was from the buried tryptophan residues. Figure 4.7(A) suggested that there were buried tryptophan residues, which gave the slightly downward curving Stern-Volmer plot for the eIF-4B, titration.

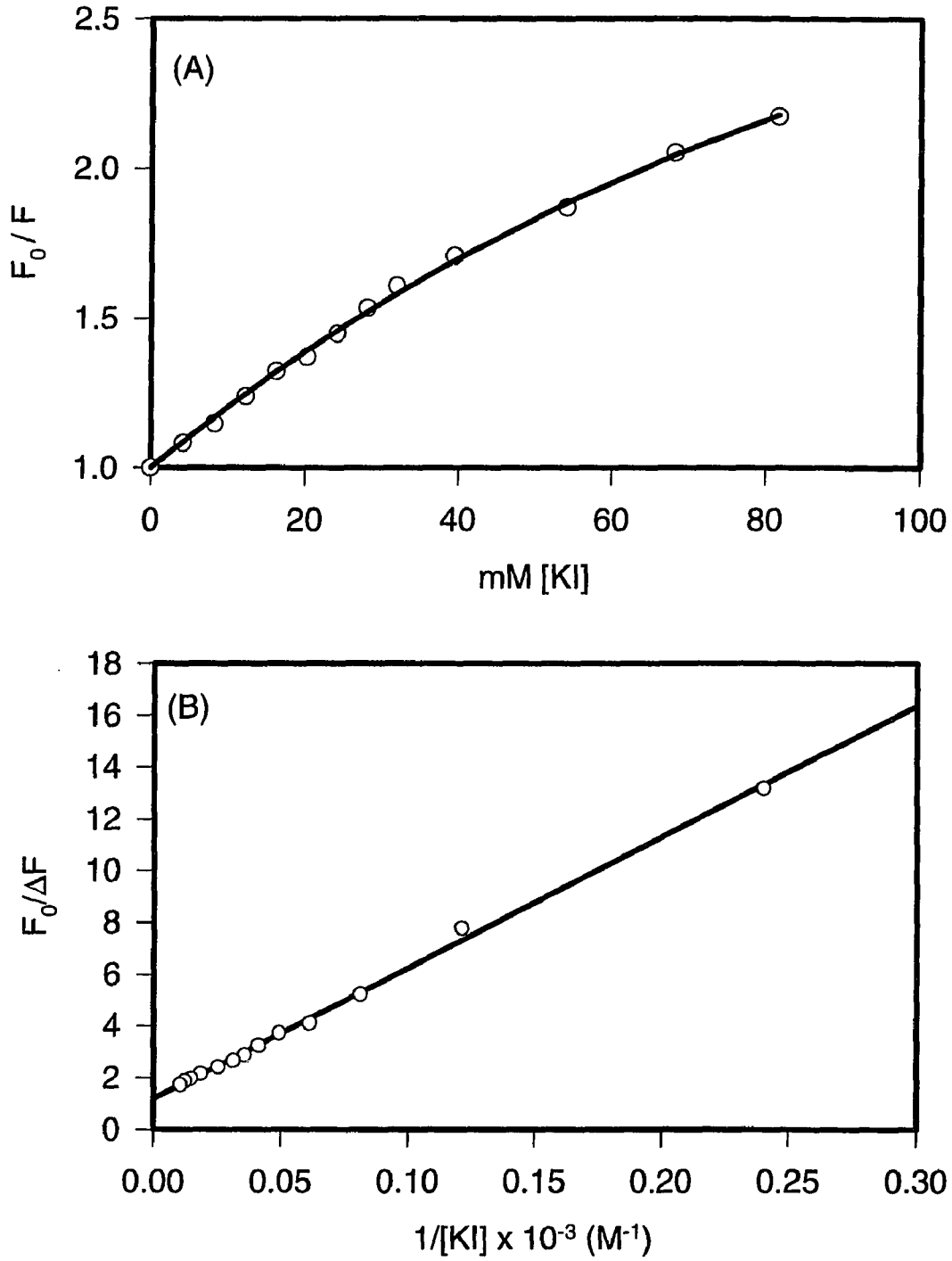

Figure 4.7. (A), Stern Volmer plot of iodide quenching to eIF-4B. (B), Modified Stern Volmer plot from (A). All experimental conditions were as in Figure 4.2.

Figure 4.7(B), the plot of $F_o/\Delta F$ versus the reciprocal of the iodide concentration, was a modified Stern-Volmer plot which explained the results from Figure 4.7(A) more clearly. The reciprocal of the Y intercept represented the fraction of accessible tryptophan residues among all observed tryptophan in the protein (Lakowicz, 1983). A Y intercept value of 1.13±0.15 acquired from Figure 4.7(B), indicated that 88.5% observed tryptophan residues were on the surface of eIF-4B. Assuming that all of the total 9 tryptophan residues in eIF-4B contributed to the observed fluorescence, likely 8(±1) of them were exposed.

ATP Effects on eIF-4B:oligonucleotide interaction — Figure 4.8 showed the binding of oligoribonucleotide VII to wheat germ eIF-4B as a function to ATP concentration. Figure 4.8(A), the Eadie-Hofstee plots, showed competitive inhibition by ATP of oligoribonucleotide to eIF-4B. This explained why the calculated equilibrium association constants from these plots, Keq, decreased with increasing concentration (0 μM ATP, Keq = 2.32 ± 0.01 x 10^6 M; 10 μM ATP, Keq = 1.44 ± 0.05 x 10^6 M; 15 μM ATP, Keq = 4.1 ± 0.2 x 10^5 M). Figure 4.8(B) showed that three Lineweaver-Burke plots met at the same Y intercept which demonstrated the competitive binding between ATP and the oligoribonucleotide for eIF-4B. The replot of the slope in Figure 4.8(B) against [I] allowed the calculation of K_I (for ATP competitive inhibition). The K_I was obtained as 1.72 x 10^{-6} M.

eIF-4B, eIF-4A, ATP and oligoribonucleotide interactions — Table 4.1 showed the results of the interaction of eIF-4B and eIF-4A, at the presence and absence of the oligoribonucleotide, in 0 and 20 μM ATP.

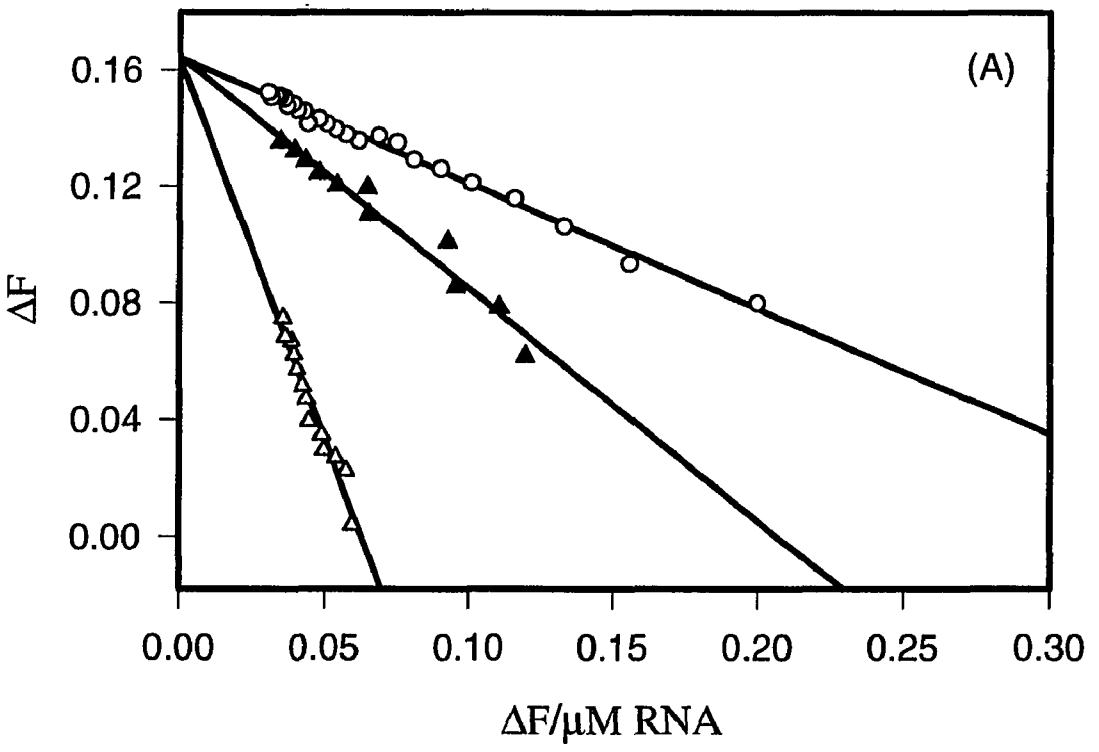

Figure 4.8. (A), Eadie-Hofstee plots of the binding of oligoribonucleotide VII for eIF-4B under 0 μM ATP (○), 10 μM ATP (▲), and 15 μM ATP (△).

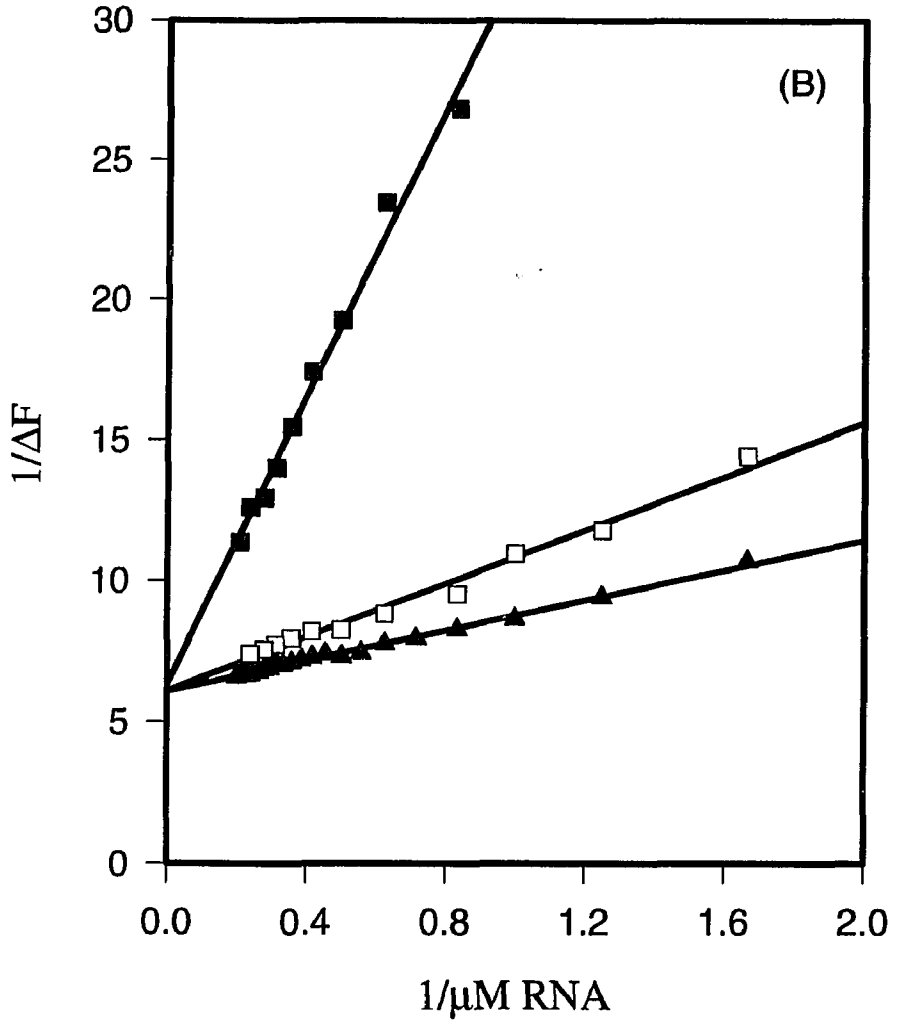

Figure 4.8. (B), Lineweaver-Burk plots of the eIF-4B oligoribonucleotide binding as a function of ATP (0 mM ATP (▲), 10 mM ATP (□), and 15 mM ATP (■)).

eIF-4A is a protein synthesis initiation factor which had been found to have helicase activity and ATPase activity. The Keq between eIF-4A and eIF-4B was measured by titrating eIF-4A into eIF-4B with or without pre added ATP (The subscript A attached to some binding constants K denoted the presence of ATP). Balasta et al. (1993) had previously observed that eIF-4A had little intrinsic fluorescence. The eIF-4A•eIF-4B complex formation was then measured by titrating the eIF-4A into eIF-4B solution, which caused approximately 20% decrease in eIF-4B fluorescence. Titrating oligonucleotide VII into eIF-4A•eIF-4B complex resulted in a further fluorescence decrease which agreed with the previous evidance of the existence of a tertiary complex eIF-4A•eIF-4B•mRNA. The Keqs (K_3, K_{3A}) were obtained from these data by varying the amount of eIF-4A•eIF-4B complex and by using the known equilibrium constant for 4B:oligonucleotide and 4A:4B interactions. Figure 4.9 showed the relationship between K_1, K_2, K_3, and K_4. K_4 and K_{4A} were obtained from the following relationships:

$$K_4 = (K_1K_3)/K_2$$

$$K_{4A} = (K_{1A}K_{3A})/K_{2A}$$

The ΔG values for above interactions were calculated from the Keq values from the equation $\Delta G = -RT \ln Keq$ and are given in Table 4.1.

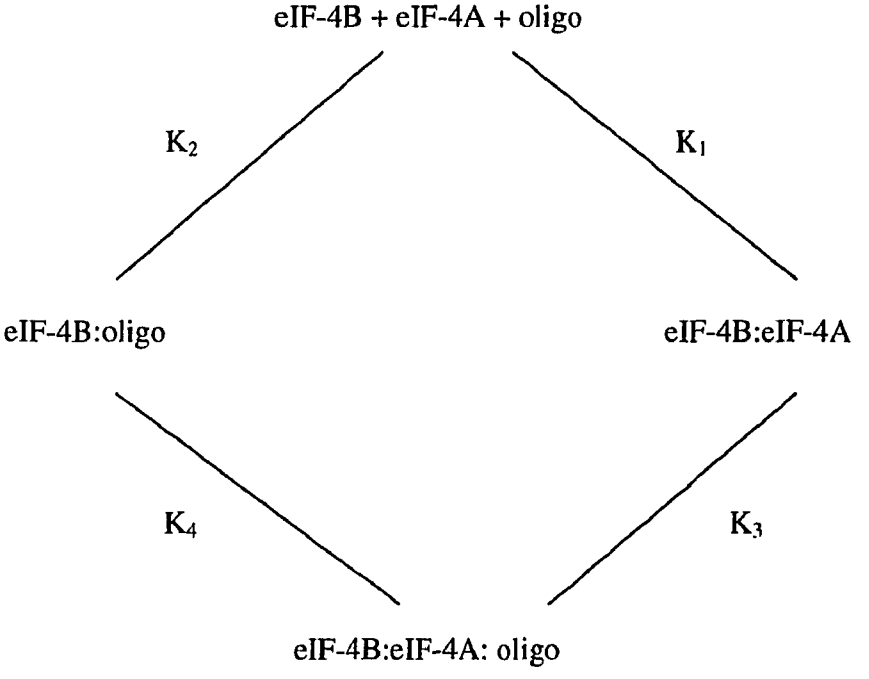

Figure 4.9. Schematic representation of the interaction of eIF-4B, eIF-4A and oligonucleotide VII without ATP. Same representation applies to the interaction with ATP except where K_1, K_2, K_3, K_4 will be K_{1A}, K_{2A}, $K_{3,A}$, K_{4A} respectively.

From the data in Table 4.1: In the absence of ATP, the binding of eIF-4A to eIF-4B reduced the affinity of oligonucleotide to eIF-4B. However, in the presence of ATP, the binding of eIF-4A enhanced the binding of the oligonucleotide to eIF-4B. This suggested that ATP induced a conformational change in eIF-4A or eIF-4B (or both) that resulted a more stable protein-oligonucleotide complex.

Discussion

Some insights into the mechanism of interaction of eIF-4B with mRNA oligoribonucleotides were obtained from the data presented in this direct binding study. eIF-4B was found to have no preference for any particular mRNA structures, such as cap, AUG, or hairpin; However, the binding affinity of eIF-4B to oligonucleotides (capped oligonucleotide IV 2.68 x 10^6 M; oligonucleotide VIII 2.46 x 10^6 M) was about ten fold stronger than that of the eIF-4F (capped oligonucleotide IV 0.25 x 10^6 M; oligonucleotide VIII 0.32 x 10^6 M) and eIF-(iso)4F (capped oligonucleotide IV 0.43 x 10^6 M; oligonucleotide VIII 0.45 x 10^6 M) (Carberry et al. 1991).

The dramatic increase of Keq from pH 6 to pH 8 indicated that an amino acid with a pK between 6.5 and 7.5 is in or near the eIF-4B binding site. When the pH increased higher than 7.5, this amino acid became deprotonated and enhanced binding by interacting with other amino acids in the oligonucleotide binding site or the oligonucleotide. A common RNA recognition motif was found in the mammalian eIF-4B through sequence analysis (Milburn, S. C. et al., 1990). Wheat germ eIF-4B was recently sequenced by Browning et al. (personal communications). Unlike the mammalian eIF-4B, the sequence analysis of wheat germ eIF-4B did not reveal a common RNA binding motif. This eIF-4B sequence was incomplete and lacked the

N-terminal sequence where the RNA binding motif was found in mammalian eIF-4B. The sequence of wheat germ eIF-4B also revealed that the protein had no net charges (seven basic and seven acidic amino acids) which agreed with the salt dependence study presented here and which excluded the possibility of strong ionic interactions.

The results from this study showed that eIF-4B bound more tightly than either of the wheat germ cap binding proteins (eIF-4F and eIF-(iso)4F). eIF-4B did not appear to interact preferentially with any particular region or sequence of the mRNA, but eIF-4B did bind mRNA 10 times stronger than either eIF-4F or eIF-(iso)4F. One possible mechanism of action was that one of the cap binding proteins interacted with the m^7G cap, eIF-4B then interacted with the protein:RNA complex and allowed release of the cap moiety while maintaining contact with the RNA. Further conformational changes might then allowed the complex to process down the RNA with corresponding helicase activity.

From Table 4.1, the equilibrium binding constants for the eIF-4A:eIF-4B interaction without oligonucleotides showed little ATP effect. But for the eIF-4B:eIF-4A interaction in the presence of oligonucleotides, more obvious ATP effects were observed. The effects of ATP on protein-protein interactions in the case of eIF-4F and eIF-(iso)4F with eIF-4A were previously examined (Balasta et al. 1993). Those experiments showed that the effects of ATP were mainly on the protein-protein interactions. As Table 4.1 showed, in this case, ATP had little effect on the protein-

protein or protein-RNA interactions except to act as a competitive inhibitor. While this study had not used physiological ATP concentrations since the inner filter effect (Lakowicz, 1983) would be too large, there appeared to be little reason to suggest more significant effects at higher ATP concentrations. ATP bound to the proteins as evidenced by the competitive inhibition of oligonucleotide binding ($K_I = 1.7 \times 10^{-6}M$) at the concentrations employed.

Table 4.1. Equilibrium binding constants for the binary and ternary eIF-4B, eIF-4A and oligoribonucleotide interactions at 0 & 20μM ATP. For K_{eq}, subscript A denotes K_{eq} in the presence of ATP.

Interactions	ATP concentration	K_{eq} x 10^{-5} M^{-1}	ΔG^o (Kcal/mol)
eIF-4B + eIF-4A	0 μM	K_1 = 4.00±0.44	ΔG^o = −7.638
	20 μM	K_{1A} = 4.53±0.47	ΔG^o = −7.712
eIF-4B + oligo	0 μM	K_2 = 23.2±0.01	ΔG^o = −8.679
	15 μM	K_{2A} = 4.10±0.20	ΔG^o = −7.653
eIF-4B:eIF-4A	0 μM	K_3 = 9.13±0.11	ΔG^o = −8.127
+ oligo	20 μM	K_{3A} = 7.04±0.14	ΔG^o = −7.973
eIF-4B:oligo	0 μM	K_4 = 1.57	ΔG^o = −7.084
+ eIF-4A	20 μM	K_{4A} = 7.78	ΔG^o = −8.032

Chapter 5

Interaction of eIF-(iso)4F and its Subunits P28 and P86 With m^7GTP and mRNA Analogues

Materials and methods

Buffer A, used for fluorescence measurements, consisted of 20 mM HEPES-KOH, 1mM DTT and 1mM $MgCl_2$ and was adjusted to the appropriate pH. mRNA analogues (capped and uncapped oligonucleotides) were transcribed from partially double stranded deoxyoligonucleotide templates containing a T7 RNA polymerase primer according to the procedures of Milligan et al. (1987) and were purified according to the method of Draper et al. (1988), the RNA concentration used in these calculation was mole of RNA single strand; the oligonucleotides used for the binding study and helicase assay were shown in Figure 5.1. Fluorescence measurements were carried out at 23 ^{o}C, unless otherwise noted, and data were collected and analyzed as described in reference (Carberry et al., 1989, 1990). The wheat germ protein synthesis initiation factor eIF-(iso)4F was purified according the procedure described in **chapter 2, Protein Purification.** The pure p28 and p86 subunits were supplied by Heerden et al. from a procedure described elsewhere (Heerden et al., 1994).

The double stranded RNA (Tm=65 ^{o}C) for the helicase assay of eIF-(iso)4F was prepared by annealing the partially complementary III and IV (Figure 5.1) single stranded RNA. Equal molar amounts of RNA III and IV were mixed and heated to 80 ^{o}C for 10 min., slowly cooled to 50 ^{o}C for 30 min., and was then cooled to 40 ^{o}C and kept overnight. The double stranded RNA was shown as the following:

3'-GCGACGCGACGGGG-5'
5'-m^7G_{ppp}GACCAUGGAACAACAUUAUCGCUGCGCUGCCCC-3'

The unwinding reaction for the helicase assay was done by incubating partially double stranded RNA with eucaryotic initiation factors (5uM eIF-4A, 2uM p28, p86 and eIF-(iso)4F where used) in 20 mM Tris-HCl buffer (pH 7.5) containing 2mM ATP, 1mM magnesium acetate. The reaction mixture was incubated at 37 ^{o}C for 20 min. and then transferred to an ice bath and 2ml 5x stopping solution containing 50% glycerol and 10% SDS was added. SDS was used to separate the protein from the RNA and to avoid the formation of a large molecular mass complex. The sample was loaded onto a 15 percent non-denaturing polyacrylamide gel. The double and single stranded RNA on the gel was silver stained (Bassam B. J. et. al., 1991), and the bands were quantitatively determined by a laser scanning densitometer.

I

U–G
G A
A A
C–G
C–G
U–A
G–C
G–C
5-GGCGCUCGAUACCU ACCAUAAUGGUAUA

II

U–G
G A
A A
C–G
C–G
U–A
G–C
G–C
5-m^7G_{PPP} GGCGCUCGAUACCU ACCAUAAUGGUAUA

III 5'-GGGGCAGCGCAGCG

IV

5'-m^7G_{PPP}GACCAUGGAACAACAUUAUCGCUGCGCUGCCCC

Figure 5.1. Structures of the capped (II, IV) and uncapped (I, III) oligonucleotides used in this chapter.

Results

Fluorescence of p28•oligonucleotide Complex—The fluorescence emission spectra of the p28 subunit of eIF-(iso)4F•oligonucleotide complex as a function of oligonucleotide concentration was shown in Figure 5.2. The fluorescence emission spectra of p28•m^7GTP complex was similar (data not shown). Upon complex formation, there was a decrease in the protein fluorescence intensity at 331 nm. Such protein fluorescence quenching was attributed to the π-π stacking interactions between an aromatic amino acid residue and the nucleic acid base (Ishida et al., 1983; Brun et al., 1975; Lawaczek & Wagner, 1974).

The K_{eq} of p28•oligonucleotide and p28•m^7GTP complex formation was calculated from the relative fluorescence intensity changes in free and complexed p28 emission spectra by construction of an Eadie-Hofstee plot, as shown in the inset of Figure 5.2. K_{eq} was found to be $(1.24\pm0.04)\times10^6\ M^{-1}$ for oligonucleotide II.

pH dependence—The pH dependence of m^7GTP binding to the p28 subunit of eIF-(iso)4F was shown in Figure 5.3. The pH optimum for m^7GTP was found to be 7.05 for p28; compared with the pH optimum of 7.6 for eIF-(iso)4F•$m^7G_{ppp}G$ complex (Carberry et al., 1991).

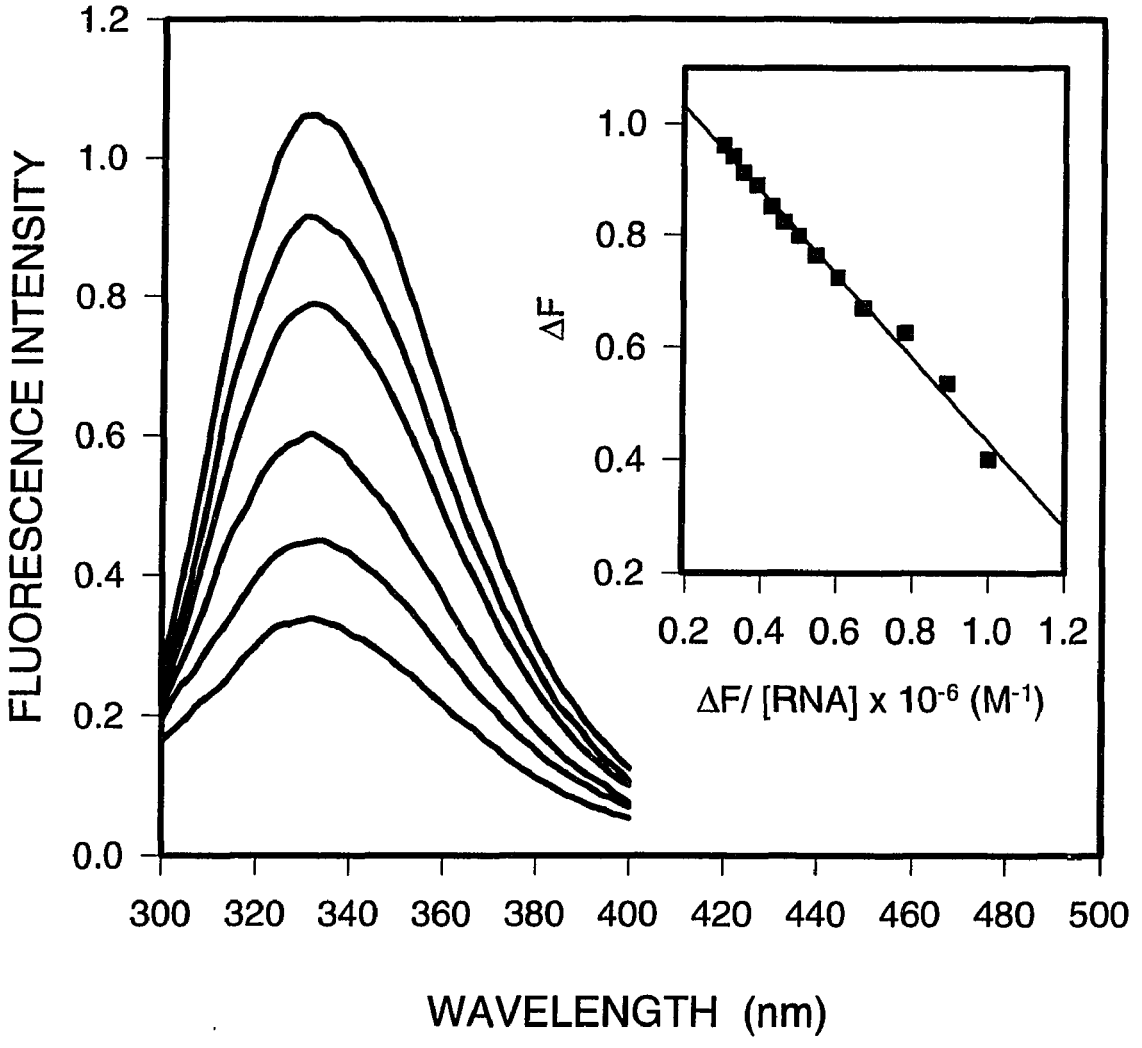

Figure 5.2. Fluorescence emission spectra of p28 (0.5 μM) titrated with capped oligonucleotide II in buffer A, pH 7.05 at 23 °C. The oligonucleotide concentration (*top to bottom*) was 0, 0.1, 0.3, 0.6, 1.2, and 2.3 μM. The excitation wavelength was 282 nm, and a 1.4 mm slit was employed. Emission maxima was observed at 331 nm. *Inset*: Eadie-Hofstee plot of the data. ΔF was calculated as $\Delta F = F_{p28} - F_{p28+oligonucleotide.}$

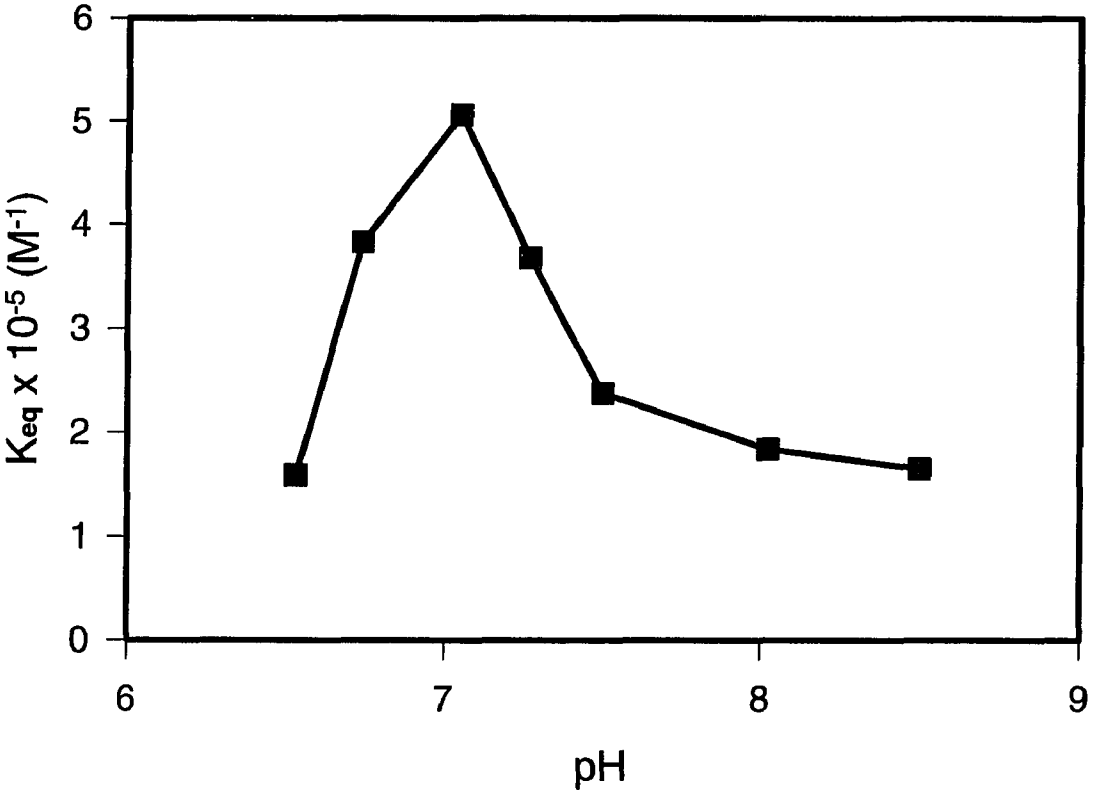

Figure 5.3. Binding of m^7GTP and p28 as a function of pH. All solutions were prepared in buffer A, adjusted to the appropriate pH at 23 °C.

Temperature Effects—A Van't Hoff plot of $-\ln(K_{eq})$ vs the reciprocal of temperature (T^{-1}) was used to calculate the thermodynamic parameters of entropy (ΔS) and enthalpy (ΔH). Figure 5.4 showed the Van't Hoff plot based on m^7GTP binding to p28; the values of ΔH and ΔS were obtained from the intercept and slope, respectively. The values of 5.8 ± 0.4 kcal/mol and 44.7 ± 1.9 cal/(mol °C) were obtained for ΔH and ΔS, respectively. These results were similar to the eIF-4E•m^7GTP interaction, where ΔH was 6.25 ± 0.25 kcal/mol and ΔS was 46.1 ± 1.8 cal/(mol ^{o}C) (Carberry et al., 1989). Similar values were also obtained for the eIF-4F•m^7GTP interaction, where ΔH was 6.84 ± 0.7 kcal/mol and ΔS was 47.4 ± 5.0 cal/(mol ^{o}C) (Carberry et al., 1991). An interpretation was given (Ross et al., 1981) that positive ΔH and ΔS values suggested either hydrophobic (Gill et al., 1967, 1976) or ionic (Pimentel & McClellan, 1971) interactions. The ionic strength dependence of m^7GTP binding with p28 was investigated in order to determine if the interaction was hydrophobic or ionic.

Ionic Strength Dependence— Debye-Huckel theory predicted that for charge-charge interactions, a plot of log K_{eq} versus the square root of the ionic strength would give a linear plot. The slope equaled to $1.02Z_AZ_B$ for ionic interactions where Z_A and Z_B were the charges of the reactants.

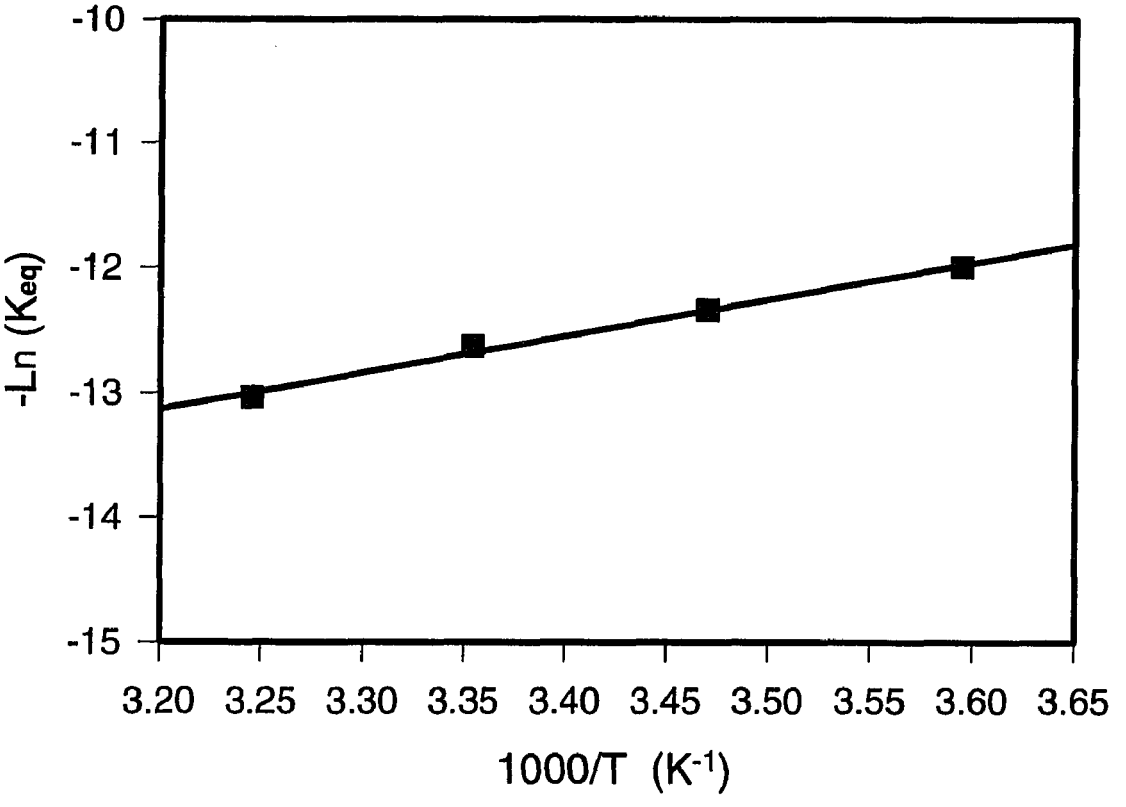

Figure 5.4. Van't Hoff plot for m^7GTP-p28 interactions. All experimental conditions as in figure 5.2.

The bindings of m^7GTP to p28 as a function of the concentration of KCl and $KC_2H_3O_2$ were shown in Figure 5.5(A) and 5.5(B) respectively, and the treatment of these data according to Debye-Huckel theory was shown in the Figure 5.6. For the interaction of a single positive and negative charge, Z_AZ_B=-1. For m^7GTP binding with p28 in $KC_2H_3O_2$, Z_AZ_B=0.008, demonstrated that the binding of m^7GTP to p28 had little dependence on ionic strength. There were no significant ionic interactions involved in the binding of m^7GTP to p28. Using KCl to vary ionic strength, the value of Z_AZ_B was -0.47. This difference between KCl and $KC_2H_3O_2$ suggested a possible uptake of Cl^- by the p28. The special effect of anions on protein-RNA binding was similar to that of the wheat germ eIF-4B protein (Chapter 4: Interaction of eIF-4B with nucleotides and mRNA analogs).

Iodide Quenching Effect—Iodide quenching to determine the accessible tryptophan residues was described in previous chapter (Chapter 4: Interaction of eIF-4B with nucleotides and mRNA analogs). The Stern-Volmer plots of iodide quenching on p28 and eIF-(iso)4F were shown in figure 5.7(A) and 5.7(B) respectively. The linearity of the 5.7(A) curve showed that all tryptophan residues in p28 which contribute to protein fluorescence were solvent accessible. The downward curve in figure 5.7(B) indicated that some tryptophan residues were buried in eIF-(iso)4F. The modified Stern-Volmer plot (Figure 5.8) showed more quantitative results for quenching of p28 and eIF-(iso)4F.

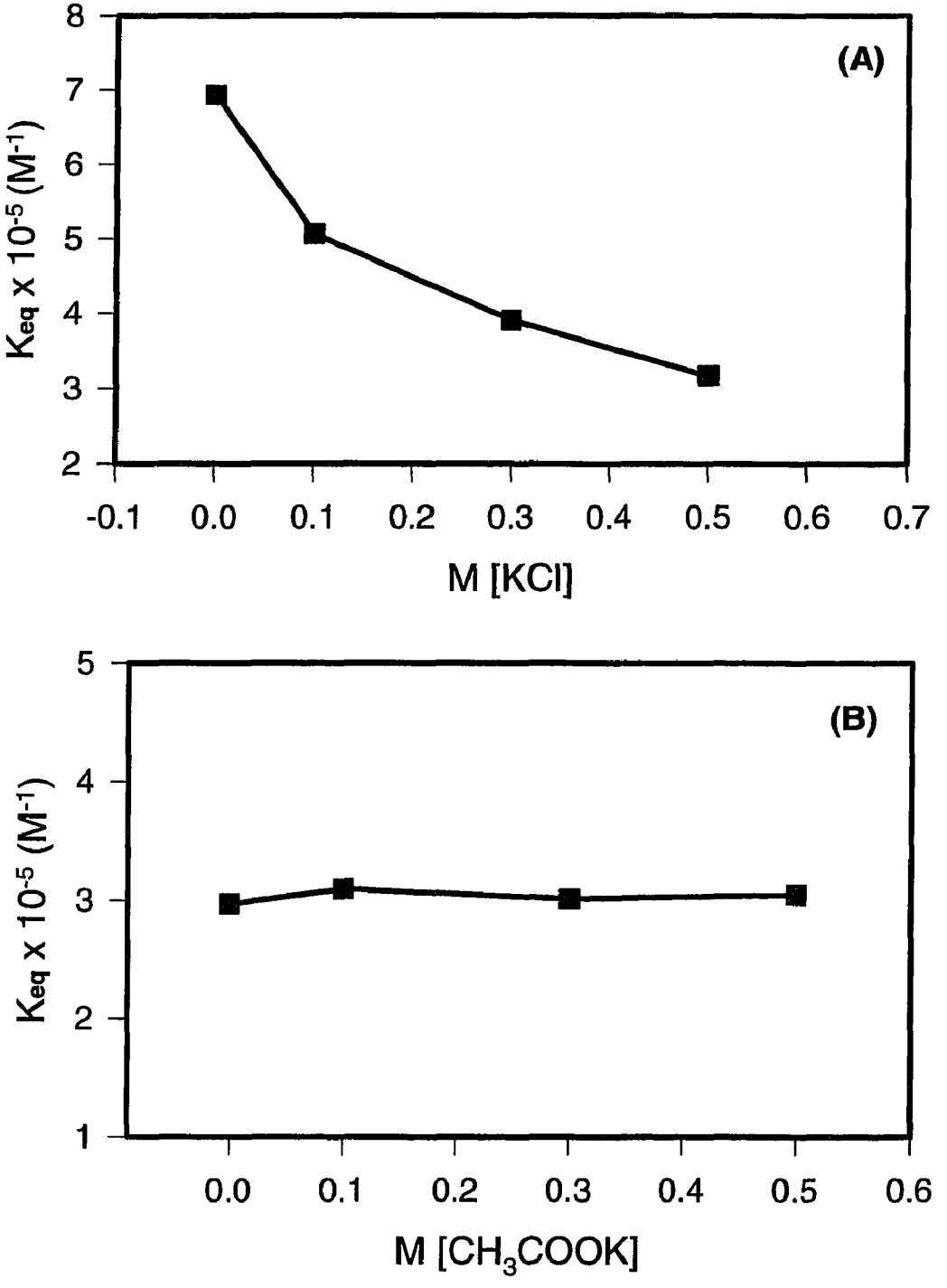

Figure 5.5. (A), K_{eq} values of m^7GTP and p28 as a function of KCl concentration. (B), K_{eq} values of m^7GTP and p28 as a function of $KC_2H_3O_2$ concentration. All solutions were prepared in buffer A, pH 7.05.

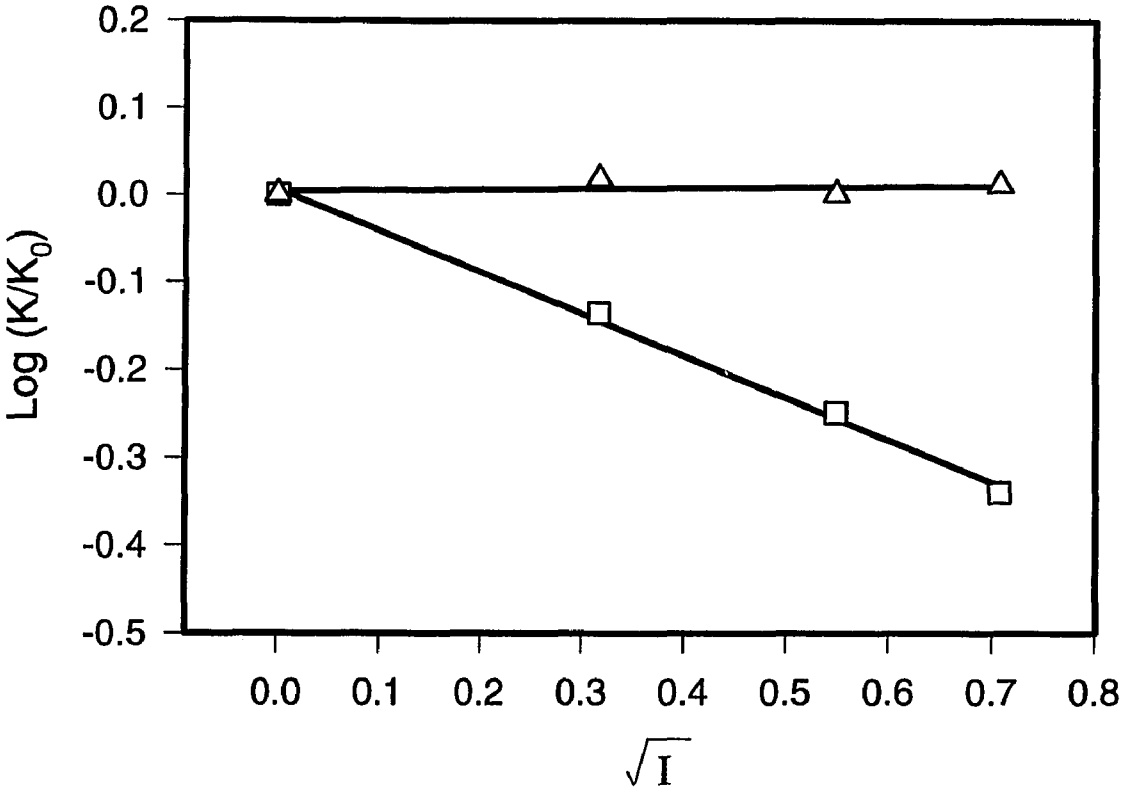

Figure 5.6. Debye-Huckel analysis of the data in Figure 5.5 (□: KCl, △: $KC_2H_3O_2$)

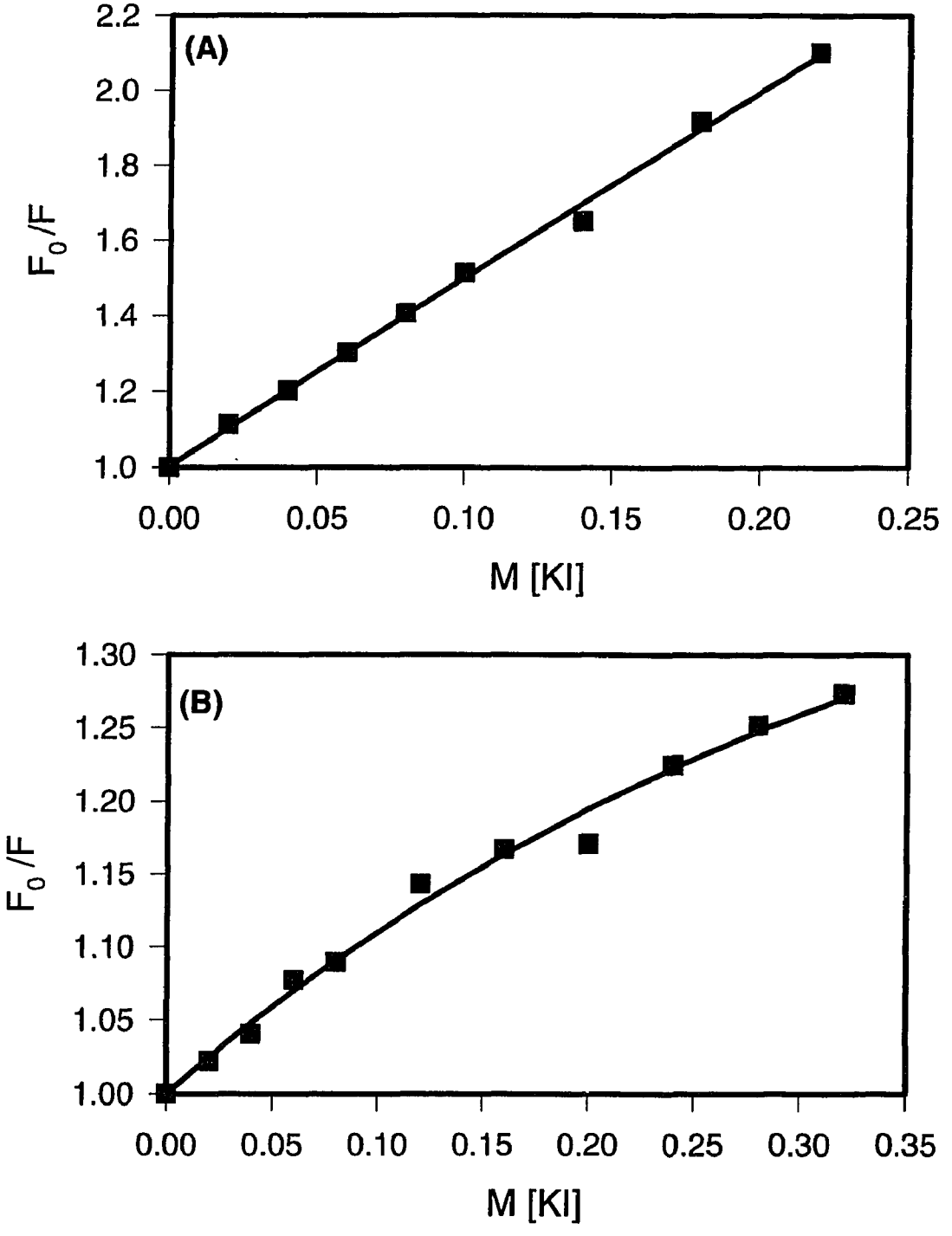

Figure 5.7. (A), Stern Volmer plot of iodide quenching to p28. (B), Stern Volmer plot for quenching of eIF-(iso)4F. All experimental conditions as in Figure 5.2.

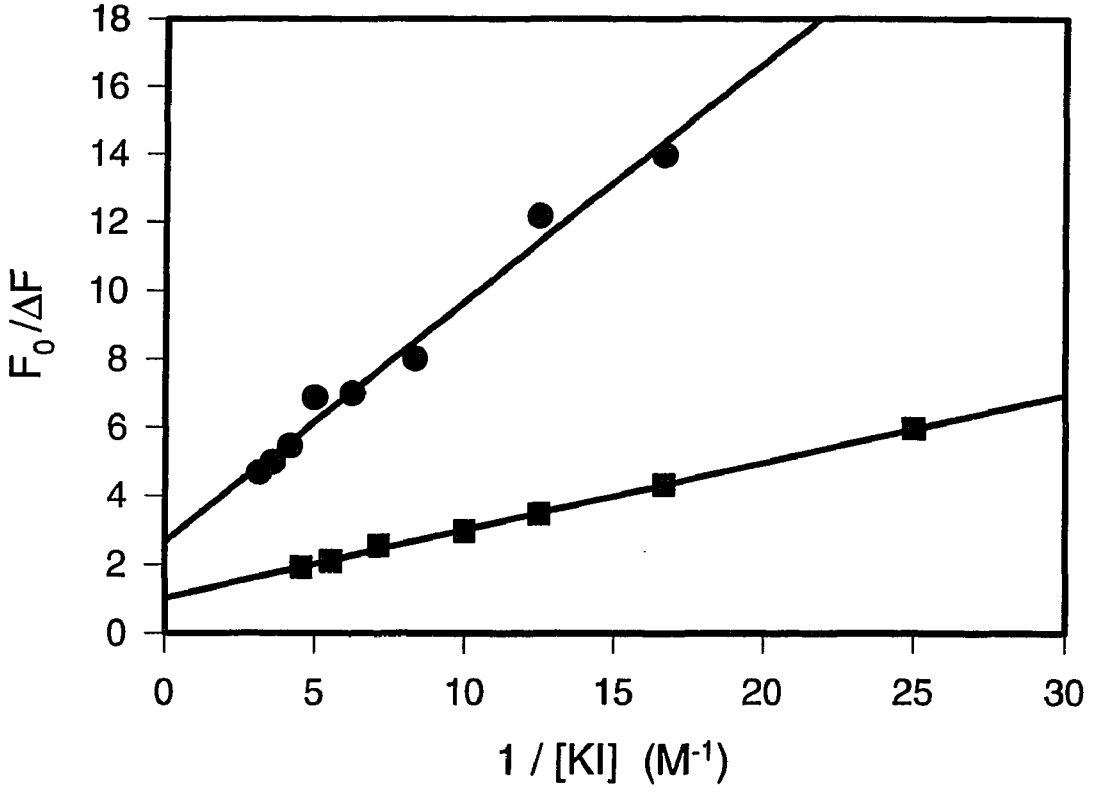

Figure 5.8. Modified Stern Volmer plot of iodide quenching to p28 (■) and eIF-(iso)4F (●).

The reciprocal of the Y intercept represented the fraction of accessible tryptophan residues among all tryptophan in the protein which contribute to the fluorescence (Lakowicz, J. R. 1983). A Y intercept of 1.02±0.05 and 2.65±0.50 was obtained for p28 and eIF-(iso)4F, respectively. Reciprocal values gave the fraction of accessible tryptophan residues as 98.0%±4.5% and 37.7%±6.0% for p28 and eIF-(iso)4F respectively. Thus, if all tryptophan residues contributed to the protein fluorescence, all 9 tryptophan residues in p28 were solvent accessible and only 6 tryptophan residues from a total of 16 in eIF-(iso)4F were solvent accessible, indicating some tryptophan residues on p28 were buried during binding with the large subunit, p82, to form eIF-(iso)4F.

Comparison of oligonucleotide binding to wheat germ eIF-(iso)4F and it's subunits —The bindings of p28, p86 and wheat germ eIF-(iso)4F with m^7GTP and mRNA analogues were measured and compared in Table 5.1. The association of p28 with p86 to form eIF-(iso)4F did not significantly increase the K_{eq} for m^7GTP and capped RNA binding, yet both subunits were required for activity.

Helicase Activity—The eIF-4A dependent helicase activity of eIF-(iso)4F and it's subunits was measured by unwinding the partially double stranded RNA annealed from oligonucleotide III and IV (Figure 5.1). It was found that neither the p28 nor the p86 subunit alone had helicase activity, while the combination of p28 and p86 gave full helicase activity as compared to eIF-(iso)4F (Table 5.2). These data demonstrated that p86, the large subunit of eIF-(iso)4F, although it did not significantly enhance the

RNA binding, was necessary for mRNA secondary structure unwinding during the translation process.

Discussion

The fluorescence emission maxima (331 nm) of wheat germ eIF-(iso)4F and it's small subunit p28 suggested the involvement of tryptophan residues in the cap-binding site, as was previously described in detail for human eIF-4E (Carberry et al., 1989) and wheat germ eIF-4F and eIF-(iso)4F (Carberry et al., 1991). The pH optimum for cap binding to p28 was found to be 7.05; compared with the pH optimum of 7.6 for eIF-(iso)4F•$m^7G_{ppp}G$ complex (Carberry et al., 1991). The change of pH optimum could be caused by a difference in conformation between separated p28 and p28 in the intact eIF-(iso)4F. The shape of the pH dependent binding profile for p28 and (iso)4F were both bell shaped, similar to that previously reported for the eIF-4E•$m^7G_{ppp}G$ interaction (Carberry et al., 1989). This latter interaction was previously characterized in terms of a model which proposed that the increase in K_{eq} at pH values below the optimum was due to the pKa of the N-7 of the cap group while the decrease above the pH optimum was due to deprotonation of an amino acid residue, probably His. The data reported in Figure 5.3 for the cap-p28 interaction suggests two pK_a's as well, one for cap and one for an amino acid residue, most likely histidine (imidazole pK_a=6.04, in solution pK = 6-8). The pK_a's of amino acids were known to be environmentally sensitive and this could account for the shift in binding profile between p28 and eIF-(iso)4F. The shift in pKa implied the binding site had become more positively charged in the separated subunit. The previous sequence comparison (Allen et al., 1992) of wheat p28 with the cap-binding protein eIF-4E from

mammals and yeast had shown about 38% sequence homology. There were three highly conserved histidine residues (position 33, 91, 193 from N-terminal) and 9 tryptophan residues in p28 (positions from N-terminal: 39, 42, 55, 72, 101, 112, 126, 161, 178), one more tryptophan residue than in mammalian and yeast cap-binding proteins (Trp 178). Mouse eIF-4E was shown to substitute for yeast eIF-4E *in vivo*, even though the identity is only 33% (Altmann et al., 1989) suggesting the relative positions of the histidine and tryptophan residues were important for cap recognition. Site-directed mutagenesis of yeast eIF-4E showed that tryptophan 1, 2, and 8 were required for cap binding activity (Altmann et al., 1988). Site-directed mutagenesis of human eIF-4E showed that tryptophan 5 and the glutamic acid residue three amino acids to the carboxyl terminal side of tryptophan 5 were involved in cap recognition. None of these studies examined the tertiary structure of the mutant protein. Ueda et al. (1991) proposed that the base stacking of the tryptophan and hydrogen-bond pairing by the glutamic acid were responsible for binding the m^7G cap of mRNA. The p28 of eIF-(iso)4F had a glutamic acid residue four amino acids to the carboxyl-terminal side of tryptophan 5 (Glu:105) which could participate in the binding proposed by Ueda et al. (1991).

1 MAEVEAALPV AATETPEVAA EGDAGAAEAK GPHKLQRQWT
His 33 Trp 39

41 FWYDIQTKPK GPAAWGTSLK KGYTFDTVEE FWCLYDQIFR
Trp 42 Trp 55 Trp 72

81 PSKLVGSADF HLFKAGVEPK WEDPECANGG KWTVISSRKT
His 91 Trp 101 Glu 105 Trp 112

121 NLDTMWLETC MALIGEQFDE SQEICGVVAS VRQRQDKLSL
Trp 126

161 WTKTASNEAV QVDIGKKWKE VIDYNDKMVY SFHDDSRSQK
Trp 161 Trp 178 His 193

201 PSRGGRYTV

Figure 5.9. Amino acid sequence of p28 subunit of wheat germ eIF-(iso)4F. Histidine and tryptophan residues are in bold and labeled by numbers. Numbers are started from N-terminal. Allen et al., 1992.

Data from Table 5.1 suggested that the p28 subunit bound m^7GTP specifically because p28 showed a significant 3 fold difference in binding between m^7GTP ($K_{eq}=(5.06\pm0.08)x10^5M^{-1}$) and GTP ($K_{eq}=(1.92\pm0.08)x10^5\ M^{-1}$). In addition, p28 showed a nearly ten fold tighter binding with capped RNA ($K_{eq}=(1.24\pm0.08)x10^6M^{-1}$) as compared to uncapped RNA ($K_{eq}=(0.17\pm0.02)x10^6M^{-1}$).

The small subunit, p28, had cap binding properties very similar to native eIF-(iso)4F. This observation was similar to the relative affinities of mammalian eIF-4E and eIF-4F binding to globin mRNA (eIF-4E: $K_{eq}=(20.9\pm1.0)x10^5\ M^{-1}$; eIF-4F: $K_{eq}=(18.6\pm1.1)x10^5\ M^{-1}$, Goss et al., 1990). In the mammalian system eIF-4E had about the same affinity for mRNA as the larger eIF-4F complex. These data suggested that the essential role of the large subunit was involved in other interactions such as protein-protein interactions and helicase activity.

The p86 subunit, which also bound to m^7GTP, although less tightly, was unlikely to be the specific cap binding subunit in eIF-(iso)4F for the following two reasons: p86 showed no significant difference between capped RNA and uncapped RNA binding (for capped RNA $K_{eq}=(1.22\pm0.05)x10^6M^{-1}$, for uncapped RNA $K_{eq}=(1.11\pm0.06)x10^6M^{-1}$) and p86 did not distinguish m^7GTP from GTP (m^7GTP $K_{eq}=(3.60\pm0.11)x10^5M^{-1}$; GTP $K_{eq}=(3.30\pm0.17)x10^5M^{-1}$). The fact that p86 had a relatively high binding affinity for RNA suggested the native protein might have an RNA site involving both subunits and that p86 might stabilize the contact with RNA during the course of protein synthesis. In addition, photoaffinity labeling with m^7GTP analogs labeled only the small subunit (Friedland et al., unpublished results).

A working model was that p28 contained the binding site for the cap and located the complex at or near the 5' end of the mRNA. In order for the eIF-(iso)4F complex to perform translation initiation activity, the complex must process down the RNA. This required the helicase activity which required both p28 and p86, Table 5.2. This would in all probability require release of the cap while maintaining contact with the RNA. p86 and other factors might stabilize the interaction with mRNA and prevent the protein complex from dissociating from the RNA. While p28 bound capped RNA specifically, the intact protein (or sum of p28+p86) was necessary to perform the helicase activity (Table 5.2) and to stimulate protein synthesis (Heerden et al., 1994). This suggested p86 might be involved in protein-protein interactions to form a complete initiation complex as well.

Table 5.1

Equilibrium binding constants for the interaction of p28, p86 and wheat germ eIF-(iso)4F with m^7GTP and oligonucleotides.

initiation factors	oligonucleotides	K_{eq} (M^{-1})
p28	m^7GTP	$(5.06\pm0.08)\times10^5$
	GTP	$(1.92\pm0.23)\times10^5$
	capped RNA (II)	$(1.24\pm0.04)\times10^6$
	uncapped RNA (I)	$(0.17\pm0.02)\times10^6$
p86	m^7GTP	$(3.60\pm0.11)\times10^5$
	GTP	$(3.30\pm0.17)\times10^5$
	capped RNA (II)	$(1.22\pm0.05)\times10^6$
	uncapped RNA (I)	$(1.11\pm0.06)\times10^6$
p28+p86	m^7GTP	$(5.59\pm0.21)\times10^5$
	capped RNA (II)	$(1.44\pm0.07)\times10^6$
eIF-(iso)4F	m^7GTP	$(5.40\pm0.08)\times10^5$
	capped RNA (II)	$(1.55\pm0.05)\times10^6$

Table 5.2

eIF-4A dependent helicase activity of eIF-(iso)4F and its subunits measured by densitometry scan of RNA bands on silver stained acrylamide gel

eIF factors		dsRNA	ssRNA IV	ssRNA III
eIF-4A alone	Band volume	242.50	2.41	13.63
	Ratio %	93.8%	1.0%	5.3%
	Unwinding%	6.2%		
eIF-4A and p28	Band volume	641.89	11.24	0
	Ratio %	98.3%	1.7%	0.0%
	Unwinding%	1.7%		
eIF-4A and p86	Band volume	606.28	-1.24	0.05
	Ratio %	100.2%	-0.2%	0.0%
	Unwinding%	-0.2%		
eIF-4A and p28+p86	Band volume	516.93	472.60	147.70
	Ratio %	45.5%	41.6%	13.0%
	Unwinding%	54.5%		
eIF-4A and eIF-(iso)4F	Band volume	707.41	566.34	227.72
	Ratio %	47.1%	37.7%	15.1%
	Unwinding%	52.9%		

Chapter 6

Anti-Cooperative Bi-Phasic Binding of Transcription Factor USF to its cognate DNA

Material and Methods

DNA oligomers and⊗ USF DNA-binding site oligomers of MLP, LCR and NS were synthesized, purified, quantitated and annealed as described elsewhere (Ferr D'Amar et al., 1993). The overexpression and purification of both protein constructs had been described previously (Ferr D'Amar et al., 1994). Cysteine-free mutants, which were indistinguishable from wild-type protein were employed.

Fluorescence Measurements—The binding buffer used for fluorescence measurements, consisted of 10 mM HEPES-KOH, 100 mM KCl, 10% glycerol and 1mM $MgCl_2$, adjusted to pH 7.5. All chemicals were reagent grade or better. Fluorescence measurements were carried out at 25 °C, unless otherwise noted, on a SPEX Fluorolog-τ2 Spectrofluorometer equipped with a high-intensity xenon arc lamp and steady-state data were collected and analyzed as previously described in detail (Sha et al., 1994; Carberry et al., 1989, 1990).

The kinetics of the binding of the E-box domain of MLP DNA to b/HLH and b/HLH/Z of USF protein were followed by measuring the changes of the intrinsic protein fluorescence after rapid mixing by a Hi-Tech Scientific SFA-11 stopped-flow apparatus. The excitation wavelength was 281 nm and the slit width 2 mm. Light emitted from the reaction mixture was monitored at a single wavelength, 335 nm, with a integration time of 1 ms. A series of stopped-flow experiments were performed at different temperatures. After rapid mixing of protein (0.1 μM b/HLH dimer or 0.1 μM b/HLH/Z tetramer) with appropriate DNA solution, the time course of the intrinsic

fluorescence intensity was recorded. The plot of ΔF vs. time was fitted to a number of nonlinear analytical equations using Peakfit software from Jandel Scientific.

Results

Steady-State Fluorescence Measurements—The fluorescence emission spectra of b/HLH•oligonucleotide complexes as a function of oligonucleotide concentration was shown in Figure 6.1. The fluorescence emission spectra of b/HLH/Z•oligonucleotide complexes were similar (data not shown). Upon complex formation, there was a decrease in the protein fluorescence intensity at 335 nm. Such protein fluorescence quenching was attributed to the π-π stacking interactions between an aromatic amino acid residue, in this case tryptophan (Three was one tryptophan residue in both b/HLH and b/HLH/Z at position 218), and the nucleic acid base (Lawaczek & Wagner, 1974; Brun et al., 1975; Ishida et al., 1983).

The K_{eq} of b/HLH•oligonucleotide and b/HLH/Z•oligonucleotide complex formation was calculated from the relative fluorescence intensity changes in free and complexed protein emission spectra by construction of an Eadie-Hofstee plot, as shown in the inset of Figure 6.1. K_{eq} was found to be $(4.7\pm0.6)\times10^{5}M^{-1}$ for the interaction of b/HLH with MLP oligonucleotide.

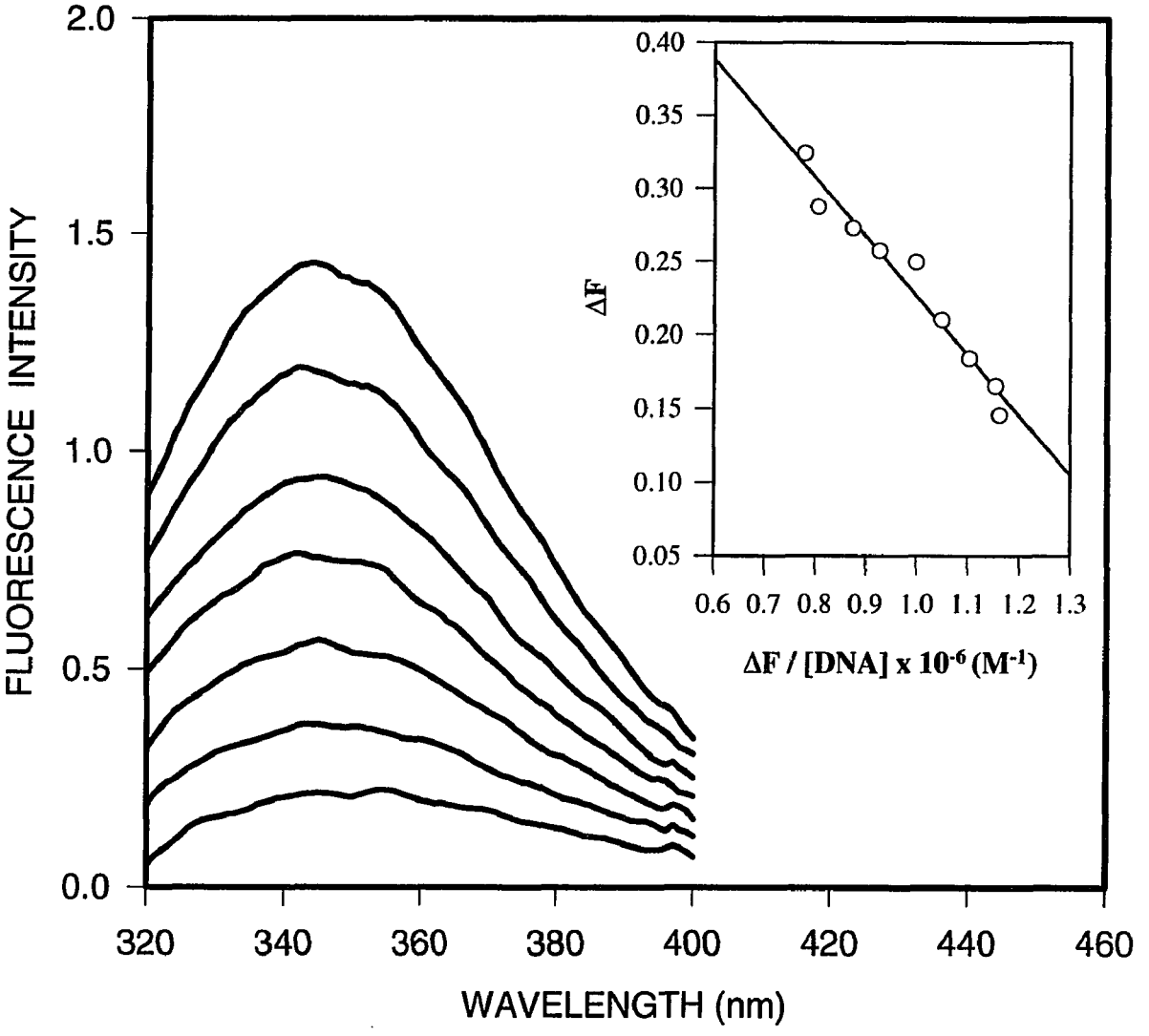

Figure 6.1. Fluorescence emission spectra of b/HLH (0.2 μM dimer) titrated with MLP DNA in the binding buffer, pH 7.5 at 25 °C. The oligonucleotide concentration (*top to bottom*) was 0.0, 0.2, 0.8, 1.8, 2.8, 4.0 and 6.0 μM. The excitation wavelength was 281 nm. Emission maxima was observed at 335 nm. *Inset*: Eadie-Hofstee plot. ΔF was calculated at 335 nm as $\Delta F=F_{b/HLH}-F_{b/HLH+DNA.}$

Quenching of b/HLH fluorescence by DNA—The recent cocrystal structure of b/HLH•DNA had shown that b/HLH binds to one duplex DNA as a dimer (Ferr D'Amar et al., 1994). We used concentration of dimer as the protein concentration in fitting the fluorescence titration data. The binding of MLP, LCR and NS DNA to b/HLH showed similar simple quenching curves (Figure 6.2). All three DNA bind b/HLH with about the same affinity (Table 6.1, MLP: Keq=(4.7±0.6)x10^5M^{-1}, LCR: Keq=(4.0±0.2)x10^5M^{-1}, NS: (3.2±0.1)x10^5 M^{-1}). The specificity of binding was defined as the equilibrium constant for binding to specific DNA sequences divided by the binding equilibrium constant for binding to non specific DNA. Thus, the binding specificity of b/HLH for MLP E-box duplex oligonucleotide compared to the non-specific (NS) sequence was only 1.47, and the binding specificity of b/HLH for LCR binding site oligonucleotide compared to the non-specific (NS) sequence was only 1.25, which suggested little specificity of binding for either oligonucleotide (Table 6.1). This was in dramatic contrast to the b/HLH/Z protein results shown bellow.

Bi-Phasic Binding of b/HLH/Z with DNA—b/HLH/Z formed a homotetrameric complex that had been shown to bind 2 DNA duplex molecules at the same time (Ferr D'Amar et al., 1994). A stoichiometry of 4 b/HLH/Z monomer : 2 DNA duplex was used for the analysis of the fluorescence titrations.

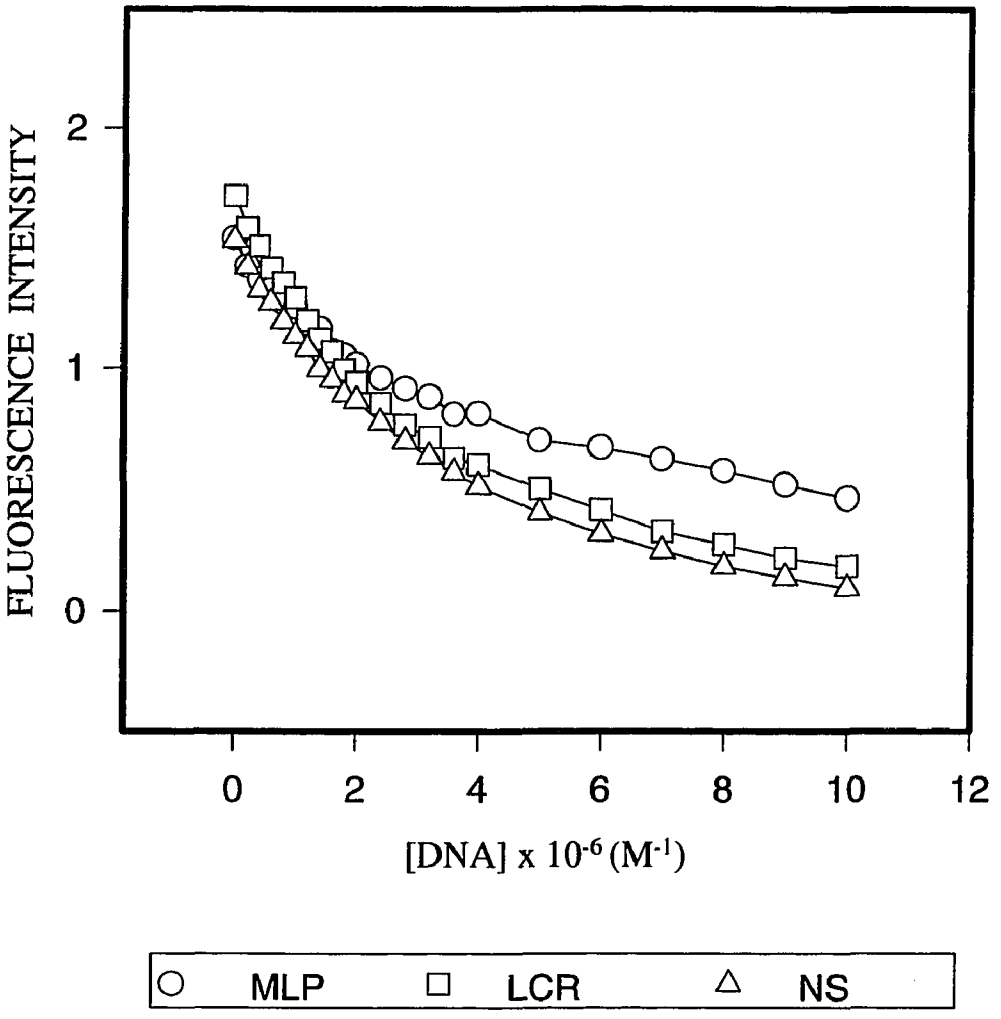

Figure 6.2. 1 μM b/HLH dimer fluorescence quenching by 0 to 10 μM double stranded MLP, LCR and NS DNA.

The binding of MLP and LCR DNA to b/HLH/Z showed a dramatic bi-phasic binding mode: enhancement of fluorescence followed by fluorescence quenching (Figure 6.3(A), 6.3(B)), while the binding of the NS sequence to b/HLH/Z showed a single binding mode (Figure 6.3(C)) as seen for the b/HLH protein. For the bi-phasic binding of b/HLH/Z to MLP and LCR, the turning point from fluorescence enhancement to fluorescence quenching was at a one to one ratio of tetramer b/HLH/Z to duplex DNA (Figure 6.3(A), 50 nM b/HLH/Z tetramer:50 nM DNA duplex; Figure 6.3(B), 0.5 μM b/HLH/Z tetramer:0.5μM DNA duplex). Which clearly indicated that two DNAs were binding to a single tetrameric b/HLH/Z and that the two DNA binding sites on the same protein tetramer were not equivalent. The first DNA molecule binding induced a fluorescence enhancement while the second DNA molecule binding induced fluorescence quenching. b/HLH/Z showed very specific binding towards MLP DNA. The binding constant of b/HLH/Z for MLP was about one to ten thousand fold stronger than the binding of the other two DNA (Table 6.1: MLP: First binding mode: $(2.2\pm2.0)\times10^{9}$ M^{-1}, Second binding mode: $(1.2\pm0.8)\times10^{8}$ M^{-1}; LCR: First binding mode: $(3.1\pm3.7)\times10^{6}$ M^{-1}, Second binding mode: $(3.3\pm0.6)\times10^{5}$ M^{-1}; NS: second binding mode only: $(1.1\pm0.3)\times10^{5}$ M^{-1}). The specificity of b/HLH/Z binding to MLP E-box compared to the NS sequence was 2.0×10^{4} for the first and 1.1×10^{3} for the second binding mode. The specificity of b/HLH/Z binding to the LCR sequence compared to the NS sequence was 28 for the first and 3.0 for the second binding mode (Table 6.1).

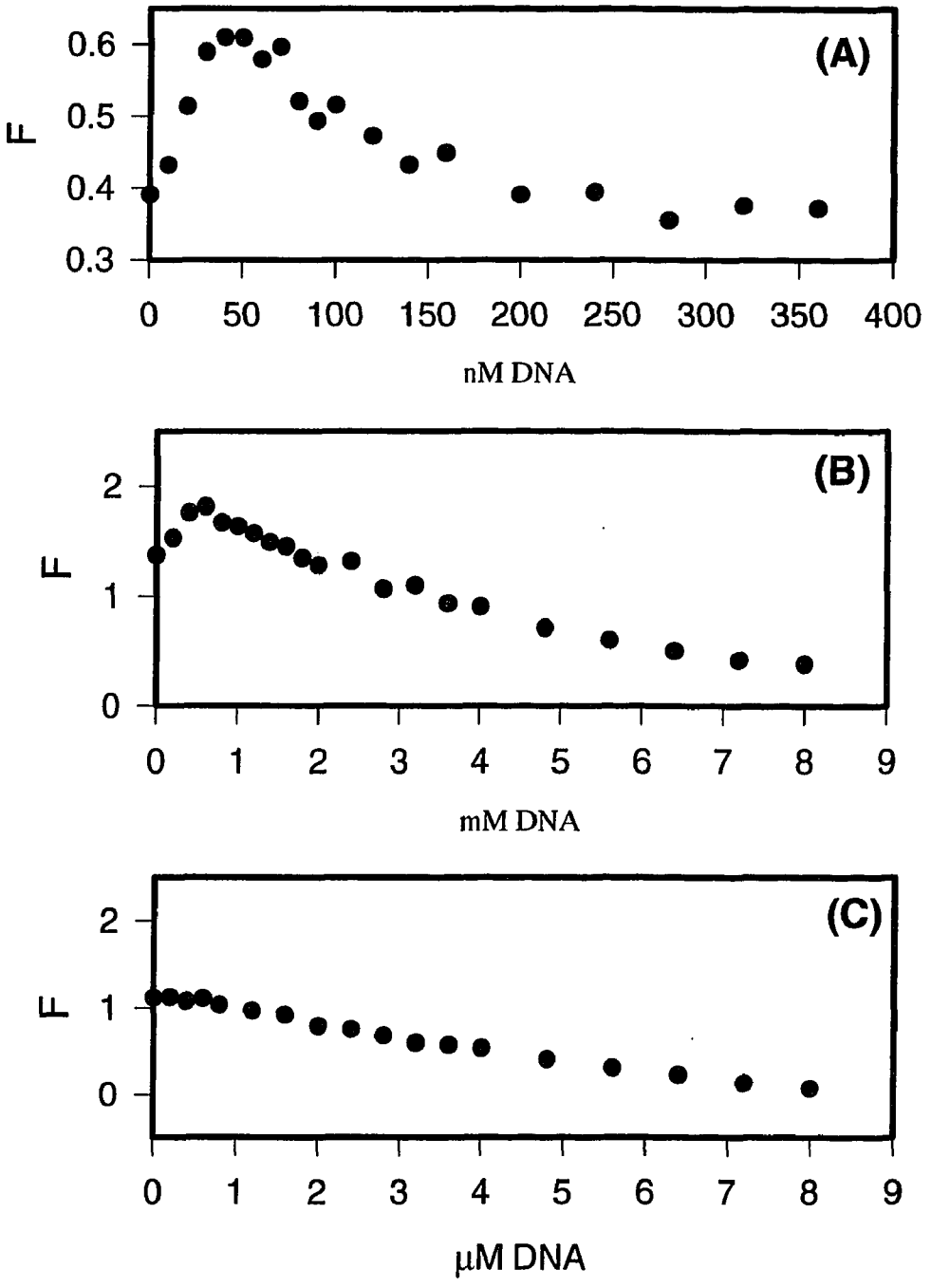

Figure 6.3. (A), Bi-phasic fluorescence changes of 50 nM tetramer b/HLH/Z upon binding to MLP E-box sequence. (B), Bi-phasic f luorescence changes of 0.5 μM tetramer b/HLH/Z binding with LCR DNA. (C), Single phase fluorescence change of 0.5 μM tetramer b/HLH/Z binding with NS DNA.

Results showed that b/HLH/Z had highly specific binding to the adenovirus major late promoter palindromic E-box sequence and moderately specific binding for human locus control region non-palindrome E-box like sequence when compared with the non specific DNA sequence.

Stopped-Flow Fluorescence Kinetics—The stopped-flow data for the binding of MLP DNA to the b/HLH and b/HLH/Z were plotted as ΔF vs. time as shown in Figure 6.4. Fitted curves corresponded to the following single-exponential equation (Olsen et al., 1993):

$$\Delta F = \Delta F\int (1-\exp(-k_{obs}t)) \qquad (1)$$

where k_{obs} was the observed first-order rate constant, and the $\Delta F\int$ was the maximum fluorescence change.

Mechanisms for MLP-b/HLH interaction—Two possible schemes, one step reaction and two step reactions, for simple quenching of b/HLH by MLP E-box sequences were considered (Garland, 1978).

Figure 6.4. Single exponential curve fitting of the ΔF vs. time for the kinetics of 0.1 μM b/HLH dimer mixing with 1 μM MLP DNA. k_{obs} was obtained from the fitted curve. Bottom inset is the residual of fitting plotted on the same x but different y axis (labeled on the right).

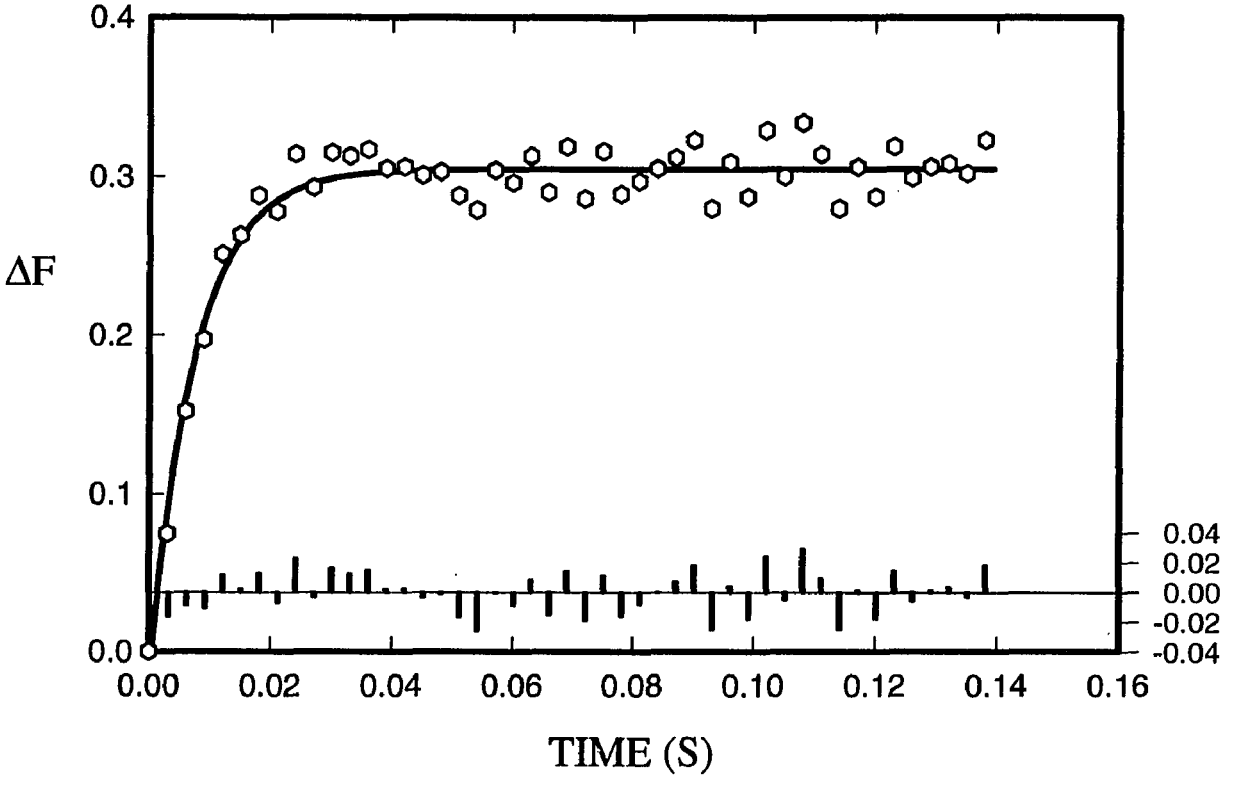

The one-step reaction was:

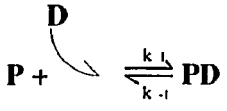

(i)

where k_1 and k_{-1} were forward and reverse rate constants, respectively; P an D refer to protein and DNA. Under the pseudo-first-order condition, the observed rate constant was predicted to be a linear function of substrate concentration, i.e., $k_{obs} = k_1[D] + k_{-1}$.

The two- step reaction was:

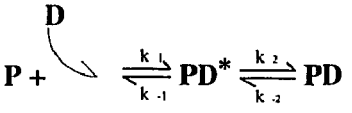

(ii)

which involved a fast association of protein and DNA followed by a slow change of conformation of the first association complex, PD^*, to the stable complex, PD.

The interaction of b/HLH (0.1 μM) with MLP E-box under different concentrations of DNA (1 μM, 2 μM and 3.5 μM) gave about the same k_{obs} (125.8±4.9 s^{-1}, 128.9±8.6 s^{-1} and 129.7±5.9 s^{-1} respectively) within experimental error. The reaction was not a single-step pseudo first order reaction (Mechanism i). Earlier CD experiments had shown that the b/HLH protein undergone a 48% conformational change upon binding to MLP sequence (Ferr D'Amar et al., 1994), in agreement with Mechanism (ii).

Mechanism (ii) can be written as (Olsen et al., 1993):

$$k_{obs} = \frac{k_2}{1 + \frac{K_1}{[D]}} + k_{-2} \qquad [2]$$

where $K_1 = \frac{k_{-1}}{k_1}$. Equation [2] rearranges to: $$k_{obs} - k_{-2} = \frac{k_2[D]}{[D] + K_1} \qquad [3]$$

If one assume $k_{-2} << k_{obs}$, then

$$k_{obs} = \frac{k_2[D]}{[D] + K_1}$$

and $$\frac{1}{k_{obs}} = \frac{1}{k_2} + \frac{K_1}{k_2[D]} \qquad [4]$$

A plot of $\frac{1}{k_{obs}}$ vs $\frac{1}{[D]}$ will give an intercept of $1/k_2$ (Figure 6.5).

This simple model gives a k_2 value of 134.4 ± 9.8 sec^{-1} for b/HLH binding with MLP DNA. While more complex model with additional conformational changes will also fit the data, at present there is no experimental data to suggest such a mechanism is required.

The study of the binding kinetics at different temperatures allowed for the calculation of the activation energy ΔE (2.1±0.2 kcal/mol), which was the forward direction energy barier for the conformational change step (Figure 6.6, Arrhenius plot). The k_{obs} for b/HLH MLP binding at different DNA concentrations (26 ^{o}C) was shown in Table 6.2.

Figure 6.5. Kinetics plot of $1/k_{obs}$ vs 1/[D] of 0.1 μM b/HLH under different MLP DNA concentrations (1 μM, 2 μM, 3.5 μM and 5 μM respectively). k_2 was obtained as the reciprocal of Y inrtercept (134.4 sec^{-1}).

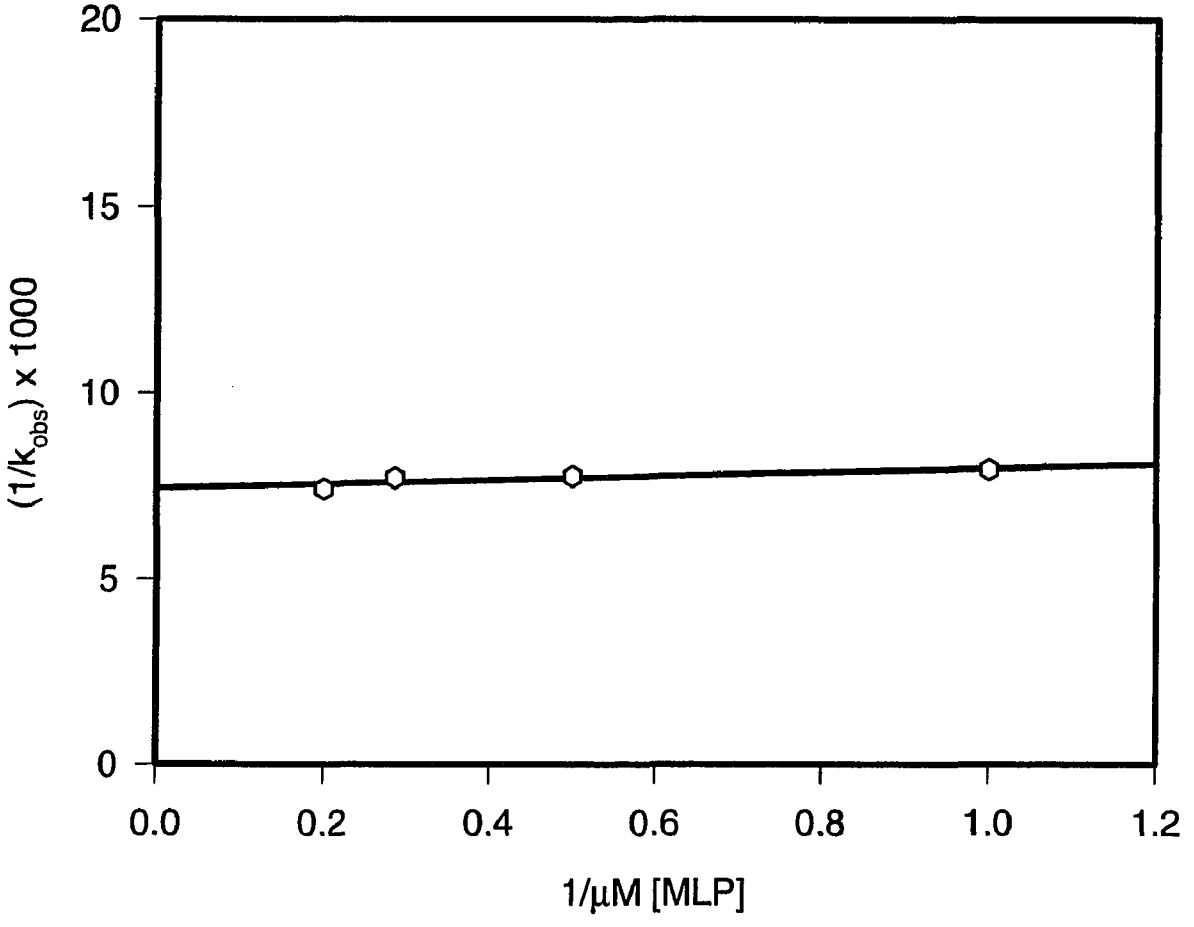

Figure 6.6. Arrhenius plot of b/HLH-MLP DNA interactions using K_2 obtained from different temperatures. The activation energy for the conformational change step, ΔE_2 = 2.1 kcal/mol, is calculated from the slope (1000 x slope = -ΔE/R, where R = 1.987 cal/K mol).

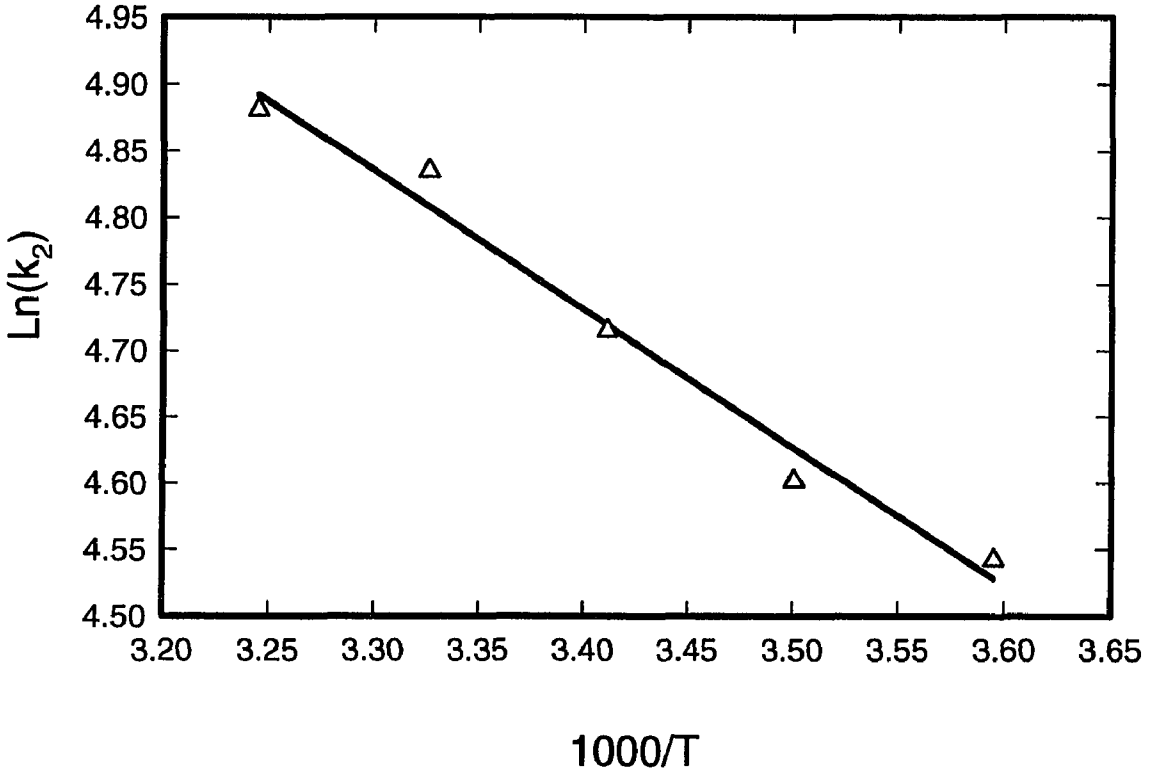

Mechanisms for MLP-b/HLH/Z interaction—Four possible mechanisms could be written for the bi-phasic (enhancement-quenching) binding behavior of MLP to b/HLH/Z which were shown below:

.

|← enhancement →|← quenching →|

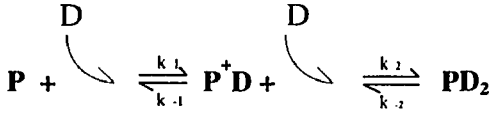

(a)

|← enhancement →|← quenching →|

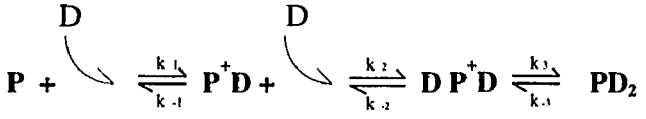

(b)

|← enhancement →|← quenching →|

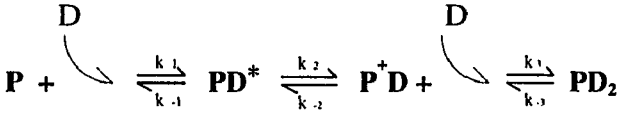

(c)

|← enhancement →|← quenching →|

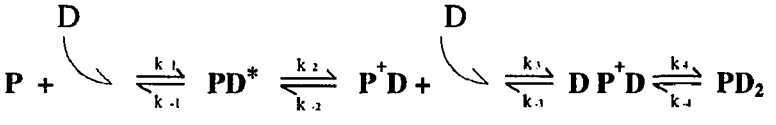

(d)

Assuming that the b/HLH/Z protein complex was a symmetrical homotetramer, the two DNA binding sites would be equivalent prior to the first DNA binding. However, the two DNA binding sites on b/HLH/Z were dramatically different, one caused fluorescence enhancement the other caused fluorescence quenching. This could be explained as the result of the first DNA binding causing a conformational change on the second DNA binding site on b/HLH/Z. The conformational change on the first DNA binding event further exposed the tryptophan on the second binding site, thus giving tryptophan fluorescence enhancement instead of fluorescence quenching. The confirmation of conformational changes for first DNA binding ruled out the possible mechanisms (a) and (b), which suggested one simple binding in the enhancement mode that did not contain a conformational change.

The stopped-flow data of b/HLH/Z interaction with MLP DNA was measured as previous described for b/HLH protein. The first DNA binding (fluorescence enhancement phase) for the kinetic interaction was too fast to be observed. We had been able to capture only the fluorescence change of the quenching phase (second DNA binding) of the b/HLH/Z DNA interaction. A simple relaxation curve resembling the curve obtained from b/HLH:DNA interaction was fitted by the same method as described earlier. The similar concentration independence of k_{obs}, (82.4±7.2) s^{-1}, (84.5±8.9) s^{-1} and (85.4±4.5) s^{-1} at different DNA concentrations respectively (Table 6.2), suggested the involvement of a conformational change as

discussed in detail for b/HLH DNA interaction. The initial binding of second DNA was much faster than the conformational change step that followed. The observed k_{obs} approximately equals to the calculated k_4 (Table 6.2, $k_4 = 87.5 \pm 10.6\ S^{-1}$), the rate constant for the last step (conformational change) in b/HLH/Z MLP binding. The only mechanism which contains two conformational changes is scheme (d) for b/HLH/Z binding with MLP DNA. This mechanism is consistent with the observed kinetics.

The only mechanism which contained two conformational changes was scheme (d) for b/HLH/Z binding with MLP DNA. This mechanism was consistent with the observed kinetics. The Arrhenius plot of k_4 vs. 1/T (Figure 6.7) was used to obtain the activation energy ΔE (2.5±0.7 kcal/mol) for the conformational change in the last step of the b/HLH/Z-DNA interaction.

Figure 6.7. Arrhenius plot of b/HLH/Z-MLP DNA interactions using k_4 obtained from different temperatures. The activation energy for the last step conformational change, $\Delta E_4 = 2.5$ kcal/mol, was calculated.

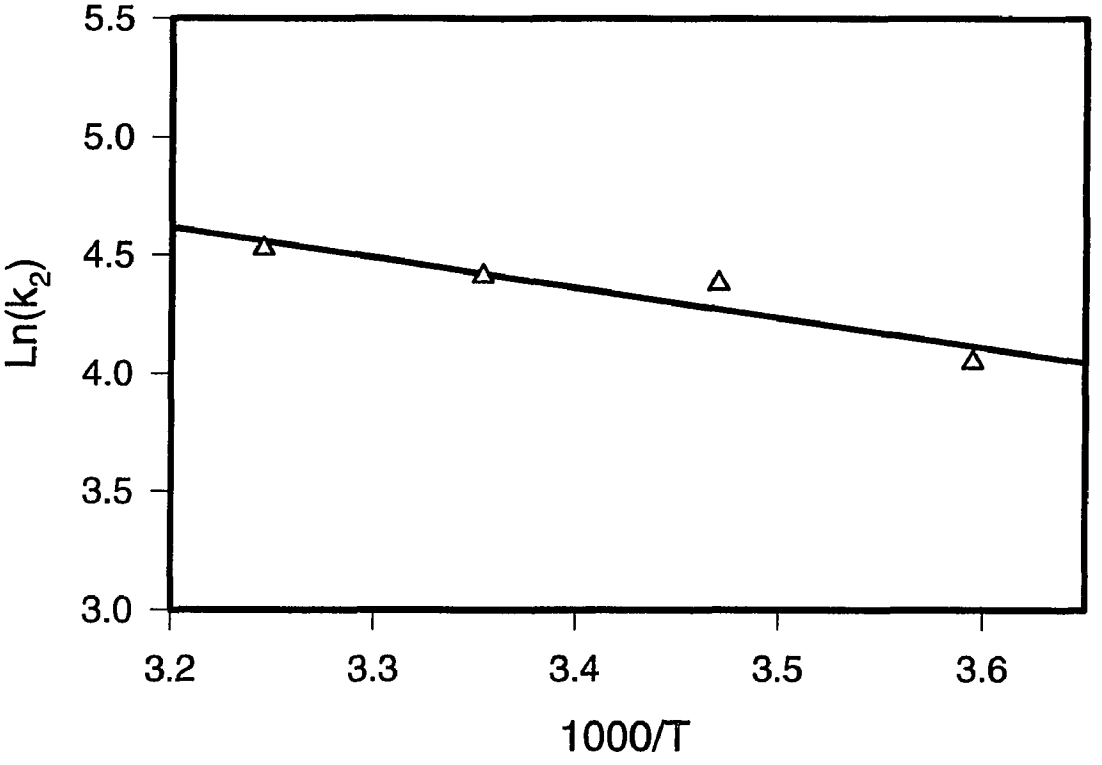

Discussion

Although the leucine zipper motif was not involved in direct contact with DNA during b/HLH/Z binding, it has some crucial effects on DNA binding to the protein. The fact that b/HLH/Z had 1000 to 100 fold (first DNA binding and second DNA binding respectively) higher affinity to MLP than b/HLH, suggested that the leucine zipper was necessary for high affinity DNA binding. Deletion of the leucine zipper caused the protein to lose the ability to discriminate among DNA sequences (Table 6.1). Presumably the leucine zipper motif maintained tetramerization of the protein which seemed to be important both in binding affinity and in specificity.

Both LCR and NS DNA had a significantly lower affinity for b/HLH/Z compared with MLP DNA (Table 6.1). However, LCR DNA still exhibited a bi-phasic interaction (enhancement, then quenching) while the NS DNA had only one quenching mode. Although no longer a palindrome, the LCR sequence maintained a less distorted E-box than that of the NS oligonucleotide, which had an extra mutation next to the E-box.

These binding affinity results demonstrated that the base immediately outside the E-box had some effect on specific binding especially on a slightly modified E-box sequence. The palindrome in the E-box was a crucial factor for high affinity binding, even a one base substitution that disturbed this symmetry (from MLP to LCR or NS) caused at least a hundred-fold affinity decrease (Table 6.1).

It was demonstrated earlier that the b/HLH/Z tetramer bound two DNA simultaneously (Ferr D'Amar et al, 1994). This study showed a sequential binding of two DNA molecules to b/HLH/Z that exhibited an unusual negative cooperativity. A ten fold decrease on the second DNA binding affinity was observed for both the MLP and the LCR sequences. An anti-cooperative binding mechanism, although unusual, will benefit DNA looping and mismatch correction in the transcription system as explained below (Figure 6.8). DNA looping for USF was suggested earlier (Ferr D'Amar et al, 1994). DNA looping by USF required two E-box sequences on the same DNA functioning together. Double E-box sequences were found in many systems. Two equivalent E-box sequences, the Insulin Enhancer Binding sequences (IEB1, IEB2) were found in human insulin gene enhancer that bound a helix-loop-helix transcription factor, insulin enhancer factor IEF1.

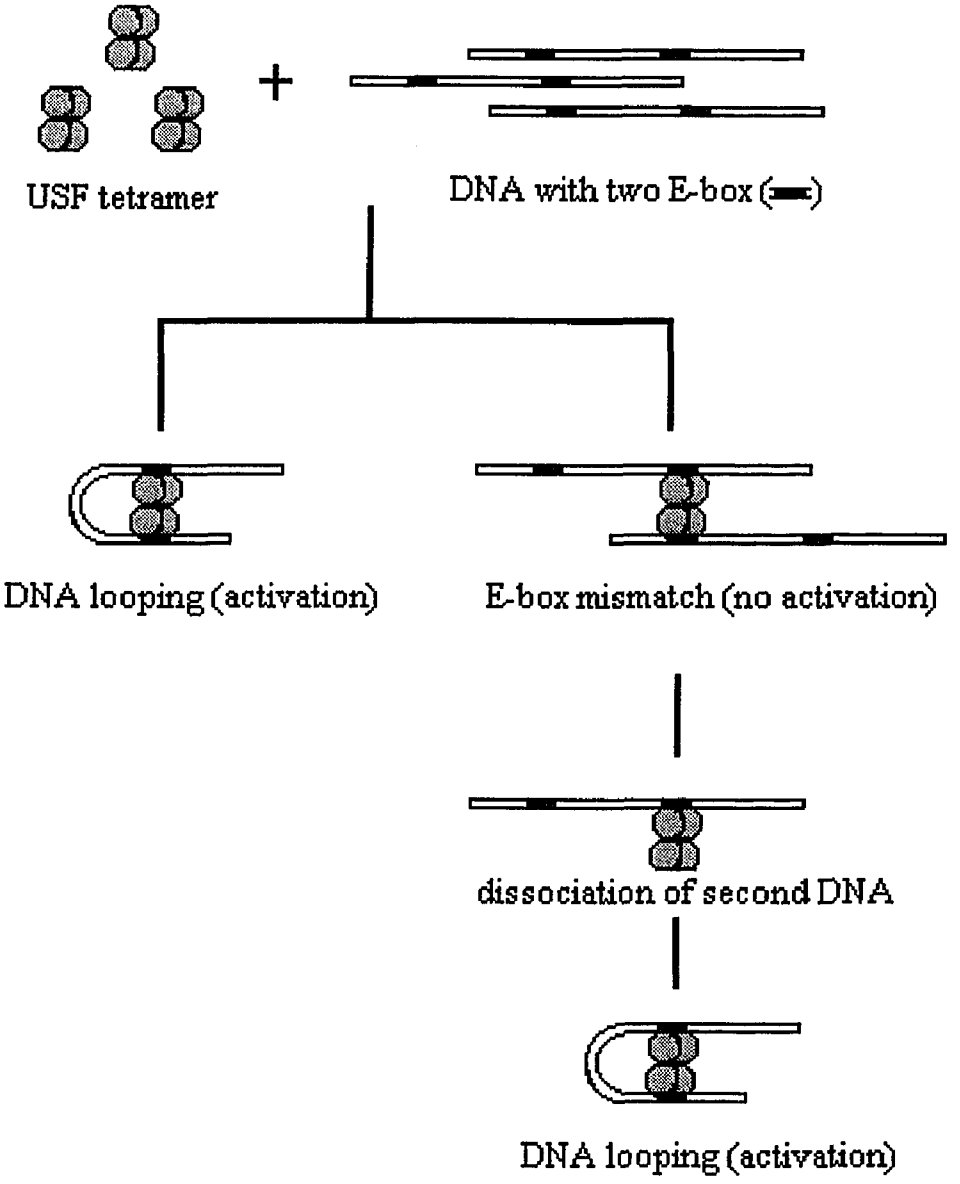

Figure 6.8. Model of selectivity for looped DNA-USF complex formation by anti-cooperative binding during transcription activation.

At least one of the IEB sequences was found to bind USF (Read et al., 1993). The in vivo transcriptional activity of the insulin gene was only modestly affected (less than two fold) when the distance between the two E-box (IEB1, IEB2) elements were changed in half-integral number of double-helical turns, and the introduction of more than two E-boxes sharply reduced the activity (Leshkowitz et al., 1992). Two copies of LCR sequences in mice were found binding to USF and functioning together. No activity was observed when there was only one LCR (Ellis et al., 1993). Paired E-box sequences were found necessary in mouse muscle creatin kinase gene enhancer, which lost activity when one E-box was removed (Martin et al., 1994).

Although USF in different systems might stimulate transcription in a variety of ways, many studies had suggested that in some double E-boxed transcription systems, USF stimulated transcription by DNA looping. In a system where DNA looping was necessary for transcription activation, the anti-cooperative binding of E-box to USF measured in this study would actually benefit DNA looping and mismatch correction (a model is shown in Figure 6.8). Because only looped DNA was activated, two DNA templates connected together by USF (mismatch) on their E-box would not function. However, the second DNA binding was 10 times less than the first one, therefore release of the second DNA from the USF-DNA complex was relatively easy and allowed reconstruction of the USF-

Looped DNA complex. The second E-box on the same DNA was generally closer and more available, i.e., had a much higher effective concentration (intra-molecular) compared with the E-box on another DNA strand. This resulted in more transcriptionally active looped DNA-USF complex than the mismatched USF-two DNA complex. The negative cooperativity derived selectivity on looped DNA formation would benefit looping and enhance transcription activation.

Although the crystal structure of complete USF or the b/HLH/Z domain of USF had not been obtained, the co-crystal structure of the b/HLH domain of USF with the MLP DNA was obtained from Dr. Steven K. Burley's lab at the Rockfeller University. This crystal structure helped me designed and conducted part of my experiments. Figure 6.9 showed the co-crystal structure of the b/HLH dimer with MLP DNA. The two monomers of b/HLH were shown in black and gray ribbon respectively. The only tryptophan residue which was responsible for the protein fluorescence in each monomer was represented by space-filled molecules (white).

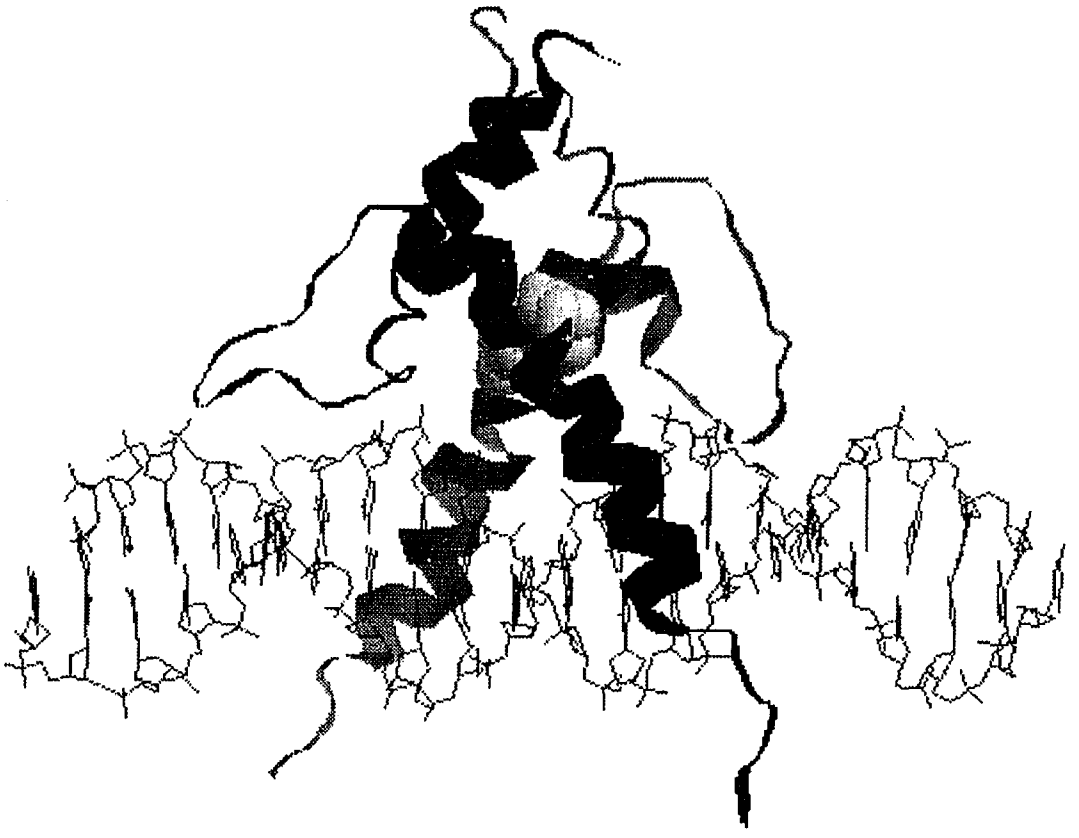

Figure 6.9. Co-crystal structure of the b/HLH dimer with MLP DNA. The two monomers of b/HLH were shown in black and gray ribbon respectively. The only tryptophan residue which was responsible for the protein fluorescence in each monomer was represented by space-filled molecules (white). All coordinates were supplied by Dr. Steven K. Burley from the Rockfeller University.

Table 6.1: The binding constants and specificities of b/HLH and b/HLH/Z binding with MLP, LCR and NS DNA. *: specific DNA (sDNA) is either MLP or LCR DNA.

DNA	b/HLH Keq	b/HLH specificity sDNA*/NS	b/HLH/Z Keq	b/HLH/Z specificity sDNA*/NS
MLP	$(4.7\pm0.6)\times10^{5}M^{-}$	1.47	F: $(2.2\pm2.0)\times10^{9}M^{-1}$ S: $(1.2\pm0.8)\times10^{8}M^{-1}$	F: 2.0×10^{4} S: 1.1×10^{3}
LCR	$(4.0\pm0.2)\times10^{5}M^{-}$	1.25	F: $(3.1\pm3.7)\times10^{6}M^{-1}$ S: $(3.3\pm0.6)\times10^{5}M^{-1}$	F: 2.8×10^{1} S: 3.0×10^{0}
NS	$(3.2\pm0.1)\times10^{5}M^{-}$	1.00	F: —————— S: $(1.1\pm0.3)\times10^{5}M^{-1}$	1.0

Table 6.2: Observed rate constants (k_{obs}) measured at different DNA concentrations for b/HLH and b/HLH/Z MLP DNA interactions at 26 °C.

MLP DNA	Dimer b/HLH (0.1μM)	Tetramer b/HLH/Z (0.1μM)
1 μM	$k_{obs} = (125.8 \pm 4.9)\ s^{-1}$	$k_{obs} = (82.4 \pm 7.2)\ s^{-1}$
2 μM	$k_{obs} = (128.9 \pm 8.6)\ s^{-1}$	$k_{obs} = (84.5 \pm 8.9)\ s^{-1}$
3.5 μM	$k_{obs} = (129.7 \pm 5.9)\ s^{-1}$	$k_{obs} = (85.4 \pm 4.5)\ s^{-1}$
5 μM	$k_{obs} = (134.9 \pm 7.0)\ s^{-1}$	$k_{obs} = (87.0 \pm 8.5)\ s^{-1}$
calculated k_2 or k_4	$k_2 = (134.4 \pm 9.8)\ s^{-1}$	$k_4 = (87.5 \pm 10.6)\ s^{-1}$

References

Abramson, R. D., Dever T. E., Lawson, T. G., Ray B. K., Thach, R. E and Merrick, W. C. (1987) *J. Biol. Chem.* **262,** 3826-3832.

Abramson, R. D., Browning, K. S., Dever, T. E., Lawson, T. G., Thach, R. E., Ravel, J. M., & Merrick, W. C., (1988) *J. Biol. Chem.* **263**, 5462-5467.

Allen, M. L., Metz, A. M., Timmer, R. T., Rhoads, R. E., & Browning, K. S. (1992) *J. Biol. Chem.* **267**, 23232-23236.

Altmann, M., Edery, I., Trachsel, H., and Sonenberg, N. (1988) *J. Biol. Chem.* **263**, 17229-17232.

Altmann, M., Muller, P. P., Pelletier, J., Sonenberg, N., and Trachsel, H. (1989) *J. Biol. Chem.* **264**, 12145-12147.

Anthony, D. D., Kinzy, T. G., and Merrick, W. C. (1990) *Arch. Biochem. Biophys.* **281**, 157-162.

Atkins, P. W. (1982) *Physical Chemistry*, 2nd ed., pp 988-989, W. H. Freeman, San Francisco.

Balasta, M. L., Carberry, S. E., Friedland, D. E., Perez, R. A., and Goss, D. J. (1993) *J. Biol. Chem.* **268**, 1-5.

Bassam B. J., Anolles G. G., and Gresshoff P. M. (1991) *Anal. Biochemistry* **196**, 80-83.

Benne, R. and Hershey, J. W. B. (1978) *J. Biol. Chem.* **253**, 3078-3087.

Bresnick, E. H. and Felsenfeld, G. (1993) *J. Biol. Chem.* **268**, 18824-18834.

Browning, K. S., Maia, D. M., Lax, S. R., and Ravel, J. M. (1987) *J. Biol. Chem.* **262**, 538-541.

Browning, K. S., Fletcher, L., Lax, S. R., and Ravel, J. M. (1989) 2*J. Biol. Chem.* **264**, 8491-8491.

Brun, F., Toulme, J.-J., & Helene, C. (1975) *Biochemistry* **14**, 558-563.

Bujalowski, W., and Lohman, T. M (1986) *Biochemistry* **25**, 7799-7802.

Bujalowski, W., Overman, L. B., and Lohman, T. M. (1988) *J. Biol. Chem.* **263**, 4629-4640.

Bungert, J., Dring, F. and Seifart, K. H. (1992) *J. Mol. Biol.* **223**, 885-898.

Carberry, S. E., Rhoads, R. E., & Goss, D. J. (1989) *Biochemistry* **28**, 8078-8083.

Carberry, S. E., Darzynkiewicz, E., Stepinski, J., Tahara, S. M., Rhoads, R. E., & Goss, D. J. (1990) *Biochemistry* **29**, 3337-3341.

Carberry, S. E., Darzynkiewicz, E. and Goss, D. J. (1991) *Biochemistry* **30**, 1624-1627.

Carberry, S. E., Friedland, D. F., Rhoads, R. E., & Goss, D. J. (1992) *Biochemistry* **31**, 1427-1432.

Carthew, R. W., Chodosh, L. A. and Sharp, P. A. (1985). *Cell* **43**, 439-448.

Conroy, S. C., Dever, T. E., Owens, C. L., and Merrick, W. C. (1990) Arch. *Biochem. Biophys.* **282**, 363-371.

Cooper, H. L., Park, M. H., Folk, J. E., and Safer, B., and Braverman, R. (1983) *Proc. Natl. Acad. Sci. USA* **80**, 1854-1857.

Dever, T. E., Ravel, J. M. and Merrick, W. C. (1989) *J. Cell Biol.* **107**, 547-552.

Draper, D. E., White, S. A., & Kean, J. M. (1988) *Methods Enzymol.* **164**, 221-237.

Dulley, J. R. (1975) *Anal. Biochem.* **67**, 91-95.

Eadie, G. S. (1942) *J. Biol. Chem.* **146**, 85-90.

Edery, I., Humbelin, M., Darveau, A., Lee, K. A. W., Milburn, S., Hershey, J. W. B., Trachsel, H., and Sonenberg, N. (1983) *J. Biol. Chem.* **258**, 11398-11403.

Ernst, H., Duncan, R., and Hershey, J. W. B. (1987) *J. Biol. Chem.* **262**, 1206-1212.

Ferr D'Amar, A. R., Prendergast, G. C., Ziff, E. B. and Burley, S. K. (1993) *Nature* **363**, 38-45.

Ferr D'Amar , A. R., Pognonec, P., Roeder, R. G. and Burley, S. K. (1994) *EMBO* **13**, 180-189.

Fiske, C. H. and Subba Row, Y. (1925) *J.Biol. Chem* **66**, 375-380.

Gill, S. J., Downing, M., & Sheats, G. F. (1967) *Biochemistry* **6**, 272-276.

Gill, S. J., Nichols, N. F., & Wadso, I. (1976) *J. Chem. Thermodyn.* **8**, 445-452.

Gordon, E. D., Mora R., Meredith S. C., Lee C., and Lindquist S. L. (1987) *J. Biol. Chem.* **262**,16585-16595.

Goss, D. J., Parkhurst, L. J., Mehta, A. M., & Wahba, A. J.
(1984) *J. Biol. Chem.* **258**, 11398-11403.

Goss, D. J., Carberry, S. E., Dever, T. E., Merrick, W. C. and Rhoads, R. E. (1990) *Biochem. Biophys. Acta* **1050**, 163-166.

Heerden A. V. and Browning K. S. (1994) *J. Biol. Chem.* (in press)

Hershey, J. W. B., Trachsel, H., and Sonenberg, N. (1983) *J. Biol. Chem.* **258**, 11398-11403.

Hershey, J. W. B. (1991) *Annu. Rev. Biochem.* **60**, 717-755.

Heufler, C., Browning, K. S., and Ravel, J. M. (1988) *Biochem. Biophys. Acta* **951**, 182-190.

Ishida, T., Katsuta, M., Inoue, M., Yamagata, Y., & Tomita, K. (1983) *Biochem. Biophys. Res. Commun.* **115**, 849-854.

Kaulen, H., Pognonec, P., Gregor, P. D. and Roeder, R. G. (1991) *Mol. Cell. Biol.*, **11**, 412-424.

Lakowicz, J. R., & Weber, G. (1973) *Biochemistry* **12**, 4171-4179.

Lakowicz, J. R. *Principles of Fluorescence Spectroscopy*, 279-284. (Plenum Prtess, New York 1983)

Lakowicz J. R. (1983) *Principles of Fluorescence Spectroscopy*, pp 343, Plenum Press, New York and London.

Lax, S. R., Fritz, W., Browning, K. S., & Ravel, J. M. (1985) *Proc. Natl. Acad. Sci. U.S.A.* **82**, 330-333.

Lax, S. R., Lauer, S. J., Browning, K. S., & Ravel, J. M. (1986a) *Methods Enzyme.* **118**, 109-128.

Lax, S. R., W., Browning, K. S., Maia, D. M., & Ravel, J. M. (1986b) *J. Biol. Chem.* **261**, 15632-15636.

Lawaczek, R., and Wagner, K. G. (1974) *Biopolymers* **13**, 2003-2014.

Lawson, T. G., Lee, K. A., Maimone, M. M., Abramson, R. D., Dever, T. E., Merrick, W. C., and Thach, R. E. (1989) *Biochemistry* **28**, 4729-4734.

Lehrer, S. S. (1971) *Biochemistry* **10**, 3254-3263.

Leshkowitz, D., Aronheim, A. and Walker, M. D. (1992) *DNA Cell Biol.* **11**, 549-558.

Lin, T., and Morales, M. (1977) *Anal. Biochem.* **77**, 10-17.

Martin, K. A., Walsh, K. and Mader, S. L. (1994) *Gene.* **142**, 275-278.

McClure, W. R., Cech, C. L. & Johnston, D. E. (1978) *J. Biol. Chem.* **253**, 8941-8948.

Meisterernst, M., Horikoshi, M. and Roeder, R. G. (1985) *Proc. Natl Acad. Sci. USA.* **87**, 9153-9157.

Merrick W. C. *Microbiological Reviews, June 1992*, 291-315.

Milburn, S. C., Hershey, J. W., Davies, M. V., Kelleher, K., & Kaufman, R. J. *EMBO-J.* 1990 Sep; **9**(9): 2783-90.

Milligan, J. F., Groebe, D. R., Witherell, G. W., & Uhlenbeck, O. C. (1987) *Nucleic Acids Res.* **15**, 8783-8798.

Mission, G. (1908) *Chem. Z.* **32**, 663-667.

Miyamoto, N. G., Moncollin, V., Egly, J. M. and Chambon, P. (1985) *EMBO J.* **4**, 3563-3570.

Murphey, R. J., and Gerner, E. W. (1987) *J. Biol. Chem.* **262**, 15033-15036.

Nielsen, P. J., and Trachsel, H. (1988) *EMBO J.*, **7**, 2097-2105.

Nygard, O., Westermann, P., and Hultin, T. (1980) *FEBS Lett.* **113**, 125-128.

Olsen, K., Christensen, U., Sierks, M. R. and Svensson, B. (1993) *Biochemistry*, **32**, 9686-9693.

Park, M. H. (1987) *J. Biol. Chem.* **262**:12730-12734.

Pathak, V. K., Nielson, P. J., Trachsel, H., and Hershey, J. W. B. (1988) *Cell* **54**, 633-639.

Pimentel, G. C., & McClellan, A. L. (1971) *Annu. Rev. Phys. Chem.* **22**, 347-385.

Pognonec, P., Kato, H. and Roeder, R. G. (1992) *J. Biol. Chem.*, **267**, 24563-24567.

Pognonec, P., Kato, H., Sumimoto, H., Kretzschmar, M. and Roeder, R. G. (1991) Nucleic Acids Res., 19, 6650-6655.

Pognonec, P. and Roeder, R. G. (1991) *Mol. Cell. Biol.*, **11**, 5125-5136.

Raychaudhuri, P., Stringer, E. A., Valcnzarla, D. M., and Maitra, U. (1984) *J. Biol. Chem.* **259**, 11930-11935.

Read, M. L., Clark, A. R. and Docherty, K. (1993) *Biochem. J.* **295**, 233-237.

Rhoads, R. E., Hellmann, G. M., Remy, P., & Ebel, J.-P. (1983) *Biochemistry* **22**, 6084-6088.

Rhoads, R. E. (1985) *Prog. Mol. Subcell. Biol.* **9**, 104-155.

Ross, P. D., & Subramanian, S. (1981) *Biochemistry* **20**, 3096-3102.

Rozen, F., Edery, I., Meerovith, K., Dever, T. E., Merrick, W. C. & Sonenberg, N. (1990) *Mol. Cell. Biol.* **10**, 1134-1141.

Russel, D. W., and Spremulli, L. L. (1979) *J. Biol. Chem.* **254**, 8796-8800.

Rychlik, W., Gardner, P. R., Vanaman, T. C., & Ravel, R. E (1986) *J. Biol. Chem.* **261**, 15632-15636.

Rychlik, W., Domier, L. L., Gardner, P. R., Hellman, G. M., and Rhoads, R. E. (1987) *Proc. Natl. Acad. Sci. USA* **84**, 945-948.

Sawadogo, M. and Roeder, R. G. (1985) *Cell* **43**,165-175.

Sawadogo, M., Van Dyke, M. W., Gregor, P. D. and Roeder, R. G. (1988) *J. Biol. Chem.* **263**, 11985-11993.

Seal, S. N., Schmidt, A., and Marcus, A. (1982) *J. Biol. Chem.* **257**, 8634-8637.

Sha M., Balasta M. L. and Goss D. J. (1994) *J. Biol. Chem.* **269**, 14872-14877.

Shatkin, A. J. (1985) *Cell* **40**, 223-224.

Studier, F. W., Rosenberg, A. H., Dunn. J. J. and Dubendorff, J. W. (1990) *Meth. Enzym.* **185**, 60-89.

Ueda, H., Maruyama, H., Doi, M., Inoue, M., Ishida, T., Morioka, H., Tanaka, T., Nishikawa, S., and Uesugi, S. (1991) *J. Biochem.* (Tokyo) **109**, 882-889.

Valencia, D. M., Chaudhuri, A., and Maitra, U. (1982) *J. Biol. Chem.* **257,** 7712-7719.

Voorma, H. O., Thomas A., Goumans, H., Amesz, H., and van der Mast C. (1979) *Methods Enzymol.* **60**, 124-135.

Wang, Y., Sha, M., Ren, W. Y., Heerden A. V., Browning K. S. & Goss D. J. (1995, submitted to J. Biol. Chem. for publication).

Webb, N. R., Chari, R. V. J., Depillis, G., Kozarich, J. W., & Rhoads, R. E. (1984) *Biochemistry* **23**, 177-181.

Weber, G. (1975) Adv. Protein Chem. **29**, 2-78.